

HYDROGEN EXCHANGE REACTIONS OF INDOLIN-2-ONES

a Thesis submitted by  
MARIA JOSÉ ROQUE ROCHA

in partial fulfilment of the requirements for the

DEGREE OF DOCTOR OF PHILOSOPHY  
OF THE  
UNIVERSITY OF LONDON

FRANKLAND LABORATORY  
DEPARTMENT OF CHEMISTRY  
IMPERIAL COLLEGE  
LONDON SW7 2AY

SEPTEMBER, 1978

### ABSTRACT

The validity of primary kinetic isotope effects (PKIE) and Brønsted exponents, as indices of transition state symmetry, is reviewed.

The  $pK_A$  and  $pK_{BH^+}$  of some 5-substituted indolin-2-ones are reported.

The rate of hydrogen exchange of indolin-2-ones was found to be susceptible to acid and general base catalysis, and increased by the electron withdrawing ability of 5-substituents. The influence of bulky substituents at the 3,4-positions upon the rate of exchange is less important in acid than in alkaline media.

Brønsted exponents and PKIE predict different transition state symmetries, therefore, the validity of one of these indices, or of both, remains dubious.

The reactivity of indolin-2-one towards hydrogen exchange is compared with that of structurally related amides. The results suggest that the facility of exchange exhibited by indolin-2-ones relates to the aromaticity of the enol/enolate, which results from hydrogen abstraction on the 3-position.

### ACKNOWLEDGEMENTS

I would like to express my gratitude to Dr. B. C. Challis for the opportunity and pleasure of working in his research group and also for the constant advice received during these three years.

I also thank Fundação Calouste Gulbenkian, Instituto Nacional de Investigação Científica and The British Council for financial support.

My thanks also go to those who gave invaluable assistance during this work, namely, Dr. H. S. Rzepa for theoretical calculations and Dr. P. Mitchell and Mr. J. Burgess for the  $^{13}\text{C}$  NMR spectra.

And, most specially, I thank my parents and old friends who have supported me psychologically from far away and also the new friends who have helped to transform a foreign country into a second homeland.

'The answer is yes or no depending  
on the interpretation'

ALBERT EINSTEIN

## INDEX

	<u>Page</u>
1. <u>INTRODUCTION</u>	1
1.1. THE HYDROGEN TRANSFER REACTION. PRIMARY KINETIC ISOTOPE EFFECTS (PKIE), BRØNSTED EXPONENTS AND TRANSITION STATE SYMMETRY	2
1.1.1. Primary Kinetic isotope effects. Tunnelling	3
1.1.2. The Brønsted relationship. Significance of the Brønsted exponents ( $\alpha$ and $\beta$ )	15
1.2. CHEMISTRY OF INDOLIN-2-ONES	20
1.2.1. Structure	20
1.2.2. Synthesis	20
1.2.3. Reactivity	24
1.3. INDOLIN-2-ONES AS SUBSTRATES IN THE STUDY OF PROTON TRANSFER REACTIONS	26
2. <u>RESULTS AND DISCUSSION</u>	28
2.1. MEASUREMENT OF pK	29
2.1.1. RESULTS	29
2.1.1.1. $pK_A$	29
2.1.1.2. $pK_{BH^+}$	34
2.1.2. DISCUSSION	34
2.1.2.1. $pK_A$	34
2.1.2.2. $pK_{BH^+}$	38

	<u>Page</u>
2.2. HYDROGEN EXCHANGE OF INDOLIN-2-ONES	45
2.2.1. RESULTS	45
2.2.1.1. Protodetrition in alkaline media	45
2.2.1.2. Protodetrition in acidic media	56
2.2.2. DISCUSSION	65
2.2.2.1. Protodetrition in alkaline media	65
A - General mechanism	65
B - Effect of 5-substituents on the rate of exchange	66
2.2.2.2. Protodetrition in acidic media	69
A - General mechanism	69
B - The site of protonation	76
C - Influence of 5-substituents on the rate of exchange	83
D - Influence of substituents on the 1,3- -positions. Steric effects	87
2.3. PRIMARY KINETIC ISOTOPE EFFECTS FOR THE IONIZATION OF INDOLIN-2-ONES	90
2.3.1. In alkaline media	90
2.3.1.1. INTRODUCTION	90
2.3.1.2. RESULTS	92
2.3.1.3. DISCUSSION	100
2.3.2. In acidic media	104
2.3.2.1. RESULTS	104
2.3.2.2. DISCUSSION	105

	<u>Page</u>
2.4. THE GEOMETRY OF THE TRANSITION STATE OF THE HYDROGEN EXCHANGE OF INDOLIN-2-ONES. BRØNSTED EXPONENTS, HAMMETT VALUES AND PKIE	107
2.5. COMPARATIVE HYDROGEN EXCHANGE OF INDOLIN-2-ONES AND RELATED AMIDES	113
2.5.1. INTRODUCTION	113
2.5.2. RESULTS	116
3-Pyrrolin-2-one	116
1-Methyl-3-pyrrolin-2-one	116
2-Pyrrolidone	116
N-Phenyl phenylacetamide	119
2-Ketotetrahydroquinoline	119
2.5.3. DISCUSSION	119
3. <u>EXPERIMENTAL</u>	122
General procedures	123
3.1. PURIFICATION OF REAGENTS AND SOLVENTS	124
3.2. SYNTHESIS OF SUBSTRATES	125
1,3-Dimethylindolin-2-one	125
4,6-Di <sup>t</sup> butylindolin-2-one	126
5-Methoxyindolin-2-one	127
5-Nitroindolin-2-one	128
1,3-Dimethyl-5-nitroindolin-2-one	128
5-Bromoindolin-2-one	129
1,3-Dimethyl-4,6-di <sup>t</sup> butylindolin-2-one	129
1-Methylindolin-2-one	130

	<u>Page</u>
2-Aminophenylacetic acid	131
N-Phenyl phenylacetamide	131
2-Ketotetrahydroquinoline	132
3-Pyrrolin-2-one	133
1-Methyl-3-pyrrolin-2-one	133
3.3. LABELLING OF SUBSTRATES	134
3.3.1. [ <sup>3</sup> H <sub>1</sub> ]-Compounds	134
3.3.2. [ <sup>2</sup> H <sub>1</sub> ]-Compounds	137
3.4. KINETIC PROCEDURES	138
3.4.1. Protodetrition reactions	138
3.4.2. Protodeuteriation reactions (Mass Spectral Analysis)	144
3.4.3. Iododeprotonation and iododeuteriation reactions (Iodometric Analysis)	148
3.5. pK MEASUREMENTS	154
3.6. PREPARATION OF BUFFER SOLUTIONS	155
3.7. <sup>13</sup> C NMR SPECTRA	156
 BIBLIOGRAPHY	 157



1. INTRODUCTION

1.1. THE HYDROGEN TRANSFER REACTION. PRIMARY KINETIC ISOTOPE EFFECTS (PKIE), BRØNSTED EXPONENTS AND TRANSITION STATE SYMMETRY

It seems probable that, in the future, the notion of a complete reaction mechanism will change from a sequence of equations identifying the initial state, transition state, intermediates and final state, to a more or less detailed picture of the atomic motions and electron flow occurring during the reaction. Chemical reactions in solution involve the repositioning and rebonding of a large number of atoms (including those of solvent), the complete behaviour of which is difficult to describe accurately. Therefore, it is understandable that a simple reaction such as hydrogen transfer should attract attention in the initial attempts to describe mechanisms in more detail. Furthermore, the proton plays an important role as a promoter and mediator in chemical reactions, with many organic and enzymic processes being either acid- or base-catalysed. Our understanding of hydrogen transfer reactions has increased enormously in the past twenty years, particularly in regard to the nature of the transition state. Two important empirical parameters used in these studies have been the primary isotope effects and the Brønsted exponents.

1.1.1. Primary kinetic isotope effects (PKIE). Tunnelling

The effect of isotopic substitution on reaction rates can yield valuable mechanistic information. Since the rate differences depend largely upon the relative masses of the isotopic atoms, the effects are larger for isotopes of hydrogen than other atoms. The relative simplicity of isotope effects lies in the fact that, for a fixed molecular geometry, the electronic distribution is virtually unaltered by isotopic substitution and the potential energy curves for a given reaction are, therefore, identical. Primary kinetic isotope effects ( $k_H/k_D$ ) depend principally on differences in zero point energies of the C-H and C-D bonds in the reactant, but, if this were the only factor,  $k_H/k_D$  would have a fairly constant value of ca. 7<sup>1,2</sup>. Experimental studies of proton transfer reactions have revealed, however, that constant values are not obtained, although regularities in their magnitude are apparent<sup>1,2</sup>. Thus, for a series of similar reactions,  $k_H/k_D$  varies smoothly with the pK of the reacting species and some investigations showed the existence of a maximum in  $k_H/k_D$  close to the point where the ~~the~~<sup>STANDARD</sup> free energy change of the reaction is zero, i.e. when  $\Delta pK = 0$ <sup>3-9</sup>. Westheimer rationalized these observations in terms of transition state symmetry<sup>10</sup>. If the transition state is represented by a linear three centre model,  $[A...H...B]^\ddagger$ , the maximum isotope effect corresponds to equality of the two force constants (symmetrical transition state) for the binding of the proton to the two basic centres: in this case the symmetrical stretching vibration in the transition state

involves no motion of the hydrogen atom and, therefore, its zero point energy contributes nothing to reducing the magnitude of  $k_H/k_D$ . When the two force constants are different (asymmetrical transition state) the frequency of the stretching vibration will be real and depend on the isotopic mass. Thus, the isotope effect due to the difference in the zero point energy of the reactants will be partially cancelled and  $k_H/k_D$  will be less than the predicted value of ca. 7. Westheimer's model for the transition state appears to be an over-simplification. More realistic, and hence more complicated treatments, which take into account bending vibrations in both linear<sup>11</sup> and non-linear<sup>12</sup> transition states and tunnelling corrections<sup>13,14</sup> have been put forward<sup>15</sup>. By and large, these suggest that  $k_H/k_D$  ratios depend on either transition state symmetry or the incidence of tunnelling.

Aromatic hydrogen exchange is one of the many reactions where a maximum primary isotope effect has been reported<sup>3,6</sup>. However Challis and Millar<sup>16</sup> studying substituted indoles found that, even for a wide variation in  $\Delta pK$  and a range of reactivity of  $10^7$ , there is practically no change in the primary isotope effect, even though the Brønsted exponents suggest a considerable difference in the the transition state symmetry. This work corroborates an earlier comment by Bordwell and Boyle<sup>17</sup> on the ionization of nitroalkanes in particular, and on the validity of kinetic isotope effects and Brønsted exponents as indices of the degree of proton transfer in the transition state.

Although Westheimer's and subsequent related treatments explain kinetic isotope effects of about 7 or lower and offer an elegant explanation for the maximum (artifactual or not),

they do not explain very high ratios reported by several authors and quoted by Bell<sup>14</sup>. These high ratios can be explained, however, by proton tunnelling effects. The concept of tunnelling, its theoretical treatment and practical implications has been reviewed by Caldin<sup>18</sup>, Jones<sup>19</sup> and Lewis<sup>20</sup>. Also, Bell<sup>13,14,21,22</sup> showed that good agreement can be obtained between calculated isotope effects and the experimental results (Figure 1.1.1) for nitroalkanes and carbonyl compounds using an electrostatic model for the transition state with tunnelling corrections, at different internuclear distances in the transition state ( $R_{AB}^\ddagger$ ). He concluded that his treatment was

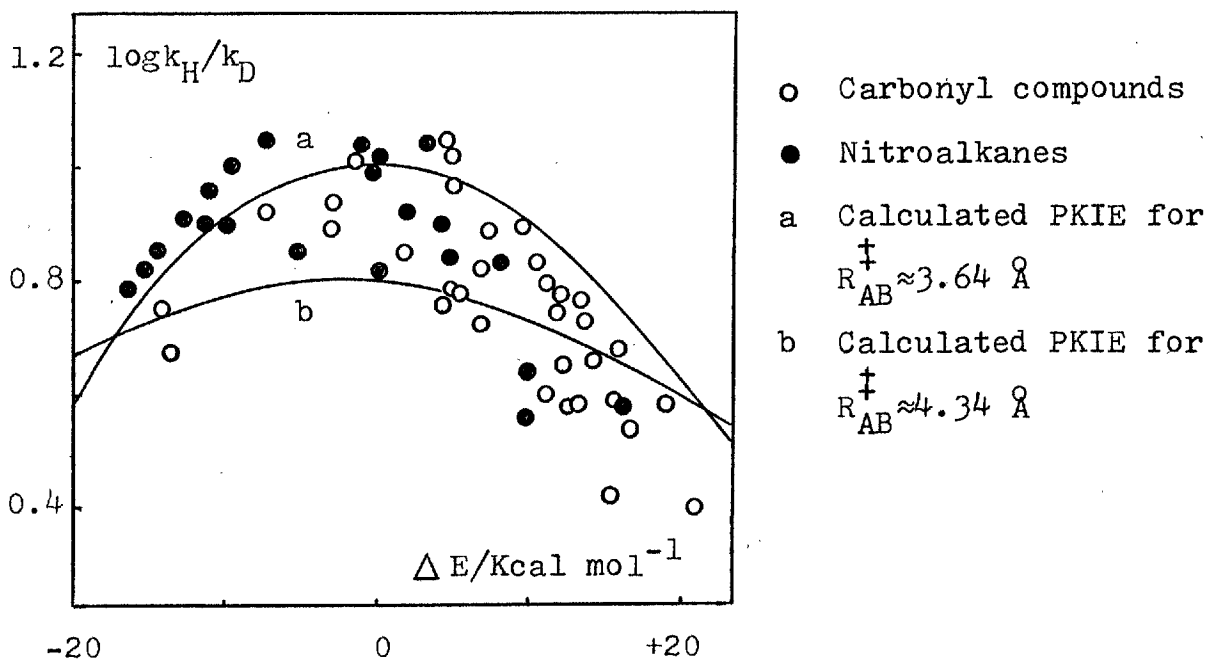


Figure 1.1.1

more satisfactory than explanations based on frequencies of the symmetrical stretching or bending modes of the transition state. The model proposed by Bell also provides an explanation for the apparent correlation between the value of the isotope effect

and the symmetry of the transition state<sup>14</sup>, since the tunnelling correction should be a maximum when  $\Delta G$  is zero, i.e., for a symmetrical barrier<sup>13</sup>. The physical basis of this statement is illustrated in Figure 1.1.2. Only that part of the barrier (shaded areas) lying above both the initial and final states is available for tunnelling and the extent of this region has its maximum for a symmetrical transition state. Another

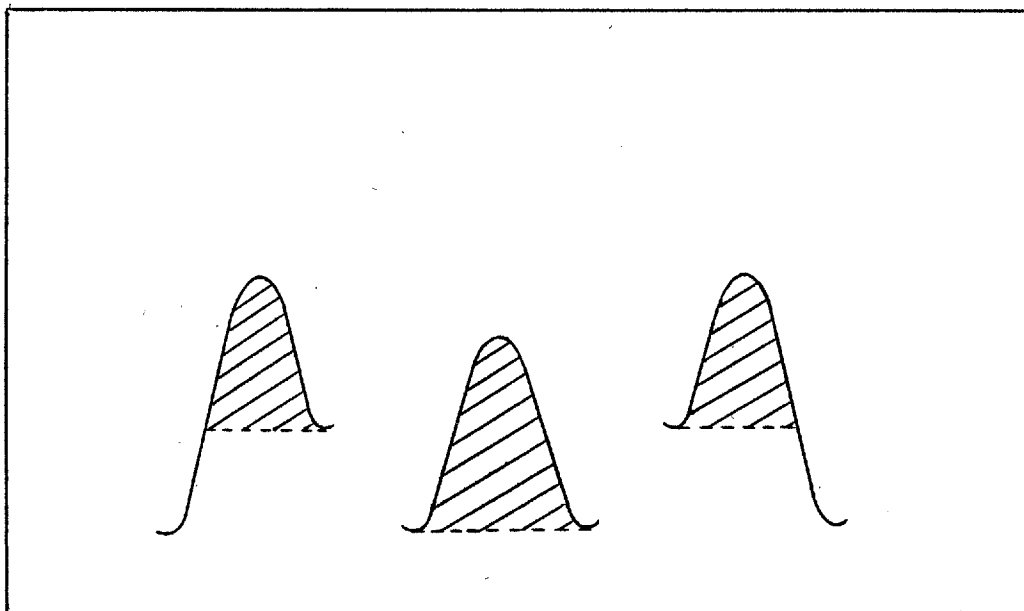


Figure 1.1.2

interesting feature of this model is that it suggests that isotope effects should be sensitive to steric hindrance. Experimental evidence appears to support this prediction. The subject has been reviewed and explained by Lewis<sup>20</sup> and the conclusion is that sterically hindered transition states for

hydrogen transfer reactions have especially large tunnelling corrections and therefore large  $k_H/k_D$  ratios.

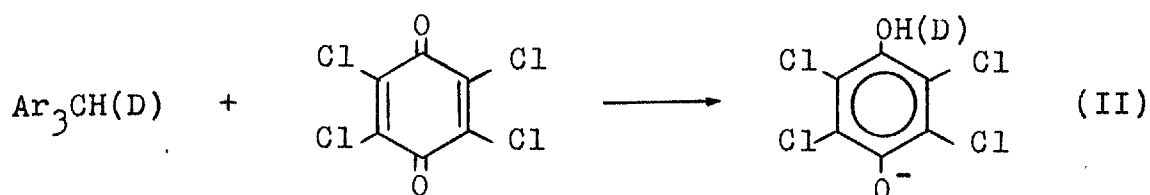
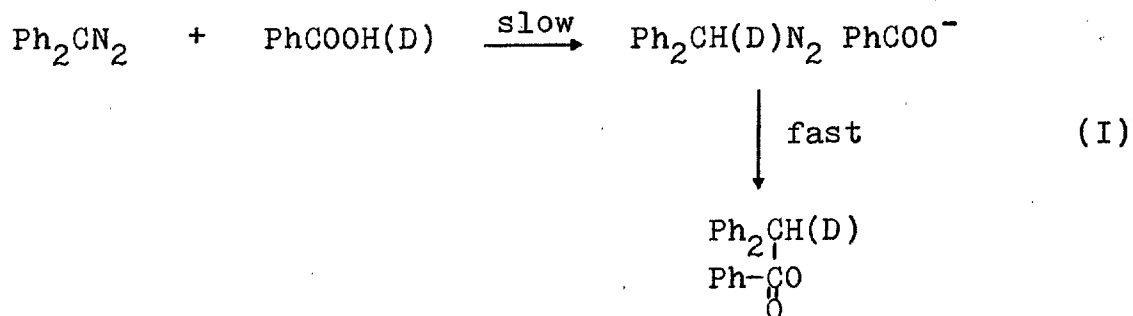
Direct chemical evidence for the existence of tunnelling is difficult to obtain. The experimental criteria for its detection are based on three empirical parameters<sup>18</sup>:

- (i) Curved Arrhenius plots and low values for the ratio of Arrhenius pre-exponential parameters ( $A^H/A^D$ )
- (ii) Very large primary kinetic isotope effects
- (iii) An anomalous Swain-Schaad exponent<sup>23,24</sup> as defined in equation 1.1.1

$$k_H/k_T = (k_H/k_D)^{1.442} \quad (1.1.1)$$

However, Arrhenius plots may deviate from linearity for reasons other than tunnelling<sup>18,25</sup> and the magnitude of the Swain-Schaad exponent is not a reliable index<sup>26,27</sup> because it is relatively insensitive to tunnelling and difficult to measure accurately. The most reliable indication of proton tunnelling remains the ratio of Arrhenius pre-exponential parameters ( $A^H/A^D$ ) which, according to collision theory<sup>13</sup>, should be ca. 1 and, according to transition state theory<sup>18</sup>, should not usually be greater than unity, the maximum limit being 2.

More recently, Isaacs et al.<sup>28</sup> have suggested that the pressure dependence of the isotope effect may also be a reliable criterion of tunnelling in proton transfer reactions. The experimental evidence for this assumption is based on the study of the effect of pressure on the  $k_H/k_D$  ratio of the reaction between diphenyldiazomethane (Scheme 1.1.1-I) and benzoic acid, for which there is no evidence of tunnelling, and of the



Scheme 1.1.1

reaction of crystal violet with chloranil (Scheme 1.1.1 - II), for which  $k_{\text{H}}/k_{\text{D}}$  ratios indicate tunnelling. The effect of pressure on  $k_{\text{H}}/k_{\text{D}}$  for both reactions is shown in Figure 1.1.3.

It is apparent that there is a difference in behaviour for both systems.  $K_{\text{H}}/k_{\text{D}}$  remains almost constant for (I) and decreases smoothly for (II), levelling off at a value near the maximum theoretical ratio of about 7. This is interpreted in terms of the decrease of the tunnelling component for  $k_{\text{H(D)}}$  of reaction (II). As an increase in external pressure lowers the potential barrier to the activation process, a higher proportion of molecules will be able to classically surmount the barrier and consequently tunnelling decreases. Since tunnelling is more probable for hydrogen than for



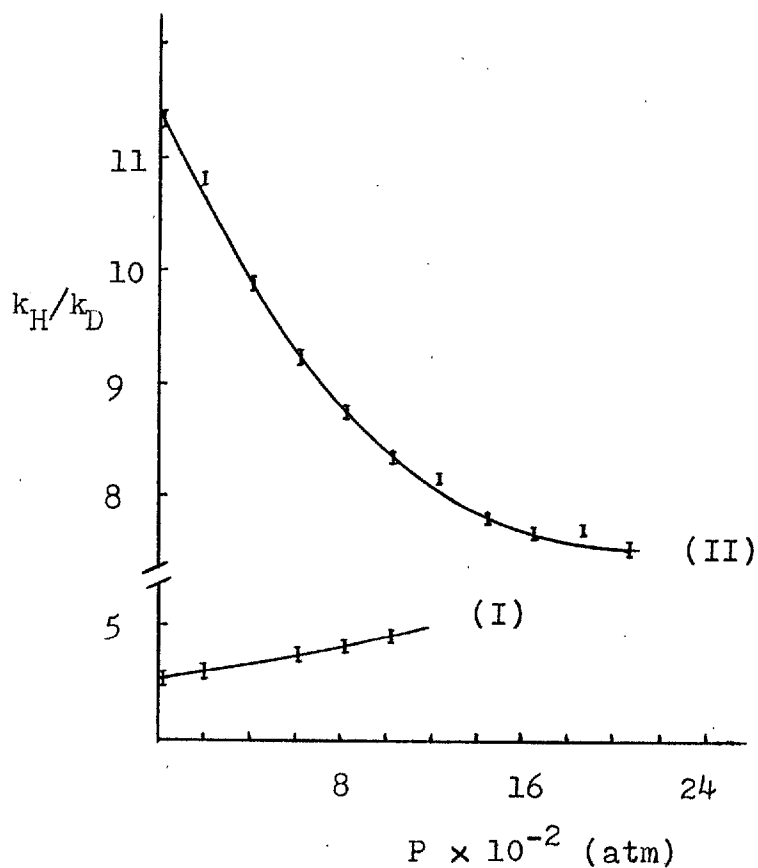
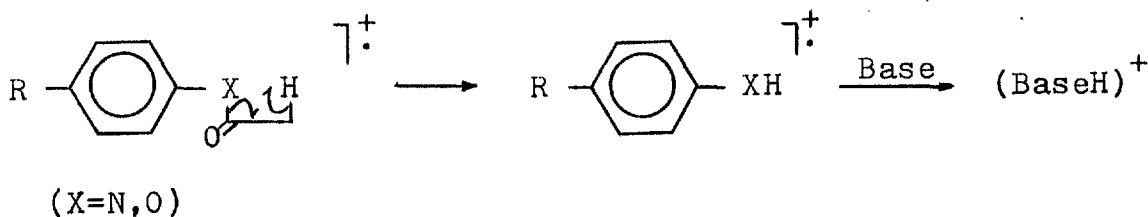


Figure 1.1.3

deuterium, the ratio  $k_H/k_D$  will decrease.

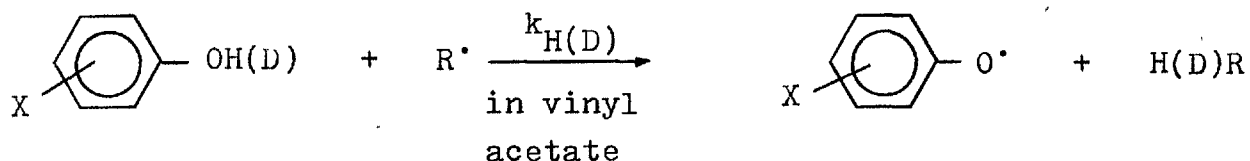
More recent work substantiates both the existence of a maximum in PKIE and the occurrence of tunnelling. Thus Underwood and Bowie<sup>29</sup> have rationalized their results for the elimination of keten from phenylacetanilide and phenylacetate radical ions, shown to proceed through a four-centred transition state (Scheme 1.1.2), on the basis of Westheimer's model. The deuterium isotope effects (calculated from peak abundances) obtained for loss of  $\text{CH}_2\text{CO}$  and  $\text{CHDCO}$  from the molecular ions of  $p\text{-RC}_6\text{H}_4\text{NHCOCH}_2\text{D}$  have been found to be greater than unity in all cases, indicating that the hydrogen transfer occurs in the rate limiting step.  $k_H/k_D$  increases (1.5 - 2.1) with the electron withdrawing ability of the substituents and exhibits a maximum ( $k_H/k_D = 2.2$  for  $\text{R}=\text{H}$ )



Scheme 1.1.2

close to the theoretical value for a four-centred transition state ( $k_H/k_D = 2.3$ )<sup>12</sup>. However this maximum is very poorly defined and may be due to scattering instead of a true Westheimer effect. Smaller PKIE (1.2 - 1.3) have been observed for loss of keten from para-substituted phenylacetate molecular ions, and, further, the value of  $k_H/k_D$  appears to be independent of the substituent. The reason for the difference between the phenylacetanilides and phenylacetates has been rationalized in terms of a difference in geometry of the transition state. In the acetanilide case, electron donating substituents which increase the electron density on nitrogen (giving a stronger N...H bond and consequently an asymmetric transition state) produce smaller isotope effects than substituents that decrease the electron density on the nitrogen. When N is replaced by O (the phenylacetate case) the asymmetry of the transition state is increased due to the formation of a stronger O...H bond and, hence the PKIE's are even smaller.

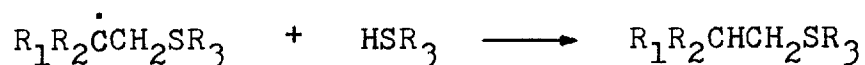
Simonyi et al.<sup>30</sup>, studying the hydrogen atom abstraction from 72 substituted phenols and 33 of their deuteriated analogues (Scheme 1.1.3) by polyvinylacetate radicals at 50°C, found that the magnitude of the isotope effect varies considerably and



Scheme 1.1.3

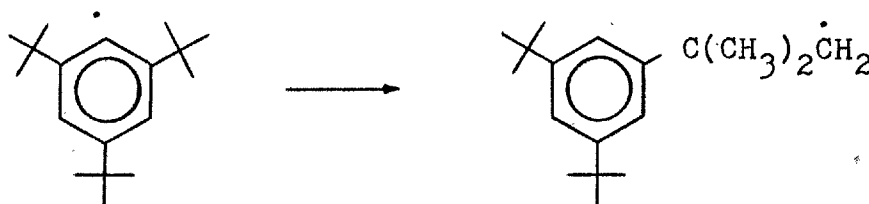
shows a maximum as function of the reactivity of the light compounds. Several  $k_{\text{H}}/k_{\text{D}}$  ratios are equal to or smaller than the semi-classical limit for C-H bonds ( $k_{\text{H}}/k_{\text{D}} = 10$  at  $50^\circ\text{C}$ )<sup>14</sup> while others are significantly higher. Assuming a mechanism in which the hydrogen atom is abstracted within the hydrogen bond, the high values of  $k_{\text{H}}/k_{\text{D}}$  can be attributed to tunnelling. However the low accuracy of the Arrhenius parameters determined over a narrow range of temperature ( $30 - 70^\circ\text{C}$ ) do not provide independent support for the above conclusion.

Other studies of hydrogen atom transfer support not only the occurrence of tunnelling but also the steric enhancement of tunnelling. Toriyama et al.<sup>31</sup> have found that iminoxy radical pairs form when single crystals of dimethylglyoxime are irradiated by ionizing radiation even at  $4.2^\circ\text{K}$  in the dark. At such low temperature the thermally activated process must be completely suppressed and therefore the conversion can only proceed through a tunnelling process. Lewis and Butler<sup>32</sup> studied the hydrogen atom transfer from mercaptans (Scheme 1.1.4) and found that the largest values of  $k_{\text{H}}/k_{\text{T}}$  occur at  $\Delta H = 0$  and that the steric hindrance enhances the isotope effect as for proton transfer. Also, Ingold et al.<sup>33</sup> studying the

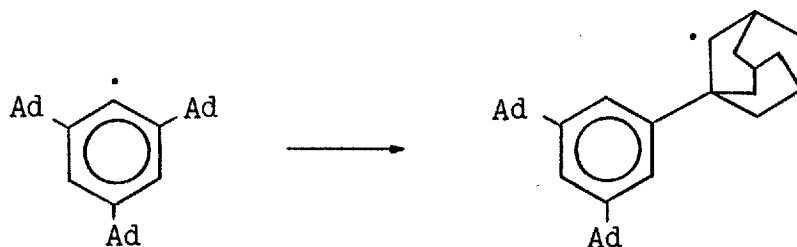


Scheme 1.1.4

isomerization of 2,4,6-tri<sup>t</sup>butylphenyl (Scheme 1.1.5) and of 2,4,6-tri(1'-adamantyl)phenyl (Scheme 1.1.6) radicals have found extremely high isotope effects accompanied by large differences in the activation energies and pre-exponential



Scheme 1.1.5

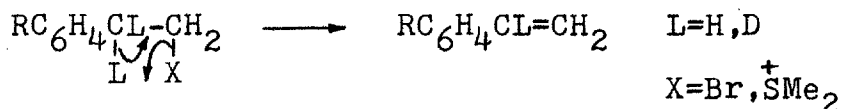


Scheme 1.1.6

Arrhenius parameters for H and D transfer. They also report that these experimental results can be quantitatively accounted for by quantum mechanical tunnelling.

Jones et al.<sup>34</sup> have found that PKIE, Brønsted plots and solvent isotope effects for the detritiation of diethyl-2-

-[<sup>3</sup>H<sub>1</sub>]- malonate give a consistent picture of transition state symmetry. Blackwell and Woodhead<sup>35</sup> have determined PKIE for 1,2-elimination from substituted phenylethyl bromides and dimethyl(phenylethyl)sulphonium bromides in dimethylsulphoxide/water (Scheme 1.1.7). For both leaving groups a systematic increase of  $k_H/k_D$  was observed as R varied from para-OMe to para-Ac. Phenylethyl bromides exhibit a maximum, but no maximum



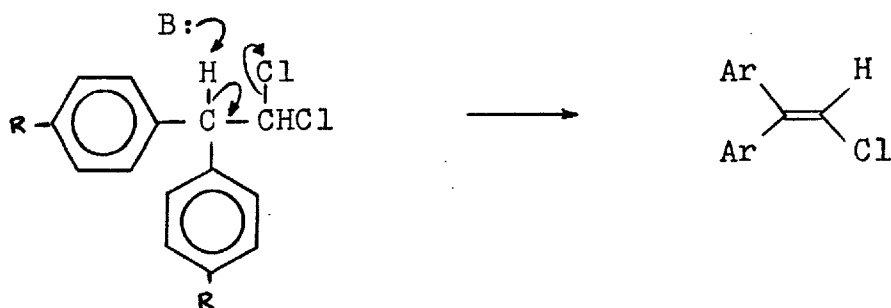
Scheme 1.1.7

was established for dimethyl(phenylethyl)sulphonium bromides. The values for X=SMe<sub>2</sub> were lower than the corresponding values for X=Br, which was interpreted in terms of a less carbanion like transition state for phenylethyl bromides. Brønsted exponents measured for PhCH<sub>2</sub>CH<sub>2</sub>Br (β = 0.54) and para-NO<sub>2</sub>C<sub>6</sub>H<sub>4</sub>CH<sub>2</sub>CH<sub>2</sub>Br (β = 0.67) with substituted phenoxide bases also indicate that the extent of proton transfer is greater for electron withdrawing substituents.

Jones<sup>36</sup> has reported the first example of an isotope effect maximum for a nitrogen acid. Studying the rates of base-catalysed decomposition of NO<sub>2</sub>NH<sub>2</sub> and NO<sub>2</sub>NHD in water and deuterium oxide, he found that the overall isotope effect passed through a maximum in the region of Δ pK ca.0.

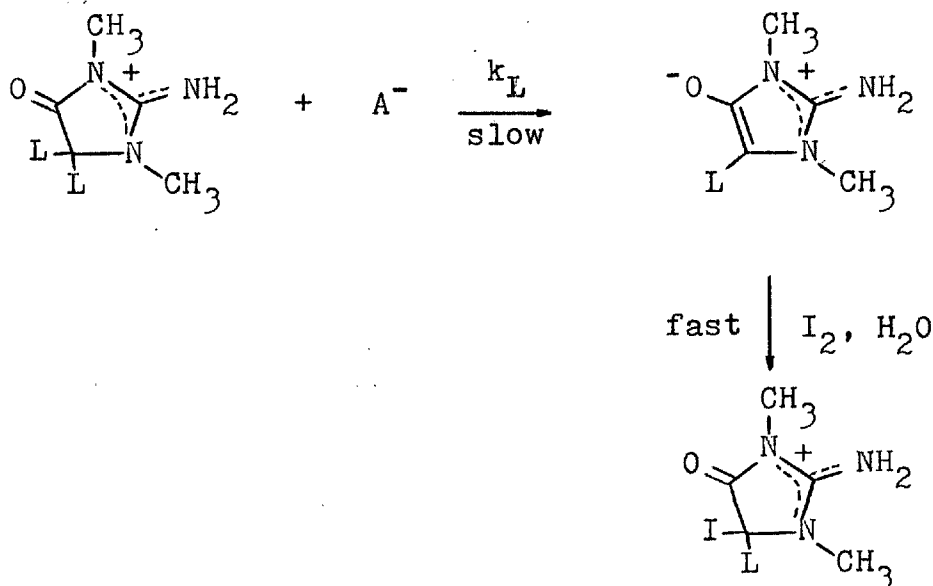
McLennan<sup>37</sup> found that Arrhenius parameters for the dehydrochlorination of 1,1-diaryl-2,2-dichloroethanes (Scheme 1.1.8)

indicate the existence of tunnelling. The variation in R produces a variation on the  $k_H/k_D$  ratio, but, as there appears to be a mechanistic change when  $R=NO_2$ , the variable isotope effects observed for the elimination cannot be related with certainty to a true isotope effect maximum.



Scheme 1.1.8

Srinivasan and Stewart<sup>38</sup> studying the general base-catalysed deprotonation of methylcreatinium ion (Scheme 1.1.9) in the presence of 39 bases found no evidence for the existence of tunnelling, even when a hindered base was used. Also, the  $k_H/k_D$  ratios did not appear to pass through a maximum.



Scheme 1.1.9

1.1.2. The Brønsted relationship. Significance of the Brønsted exponents (  $\alpha$  and  $\beta$  )

The Brønsted relationship<sup>39</sup> correlates the ability of an acid- or base-catalyst to donate or remove a proton in a chemical reaction with the acid/base strength of the catalyst. The relationships are defined by equations 1.1.2 and 1.1.3 where  $k_A$  and  $k_B$  are the catalytic rate coefficients,  $K_A$  the

General acid catalysis

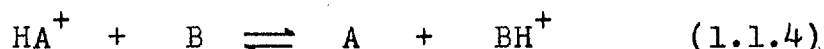
$$k_A = G_A (K_A)^\alpha \quad (1.1.2)$$

General base catalysis

$$k_B = G_B (K_B)^\beta = G_B (1/K_A)^\beta \quad (1.1.3)$$

dissociation constant of the catalyst,  $\alpha$  and  $\beta$  the Brønsted exponents and  $G_A$  and  $G_B$  proportionality constants.  $\alpha$  and  $\beta$  are usually positive and less than unity. This relationship has been widely used<sup>40,41</sup> to interpret reaction mechanisms and to provide information on the transition state of proton transfer reactions. Thus, the value of  $\alpha$  has been interpreted as a measure of the extent of proton transfer in the transition state, with low values indicating little transfer (*i.e.* reactant-like transition state) and high values indicating product-like transition states. Until relatively recently, the Brønsted relationship was believed to be linear over large ranges of  $pK_A$ , but this is now known to be untrue. Also it has become apparent that the Brønsted exponents may exceed the limiting values anticipated by Brønsted and Pedersen<sup>17,42,43,44</sup>.

Anomalous behaviour in the Brønsted relationship such as curvature,  $\alpha$  or  $\beta$  values  $< 0$  or  $> 1$  and systematic deviations of  $\text{OH}^-$  and  $\text{H}_3\text{O}^+$  have been reviewed and discussed by Kresge<sup>45</sup>. One cause of curvature arises when the reaction involves two or more consecutive steps and a change in reactivity leads to a shift in the rate determining step<sup>46</sup>. The other cause of curvature had already been predicted by Brønsted and Pedersen and has been quantitatively treated by Eigen<sup>47</sup>. In any proton transfer from an acid to a base such as in equation 1.1.4,



the rate will increase with increasing strength of the acid until a stage is reached where reaction occurs at every encounter between the acid and the base molecules. When this limit is reached, increasing the acid strength will have no effect on the rate and  $k_A$  will then be constant and independent of  $K_A$  (i.e. independent of  $\Delta G^\circ$ ) and, therefore,  $\alpha = 0$ . If on the other limit, the acid strength is continuously decreased,  $K_B$  will increase until the rate in this direction becomes also encounter controlled and  $\beta$  will be equal to zero; under these conditions  $\alpha = 1$ . The complete picture of a plot of  $\log k$  vs.  $\text{pK}$  (i.e. of  $\Delta G^\ddagger$  against  $\Delta G^\circ$ ) will therefore resemble Figure 1.1.4 where, it is evident that, as the reaction becomes faster and faster and approaches the diffusion control limit, the rate becomes less and less sensitive to the change in the  $\text{pK}$  and the linear plot becomes a curve. This curvature only became apparent when temperature-jump techniques allowed the measurement of rates of very fast reactions. Sharp curvature



is almost invariably found in proton tranfers between oxygen and nitrogen acids and basés. Systems giving linear plots involve proton transfer to and from carbon, although some carbon

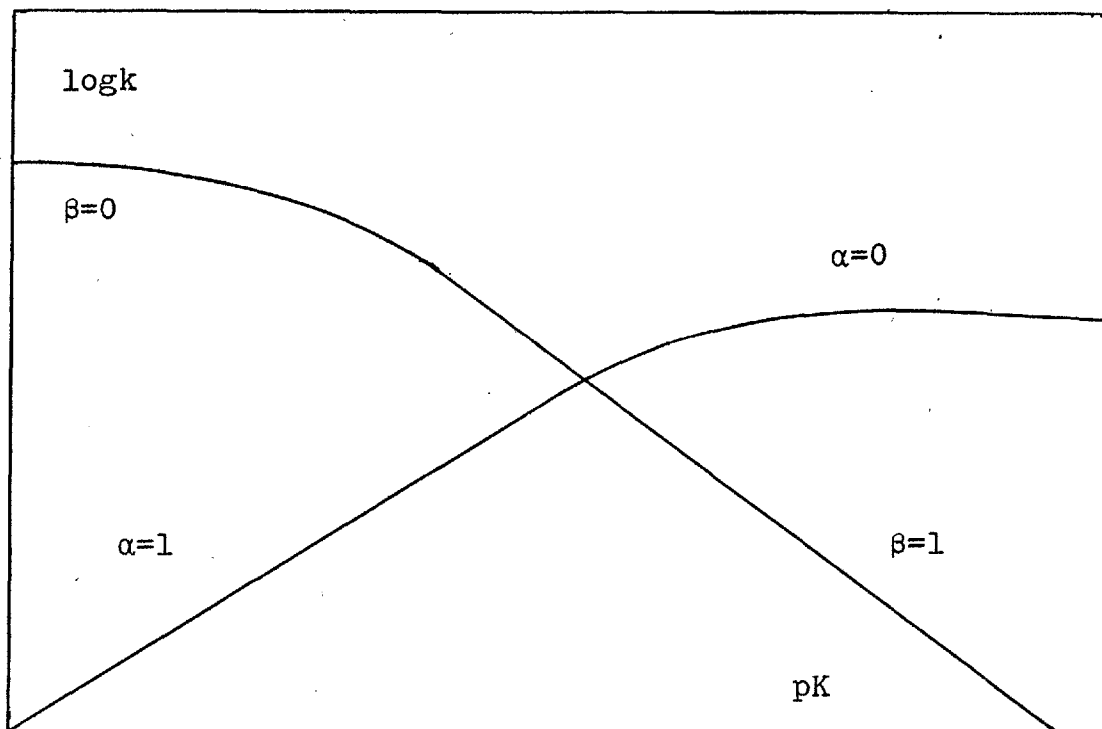


Figure 1.1.4

acids showing curved plots have also been reported, for instance, in cyanocarbons<sup>48,49,50</sup>, chloroform<sup>51</sup> and phenylacetylene<sup>52</sup>. Proton transfer between oxygen and nitrogen acid-base pairs, giving sharply curved Brønsted plots, is very fast and the same is true for cyanocarbons, chloroform and phenylacetylene. However, proton transfer to and from carbon compounds is slow and the rates are always far from the encounter control limit. The factors that control the rate of proton transfer in a particular system have been discussed by Kresge<sup>53</sup> in terms of charge delocalization, thermodynamic effects and intramolecular hydrogen bonding.

Marcus<sup>54,55</sup> has theoretically shown a correlation between curvature of Brønsted plots and reactivity. Marcus relates the free energy of activation,  $\Delta G^\ddagger$ , for a proton transfer process to the standard free energy of activation,  $\Delta G^\circ$ , through the free energy of activation when  $\Delta G^\circ=0$ ,  $\Delta G_0^\ddagger$  (Equation 1.1.5).

$$\Delta G^\ddagger = \left( 1 + \Delta G^\circ / 4 \Delta G_0^\ddagger \right)^2 \Delta G_0^\ddagger \quad (1.1.5)$$

$\Delta G_0^\ddagger$  is the energetic barrier to reaction when the process is neither exothermic nor endothermic; it expresses adequately the intrinsic reactivity of the system and, in fact, it is called the "intrinsic barrier". As  $\alpha$  may be identified with the derivative  $d\Delta G^\ddagger/d\Delta G^\circ$  (Equation 1.1.6) and the curvature of the Brønsted plot with the second derivative of  $\Delta G^\ddagger$  with respect to  $\Delta G^\circ$  (Equation 1.1.7), it is apparent that intrinsically slow reactions (large  $\Delta G_0^\ddagger$ ) will show little

$$\alpha = d\Delta G^\ddagger/d\Delta G^\circ = 1/2 \left( 1 + \Delta G^\circ / 4 \Delta G_0^\ddagger \right) \quad (1.1.6)$$

$$d\alpha/d\Delta G^\circ = d^2\Delta G^\ddagger/d(\Delta G^\circ)^2 = 1/8\Delta G_0^\ddagger \quad (1.1.7)$$

curvature and intrinsically fast reactions (small  $\Delta G_0^\ddagger$ ) will show sharp curvature. This is consistent with the chemical evidence for Brønsted plots concerning fast and slow proton transfers. However, the theory has limitations. Theoretical studies<sup>56</sup> have shown that values of  $\Delta G_0^\ddagger$  can be less than the true intrinsic barriers, sometimes by appreciable amounts.

This implies that the Marcus theory tends to underestimate  $\Delta G_0^\ddagger$ .

The anomalous exponents, that is,  $\alpha$  ( $\beta$ ) outside the limits of 1 and 0, have been attributed by Kresge<sup>45</sup> to interactions which develop in the transition state and are absent from initial and final states. The systematic deviations exhibited by  $H_3O^+$  and  $OH^-$  have been discussed in terms of Brønsted plot curvature<sup>57</sup>, electrostatic interactions<sup>58</sup>, reversible ionization of carbon acids<sup>51</sup> and strong solvation of those ions by water<sup>52</sup>.

The validity of Brønsted exponents as a guide to the extent of proton transfer in the transition state is a question of current debate. One view<sup>44</sup> based on experimental data suggests that they are a very poor guide but others think that, with certain modifications<sup>59</sup> to the theory,  $\alpha$  and  $\beta$  values may be of significance. Despite this controversy, the Brønsted relationship continues to be used to correlate rate-equilibria data for proton transfer reactions.

## 1.2. CHEMISTRY OF INDOLIN-2-ONES

### 1.2.1. Structure

Although three possible structures can be written for indolin-2-ones (Figure 1.2.1), physical evidence (mainly infrared)<sup>60,61</sup> suggests that the carbonyl tautomer (I) is the most stable.

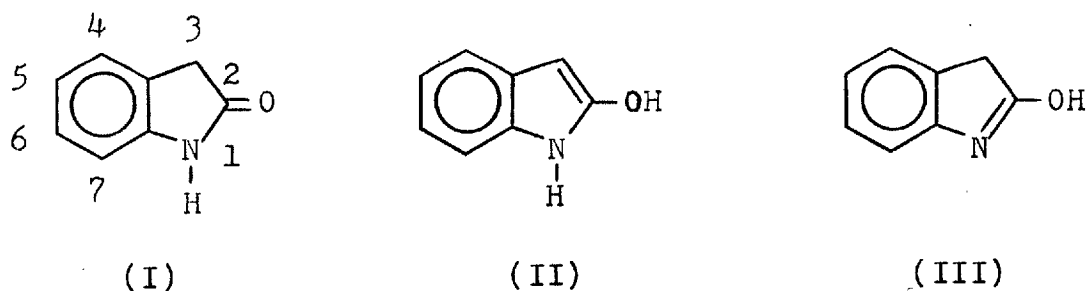


Figure 1.2.1

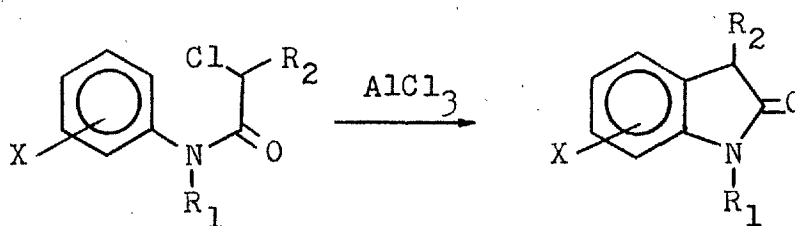
Thus indolin-2-ones are believed to exist mainly in the lactam form (I) in equilibrium with a small percentage of the enol-tautomer (II), which, being an aromatic species, is more stable than (III).

### 1.2.2. Synthesis

The synthesis of indolin-2-ones has been reviewed by Sumpter<sup>62</sup> and Sundberg<sup>63</sup>, but subsequently an important new general synthetic method has been reported by Gassman<sup>64</sup>. Also, Bailey and Bogle have developed a simple route to 3-arylindolin-2-ones<sup>65</sup>

and Mori and Ban<sup>66</sup> reported a more general synthesis based on the cyclization of 2-chloro-N-alkylacrylanilides with an organonickel complex. In the present investigation indolin-2-ones were synthesized by three procedures. Only these are discussed below.

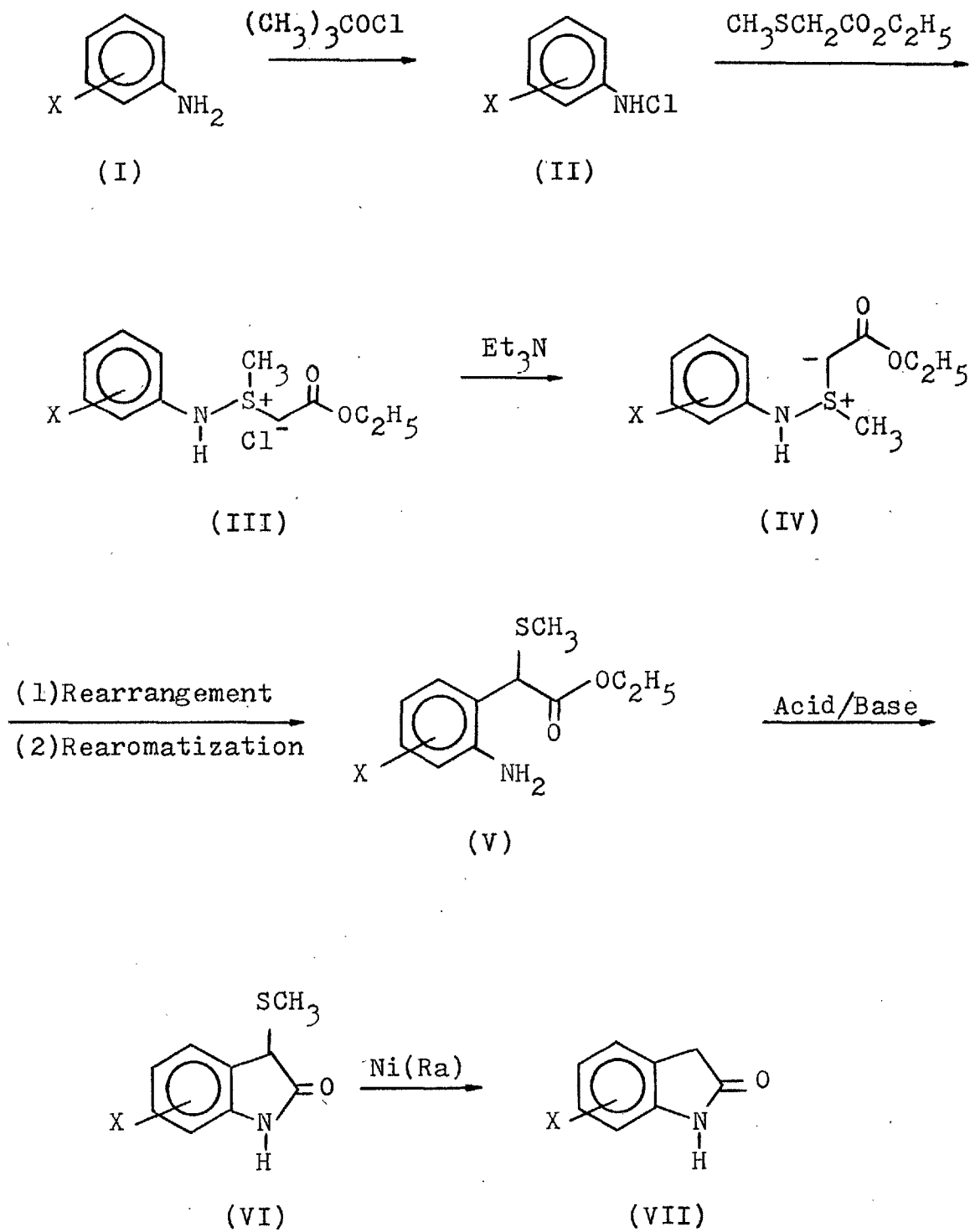
(i) Julian synthesis<sup>67,68</sup>. This involves the Lewis acid-catalysed cyclization of  $\alpha$ -haloacetanilides (Scheme 1.2.1)



Scheme 1.2.1

The reaction gives reasonable yields except when electron-withdrawing substituents are present on the ring. This is due to deactivation towards the electrophilic cyclization.

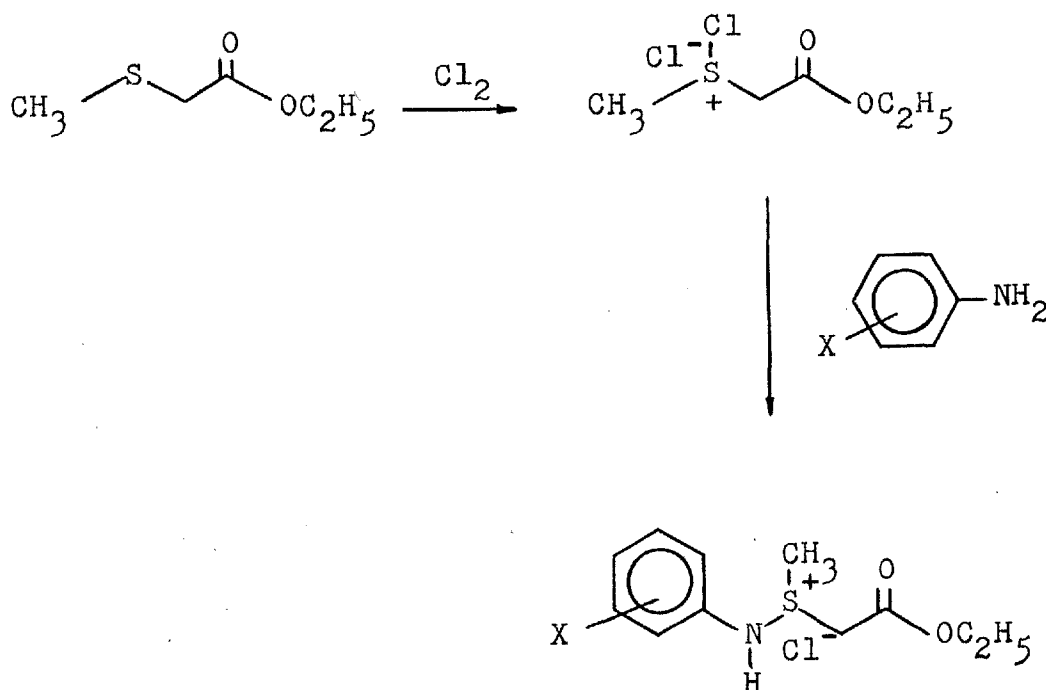
(ii) Electrophilic substitution on the ring of a parent indolin-2-one. For instance, direct nitration of indolin-2-one<sup>69</sup> at low temperature yields the 5-nitroderivative. To avoid oxidation on the 3-position, the amount of nitrating agent, the rate of addition and the temperature must be carefully controlled. Direct bromination<sup>70</sup> in aqueous solution yields mainly the 5-bromoderivative, but, if two or three molar equivalents of bromine are employed, the 5,7- and 3,5,7-derivatives will also be obtained. The bromination of indolin-2-one in anhydrous



Scheme 1.2.2

carbon tetrachloride yields 3,3-dibromoindolin-2-one.

(iii) Gassman synthesis (Scheme 1.2.2). This two step synthesis involves the reaction of a mono-N-chloroaniline (II) with a sulphide to give the azasulphonium salt (III) which, on treatment with a base, yields IV via a Sommelet-Hauser type rearrangement. Product VI can then be transformed into an indolin-2-one by desulphurization with Raney nickel<sup>71</sup>. Good yields were reported by Gassman<sup>64</sup> with a variety of substituents such as X=CH<sub>3</sub>, H, Cl, CO<sub>2</sub>R, NO<sub>2</sub>. However, when powerful cation stabilizing groups are present on the ring, for instance X=OCH<sub>3</sub>, the yield was very poor due to the extreme instability of the N-chloroanilide<sup>72</sup>. To overcome this difficulty Gassman modified the sequence of steps to obtain the azasulphonium salt according to scheme 1.2.3.



Scheme 1.2.3

### 1.2.3. Reactivity

Nitriles, amides and esters are weak acids compared to ketones and nitroalkanes. The effect of the common activating groups on the acidity of carbon acids of the  $\text{CH}_3\text{X}$  type decreases along the series<sup>73</sup>  $\text{NO}_2 > \text{COR} > \text{SO}_2\text{R} > \text{COOH} > \text{CN} > \text{CONH}_2 > \text{halogen}$ , implying that the carboxamide moiety has little power to ionize  $\alpha$ -hydrogen atoms. Early work<sup>74</sup> demonstrated that the methyl hydrogen atoms of acetamide can undergo deuterium exchange, and although the results are probably unreliable, exchange proceeds very slowly relative to nitroalkane and carbonyl compounds. Cram<sup>75</sup> examined the ionization of 2-phenylpropionamides in  ${}^t\text{BuOH}/{}^t\text{BuO}^-\text{K}^+$  and found that the N,N-diethylcarboxamide group was  $10^4$  times less effective than the  ${}^t$ butyl ester group in activating the  $\alpha$ -hydrogen atoms. Matsuo et al.<sup>76</sup>, however, showed by nmr measurements that the  $\alpha$ -hydrogen atoms of primary, secondary and tertiary amides do exchange more rapidly than those in corresponding acids and esters (ethyl and benzyl). The apparent conflict with Cram's results is not easy to rationalize, but it probably arises from competing solvolysis of the substrate in strongly alkaline reaction conditions.

The chemistry of indolin-2-ones is similar to that of typical lactams when reactions of the carbonyl carbon or oxygen are considered. However, reactions that involve abstraction of a proton from the 3-position are exceedingly facile compared to those of lactams and amides in general. In fact, it has been shown<sup>77</sup> that the C-3 hydrogen atoms of 1-methylindolin-2-one exchange on heating under reflux in mildly alkaline deuterium oxide. Further, the hydrogen exchange of 1,3-dimethylindolin-2-one has been shown to be subject to general base



catalysis<sup>78</sup> and the reported rate values show that it ionizes nearly 100 times faster than acetone and at least  $10^6$  times faster than a simple amide such as acetamide. This particular behaviour probably arises from the heteroaromatic structure of the enolate anion (Figure 1.2.2) obtained by the hydrogen abstraction<sup>63</sup>.

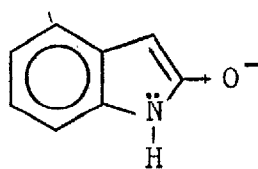
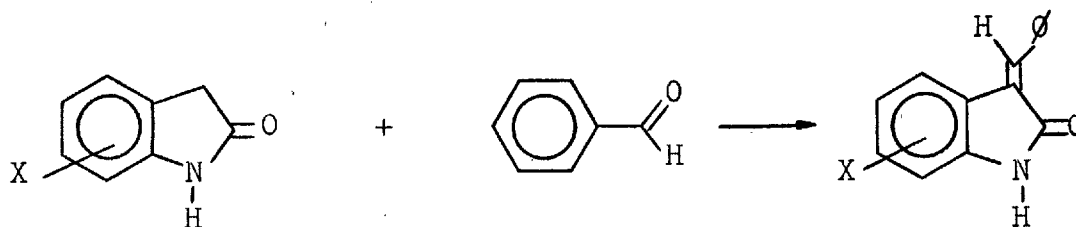


Figure 1.2.2

Although indolin-2-ones have been widely used as reagents<sup>63,79</sup> due to the extraordinary lability of the hydrogen atoms on the 3-position, little work has been done to quantify this aspect of their reactivity. Daisley and Walker<sup>80</sup> studied the condensation of benzaldehyde with various indolin-2-ones substituted at the 5-, 6- and 7-positions (Scheme 1.2.4), and found that electronwithdrawing groups meta to the methylene group facilitated proton loss from that site, hence increasing the rate of the reaction. Accordingly, the effect of a methoxy group on the 6-position (para to the methylene group) was reflected in a decrease in the rate of condensation. Gruda<sup>81</sup> examined the Michael addition of indolin-2-one and 1-methylindolin-2-one to methylvinylketone, and found that indolin-2-one reacted faster by a factor of ca.4.

The fact that indolin-2-ones easily exchange the hydrogen atoms on the 3-position suggests a close similarity between



Scheme 1.2.4

them and carbonyl compounds with respect to  $\alpha$ -hydrogen exchange. The mechanism of this exchange is well established both in acid<sup>22,82</sup> and in alkaline<sup>19,82</sup> media, and indolin-2-ones are expected to show acid and base-catalysed exchange by similar routes.

### 1.3. INDOLIN-2-ONES AS SUBSTRATES IN THE STUDY OF PROTON TRANSFER REACTIONS

Indolin-2-ones appear to be ideal models for the study of proton transfer reactions. They are stable relative to the acyclic aminoacid<sup>83,84,85</sup> and, therefore, their hydrolysis is not a problem under the reaction conditions. The rate of exchange can be conveniently measured by classical methods and can be varied by placing adequate substituents both on the ring and on the 1-position<sup>80,81</sup> without disturbing the steric neighbourhood of the reaction site. The study of

hydrogen exchange in these compounds may provide a better understanding on the remarkable differences observed in the magnitude of the PKIE for aliphatic<sup>5</sup> and heteroaromatic<sup>16</sup> hydrogen exchange. Also, by placing bulky groups on the 3- or 4-positions it may be possible to study the influence of steric hindrance on the conformational properties of the transition state for proton transfer reactions and the particular implications of those properties on the value of PKIE.

2. RESULTS AND DISCUSSION

2.1. MEASUREMENT OF pK

2.1.1. RESULTS

2.1.1.1. pK<sub>A</sub>

The ionization ratios of four indolin-2-ones at various pH in both sodium hydroxide solutions and in alkaline buffers are reported in Tables 2.1.1 to 2.1.6, together with the calculated values of the pK<sub>A</sub> for each experimental solution. pK<sub>A</sub> values were calculated according to Equation 2.1.1<sup>86</sup>

$$\text{pH} = \text{pK}_A - \log[\text{BH}^+]/[\text{B}] \quad (2.1.1)$$

where  $[\text{BH}^+]/[\text{B}] = \frac{[A - A_B]}{[A_{\text{H}_2\text{O}} - A]}$ . A is the absorbance of a given solution, A<sub>B</sub>- the absorbance of the anion and A<sub>H<sub>2</sub>O</sub> the absorbance of the neutral substrate measured in water. Average values of the pK<sub>A</sub> and their correlation with σ<sub>m</sub> are shown in Table 2.1.7 and Figure 2.1.1

Table 2.1.1 - Ionization ratios of indolin-2-one in aqueous sodium hydroxide solutions (1% EtOH) at 265 nm

10 <sup>2</sup> Experimental [OH <sup>-</sup> ]	Calculated pH	log[BH <sup>+</sup> ]/[B]	pK <sub>A</sub>
1.0	12.00	0.778	12.78
3.9	12.59	0.193	12.78
6.0	12.78	-0.037	12.74
8.0	12.90	-0.125	12.78
9.9	13.00	-0.246	12.75
19.9	13.30	-0.505	12.80
40.0	13.60	-0.813	12.79

Table 2.1.2 - Ionization ratios of 5-methoxyindolin-2-one in aqueous sodium hydroxide solutions (1% EtOH) at 265 nm

$10^2$ Experimental [OH <sup>-</sup> ]	Calculated pH	$\log[BH^+]/[B]$	pK <sub>A</sub>
1.05	12.02	0.556	12.58
2.95	12.47	0.192	12.66
3.90	12.59	0.076	12.66
4.80	12.68	0.000	12.68
5.90	12.77	-0.114	12.66
8.00	12.90	-0.232	12.67
9.90	13.00	-0.404	12.60

Table 2.1.3 - Ionization ratios of 5-bromoindolin-2-one in aqueous sodium hydroxide solutions (1% THF) at 268 nm

$10^2$ Experimental [OH <sup>-</sup> ]	Calculated pH	$\log[BH^+]/[B]$	pK <sub>A</sub>
0.4	11.60	0.539	12.14
1.0	12.00	0.121	12.12
2.0	12.30	-0.182	12.12
3.0	12.47	-0.347	12.12
3.9	12.59	-0.497	12.09
5.0	12.70	-0.630	12.07
7.1	12.85	-0.795	12.06

Table 2.1.4 - Ionization ratios of 5-bromoindolin-2-one in aqueous glycine buffers (1% THF) at 268 nm

Experimental pH	$\log[\text{BH}^+]/[\text{B}]$	$\text{pK}_A$
11.680	0.437	12.12
12.000	0.117	12.12
12.070	0.040	12.11
12.175	-0.094	12.08
12.225	-0.121	12.10
12.240	-0.176	12.06
12.270	-0.202	12.07
12.335	-0.261	12.07

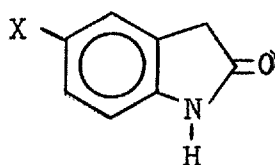
Table 2.1.5 - Ionization ratios of 5-nitroindolin-2-one in aqueous borax buffers (1% dioxan) at 329 nm

$\text{pH}^{87}$	$\log[\text{BH}^+]/[\text{B}]$	$\text{pK}_A$
11.00	0.176	11.18
11.10	0.082	11.18
11.30	-0.138	11.16
11.40	-0.215	11.19
11.50	-0.294	11.20
11.60	-0.424	11.18
11.70	-0.521	11.18

Table 2.1.6 - Ionization ratios of 5-nitroindolin-2-one in aqueous glycine buffers (1% dioxan) at 329 nm

Experimental pH	$\log[BH^+]/[B]$	$pK_A$
10.495	0.426	10.92
10.620	0.331	10.95
10.785	0.119	10.90
11.280	-0.286	10.95
11.435	-0.426	11.01
11.525	-0.531	10.99
11.605	-0.589	11.02

Table 2.1.7 - Correlation of  $pK_A$  with  $\sigma_m^{88}$



X	$pK_A$	$\sigma_m^{88}$
H	$12.77 \pm 0.03^*$	0
OCH <sub>3</sub>	$12.64 \pm 0.06^*$	0.115
Br	$12.10 \pm 0.04^*$ $12.09 \pm 0.03^{**}$	0.391
NO <sub>2</sub>	$11.18 \pm 0.02^\ddagger$ $10.96 \pm 0.06^{**}$	0.710

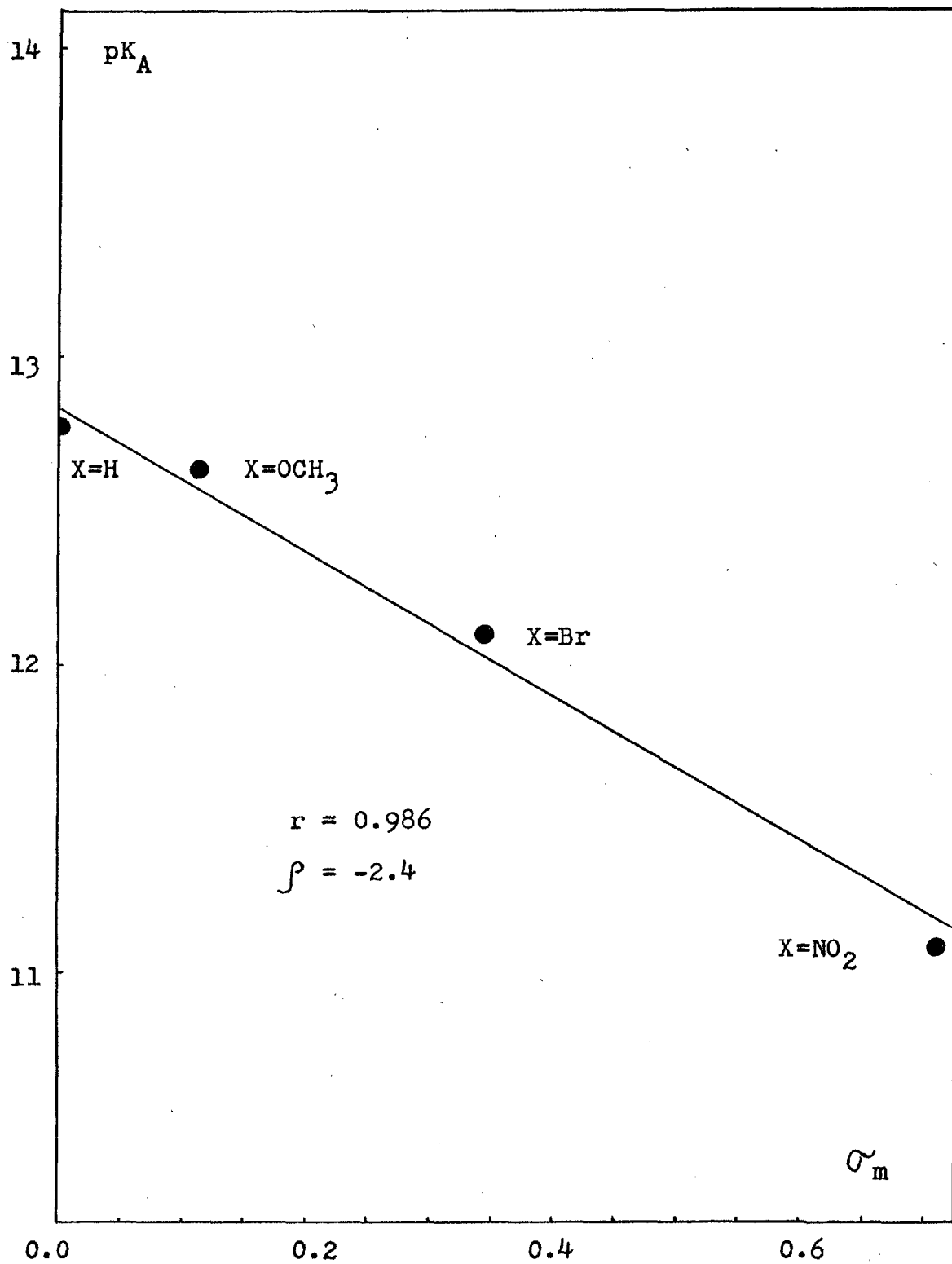
\* Measured in NaOH solutions

\*\* Measured in glycine buffers

‡ Measured in borax buffers



Figure 2.1.1 - Correlation of  $pK_A$  with  $\sigma_m$  for 5-X-indolin-2-ones



### 2.1.1.2. $pK_{BH^+}$

Spectroscopic details ( $\lambda_{max}$  and  $\epsilon$ ) of both neutral and protonated indolin-2-ones together with the acidity at which extinction coefficients of the free base and conjugate acid were measured are shown in Table 2.1.8. Ionization ratios of three indolin-2-ones in various sulphuric acid solutions are reported in Tables 2.1.9 to 2.1.11 together with the calculated values of  $pK_{BH^+}$  and the  $H_A$  acidity function<sup>89</sup> for each solution.

$pK_{BH^+}$  values were also calculated according to equation 2.1.1 where, for 5-nitroindolin-2-one  $[BH^+]/[B] = [A - A_B] / [A_{BH^+} - A]$  and for 5-methoxy and 5-bromoindolin-2-one  $[BH^+]/[B] = [A_B - A] / [A - A_{BH^+}]$ .  $A$  is the absorbance of a given solution,  $A_B$  the absorbance of the free base and  $A_{BH^+}$  the absorbance of the protonated species.

The gradients of the lines obtained by plotting  $\log[BH^+]/[B]$  vs.  $H_A$  are 1.05, 1.05 and 0.95 for 5-methoxyindolin-2-one, 5-bromoindolin-2-one and 5-nitroindolin-2-one respectively.

## 2.1.2. DISCUSSION

### 2.1.2.1. $pK_A$

Amides can lose a proton from the nitrogen atom and, therefore, behave as weak acids. Although the process is facilitated by the neighbouring carbonyl group, (Scheme 2.1.1) amides are still only relatively weak acids. Trihaloacetanilides appear to be the most acidic amides, with  $pK_A$ 's in

Table 2.1.8 - Absorption maxima and  $pK_{BH^+}$  values of 5-X-indolin-2-ones

X	$\lambda_B^{\max}$ (nm)	$\log \epsilon_B^{\max}$	$[H_2SO_4]$ M*	$\lambda_{BH^+}^{\max}$ (nm)	$\log \epsilon_{BH^+}^{\max}$	$[H_2SO_4]$ M**	$pK_{BH^+}$	slope
OCH <sub>3</sub>	255	4.06	0	268	3.87	10.95	$2.35 \pm 0.06$	1.05
Br	253	5.55	2.80	260	4.40	12.60	$2.69 \pm 0.08$	1.05
NO <sub>2</sub>	333	4.10	3.60	301	4.10	14.65	$3.24 \pm 0.07$	0.95

\* Solution used to determine the absorption of the free base

\*\* Solution used to determine the absorption of the conjugate acid

‡ Slope of  $\log[BH^+]/[B]$  against  $H_A$  determined by the least squares procedure

Table 2.1.9 - Ionization ratios of 5-methoxyindolin-2-one in aqueous sulphuric acid solutions (1% EtOH) at 255 nm

$-H_A^{89}$	$\log[BH^+]/[B]$	$-pK_{BH^+}$
1.20	-1.122	2.32
1.85	-0.487	2.34
1.95	-0.447	2.40
2.15	-0.170	2.29
2.35	0.015	2.34
2.50	0.107	2.39
2.65	0.336	2.31
2.90	0.530	2.37
3.20	0.853	2.35

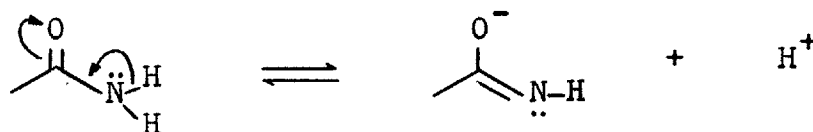
Table 2.1.10 - Ionization ratios of 5-bromoindolin-2-one in aqueous sulphuric acid solutions (1% THF) at 253 nm

$-H_A^{89}$	$\log[BH^+]/[B]$	$-pK_{BH^+}$
1.45	-1.166	2.62
1.85	-0.924	2.77
1.95	-0.757	2.71
2.15	-0.568	2.72
2.50	-0.130	2.63
2.65	-0.055	2.71
2.90	0.246	2.65
3.20	0.568	2.63
3.40	0.662	2.74

Table 2.1.11 - Ionization ratios of 5-nitroindolin-2-one in aqueous sulphuric acid solutions (1% dioxan) at 333 nm

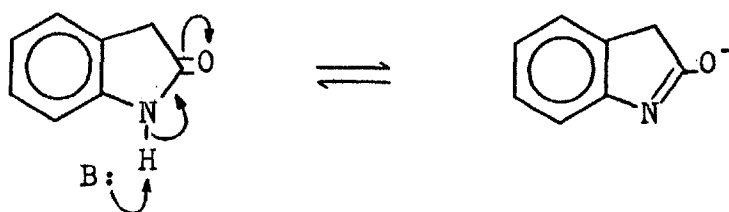
$-H_A^{89}$	$\log[BH^+]/[B]$	$-pK_{BH^+}$
1.85	-1.315	3.17
2.15	-1.079	3.23
2.35	-0.853	3.20
2.50	-0.691	3.19
2.65	-0.602	3.25
2.90	-0.417	3.31
3.40	0.121	3.28
3.60	0.352	3.25

the range  $9.5 - 10^{90}$ . Otherwise, amides usually have  $pK_A$  values higher than  $14^{90}$ . Phenylacetanilide has a  $pK_A$  of

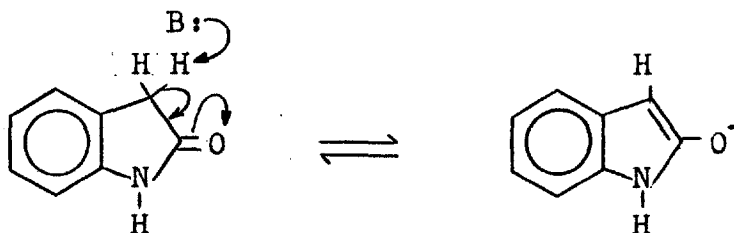


Scheme 2.1.1

$17.31^{90}$ . Substitution at nitrogen should decrease the acidity by a small factor, hence, indolin-2-ones would be expected to have  $pK_A$ 's in the range 17-18. However our measurements show that they are much more acidic. This is because, instead of behaving as weak nitrogen acids (Scheme 2.1.2), they resemble ketones with a labile  $\alpha$ -hydrogen atom, according to Scheme 2.1.3. This unexpected behaviour probably relates



Scheme 2.1.2



Scheme 2.1.3

to the structural properties of the resultant anion. The effect of 5-substituents on the acidity of indolin-2-ones is small as expected for an inductive effect between the 5- and the 3-positions. The observation that  $pK_A$  values correlate better with  $\sigma_m$  than with  $\sigma_p$  parameters supports our conclusion that N-H ionization does not occur. In fact, the  $pK_A$  of indolin-2-ones show that they are even more acidic than most ketones<sup>19</sup>.

#### 2.1.2.2. $pK_{BH^+}$

Although amides were included by Hammett<sup>91</sup> in the list of compounds completely protonated in 100%  $H_2SO_4$  and assumed to obey the  $H_0$  acidity function, Katritzky *et al.*<sup>92</sup> have shown that the slopes of their  $\log[BH^+]/[B]$  against  $H_0$  were far from unity, as required by Equation 2.1.2<sup>91</sup>, where

$$H_0 = -\log(a_{H^+} f_B / f_{BH^+}) = pK_{BH^+} - \log[BH^+]/[B] \quad (2.1.2)$$

$K_{BH^+} = a_{H^+} a_B / a_{BH^+}$  is the thermodynamic equilibrium constant defined in terms of molar activities. Yates et al.<sup>89</sup> investigated the ionization behaviour of a series of primary amides and established a new acidity function,  $H_A$ . The  $\log[BH^+]/[B]$  values of the three indolin-2-ones plotted vs. the  $H_0$  acidity function generate straight lines of non-unit slope ( ca. 0.40 - 0.55). However, when  $H_A$  acidity function is used, the slopes are all nearer unity. It is difficult to choose the appropriate optical densities corresponding to zero and complete ionization because solvent shifts usually occur for both the ionized and non-ionized forms, but particularly for the latter<sup>91</sup>. In the case of indolin-2-ones, if the values for the absorbance of the ionized and non-ionized forms are assumed to be the absorbance measured in concentrated  $H_2SO_4$  and in water respectively, the slope of  $\log[BH^+]/[B]$  vs.  $H_A$  is 0.95 for 5-methoxyindolin-2-one, 0.80 for 5-nitroindolin-2-one and 0.65 for 5-bromoindolin-2-one. Solvent shifts are noticeable for indolin-2-ones, as shown in Figures 2.1.2 and 2.1.3, by the lack of well defined isosbestic points. When measuring the  $H_A$  acidity function, Yates et al.<sup>89</sup> used the method indicated by Stewart and Granger<sup>93</sup>, whereby the solvent shifts were corrected by choosing  $A_B$  and  $A_{BH^+}$  values from solutions approximately 1.5  $H_0$  units in either direction from the rough estimate of the  $pK_{BH^+}$ . Using the same method for indolin-2-ones, the slopes of the ionization curves become 1.05, 1.05 and 0.95 for 5-methoxyindolin-2-one, 5-bromoindolin-2-one

Figure 2.1.2 - Variation of the UV spectrum of 5-methoxyindolin-2-one with acidity ( $H_2SO_4$ )

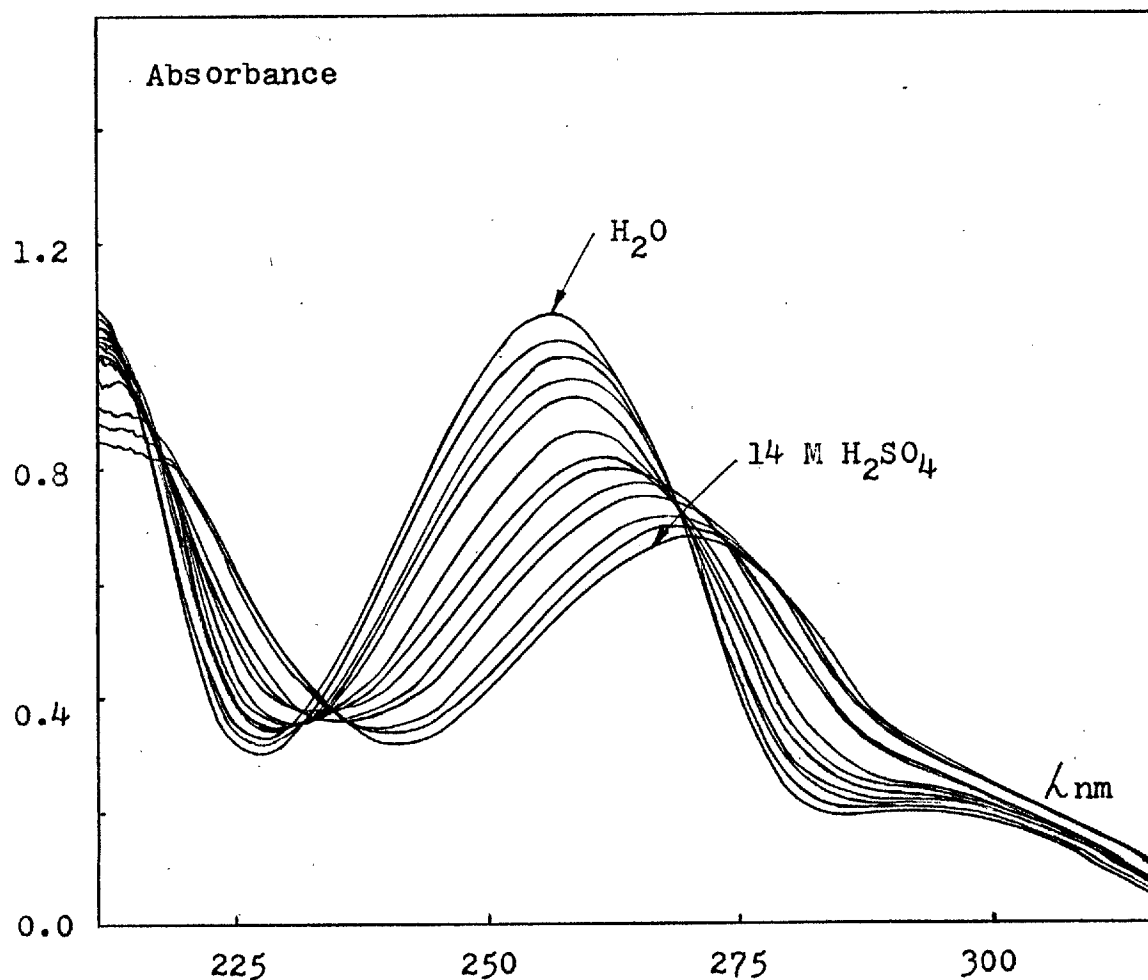
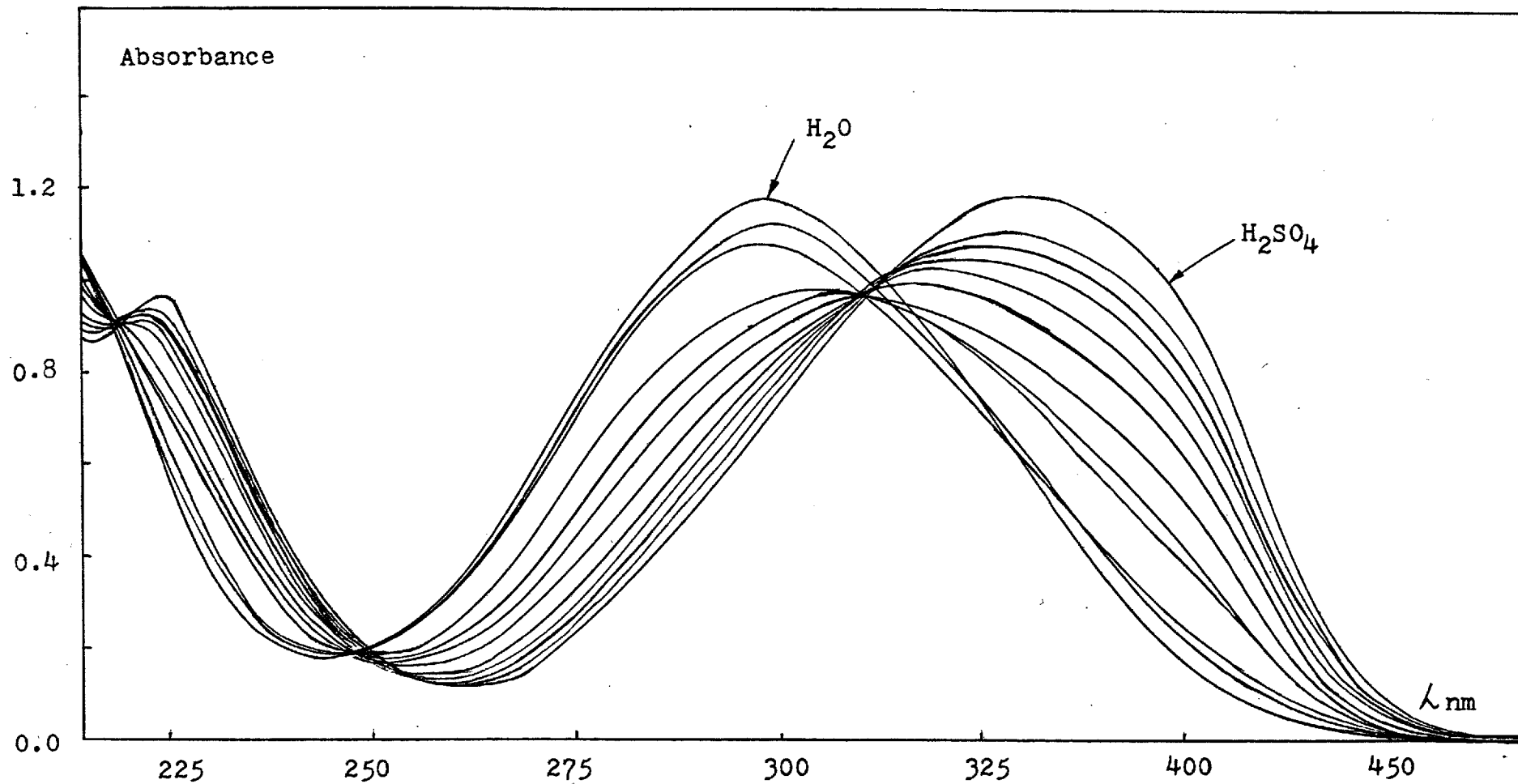




Figure 2.1.3 - Variation of the UV spectrum of 5-nitroindolin-2-one with acidity ( $H_2SO_4$ )



and 5-nitroindolin-2-one respectively, and the  $pK_{BH^+}$  values increase by ca. 0.2 pK units for all of them (Figure 2.1.4).

It was not possible to measure the  $pK_{BH^+}$  of indolin-2-one in sulphuric acid because at high acidities sulphonation becomes important and  $A_{BH^+}$  is uncertain. In aqueous perchloric acid the difference between the extinction coefficients of the free base and of the conjugate acid is too small to allow the measurement to be made by spectrophotometry. The  $pK_{BH^+}$  of indolin-2-one has been measured by Huisgen et al.<sup>94</sup> in mixtures of acetic acid/perchloric acid. Using the  $H_0$  acidity function they found a value of -2.36. Since indolin-2-ones do not follow the  $H_0$  acidity function this value is probably slightly high. Using the  $pK_{BH^+}$  of 5-nitro, 5-bromo and 5-methoxyindolin-2-one and the corresponding  $\sigma_m$  parameters, the  $pK_{BH^+}$  of indolin-2-one can be calculated as shown in Figure 2.1.5. This calculated  $pK_{BH^+}$  (-2.18) agrees with the experimental value reported by Huisgen within 0.2 pK units. Considering that he used a different experimental method and a different acidity function, the agreement is reasonable.

The correlation of the  $pK_{BH^+}$  with  $\sigma_m$  will be discussed in Section 2.2.2.2-B

Figure 2.1.4 - Correlation of ionization ratios of 5-X-indolin-2-ones with  $H_A$  ( $H_2SO_4$ ) acidity function

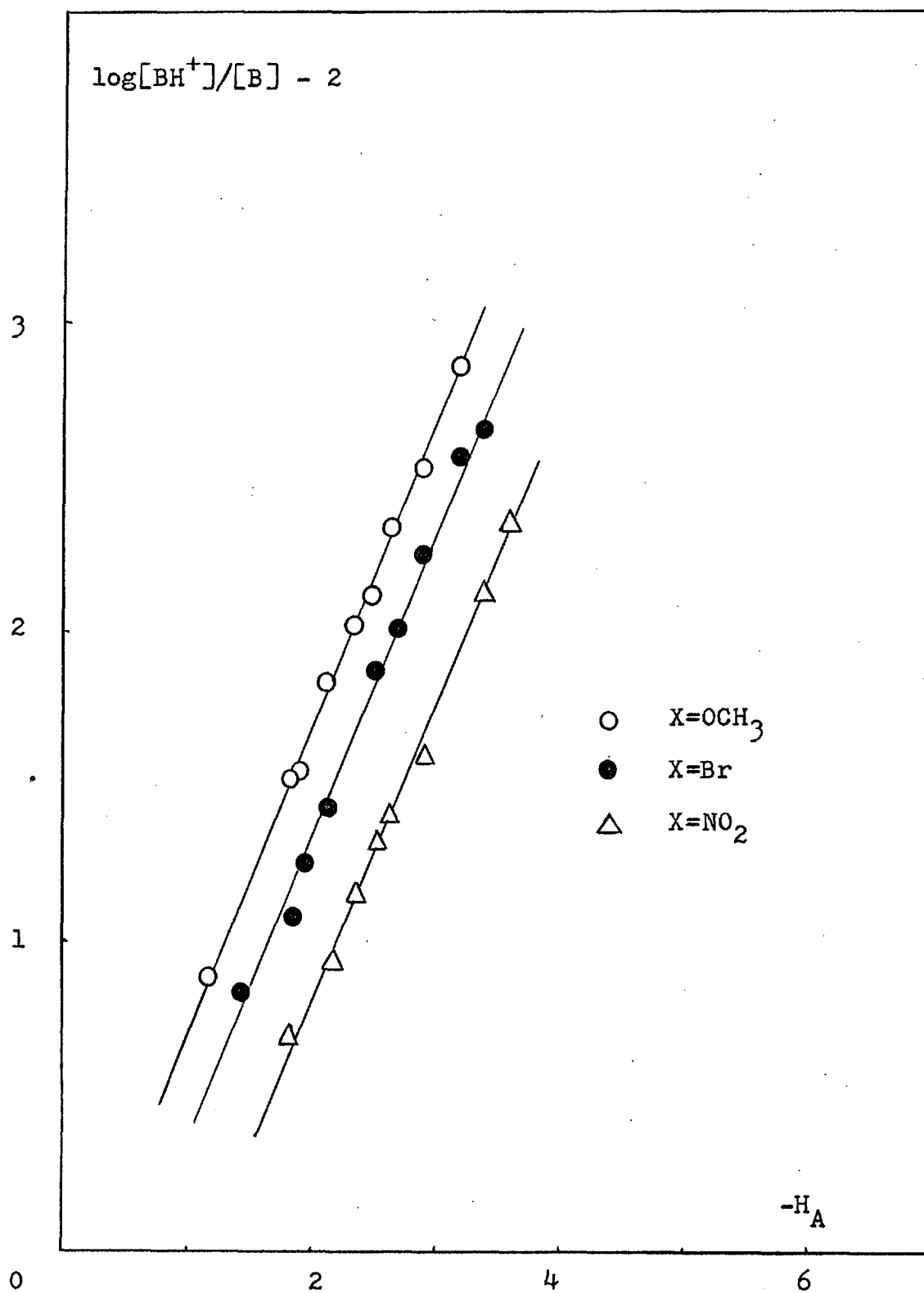
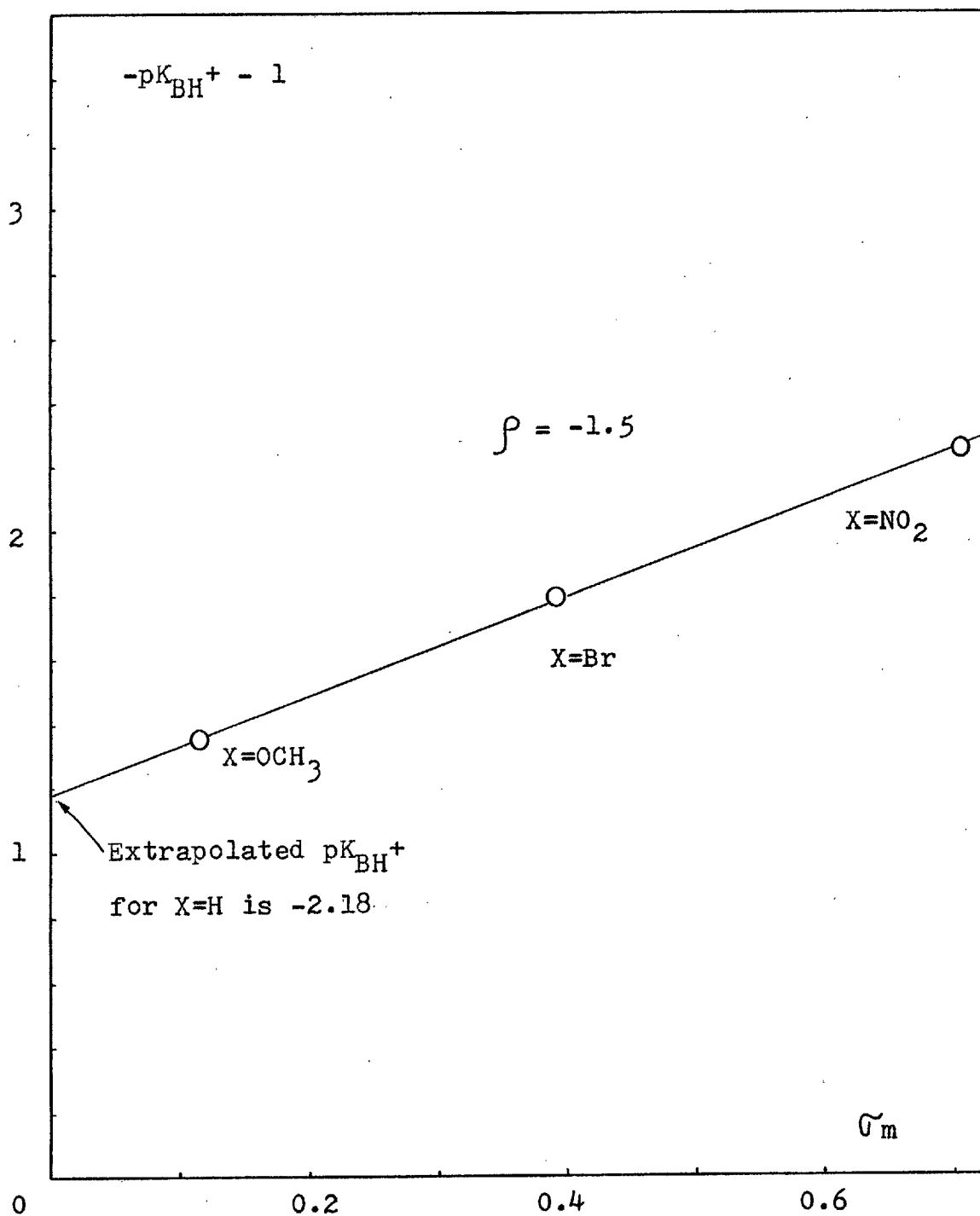


Figure 2.1.5 - Correlation of  $pK_{BH^+}$  of 5-X-indolin-2-ones with  $\sigma_m$



## 2.2. HYDROGEN EXCHANGE OF INDOLIN-2-ONES

Previous work<sup>78,95</sup> demonstrated that the hydrogen exchange of indolin-2-ones occurred readily in aqueous borax solutions at pH 8-10. Steric effects and electronic effects were partially established, as well as PKIE. The purpose of the present work was to extend that study to a wider range of substrates and catalysts in alkaline media as well as in acidic media and to measure Brønsted exponents and PKIE.

Electronic effects and steric effects were established by measuring rates of protodetrition for three main reasons: (i) Small incorporation of tritium is enough to be accurately measured (ii) Small concentrations of substrate can be used (iii) The results are reliable to approximately 1% error. The detrition was followed by the method which is indicated in Section 3.4.1.

### 2.2.1. RESULTS

#### 2.2.1.1. Protodetrition in alkaline media

The protodetrition was examined in aqueous buffer solutions. The exchange reaction followed Equation 2.2.1

$$\text{Rate} = k_0 [\text{3-L-indolin-2-one}] \quad (2.2.1)$$

and good first order kinetics were observed for at least 95% reaction. Values of  $k_0$  were found to depend both on the pH of the reaction solution and on the concentration of buffer base as well as on the nature of the substituent present on

the 5-position. Evidence for these effects is given in Tables 2.2.1 and 2.2.2. Plots of this data for reactions at constant pH and at varying pH with constant [Morpholine] are shown in Figures 2.2.1 and 2.2.2 respectively, for the four indolin-2-ones studied.

The study of the protodetrition of 5-nitro-3- $^{3}\text{H}_1$ -indolin-2-one was extended to bases other than morpholine. The data for several buffers is given in Tables 2.2.3 to 2.2.11. Measurement of  $k_0$  in acetate and pyridine buffers at different buffer ratios shows no evidence of general acid catalysis for the exchange reaction. The data supporting this conclusion is shown in Tables 2.2.8 to 2.2.11 and Figures 2.2.3 and 2.2.4.

These results clearly imply that the reaction is subject to general base catalysis, and that the full rate equation for the protodetrition can be written under the form of Equation 2.2.2. On basis of Equation 2.2.2 and 2.2.1 the

$$\text{Rate} = [\text{Sub}] \left\{ k_1^{\text{OH}^-} [\text{OH}^-] + k_1^{\text{Base}} [\text{Base}] \right\} \quad (2.2.2)$$

general relationship between  $k_0$  and the and the catalytic rate coefficients ( $k_1$ ) is given by Equation 2.2.3.

$$k_0 = k_1^{\text{OH}^-} [\text{OH}^-] + \sum_{0,i} k_1^{\text{Base}_i} [\text{Base}_i] \quad (2.2.3)$$

Table 2.2.1 - Protodetrition of 5-X-3-[<sup>3</sup>H<sub>1</sub>]-indolin-2-ones in morpholine buffers at constant pH

[Cl<sup>-</sup>] = 0.018 M, μ = 0.018 M, Buffer ratio 2:7

10 <sup>3</sup> [Morpholine]/ mol l <sup>-1</sup>	Experimental pH	10 <sup>4</sup> k <sub>o</sub> <sup>-T</sup> /s <sup>-1</sup>			
		X=H	X=OCH <sub>3</sub>	X=Br	X=NO <sub>2</sub>
7.77	9.080	6.12	9.25	24.3	91.1
3.84	9.070	3.09	4.78	12.2	48.5
1.94	9.030	1.44	2.40	6.67	26.7
0.78	9.030	0.60	-	1.86	11.6

Table 2.2.2 - Protodetrition of 5-X-3-[<sup>3</sup>H<sub>1</sub>]-indolin-2-ones in morpholine buffers at varying pH

[Morpholine] = 5 × 10<sup>-3</sup>M, [Cl<sup>-</sup>] = 0.018 M, μ = 0.018

10 <sup>6</sup> [OH <sup>-</sup> ]/mol l <sup>-1</sup>	Experimental pH	10 <sup>4</sup> k <sub>o</sub> <sup>-T</sup> /s <sup>-1</sup>			
		X=H	X=OCH <sub>3</sub>	X=Br	X=NO <sub>2</sub>
16.00	9.205	3.75	6.18	16.2	64.4
8.22	8.915	3.54	5.89	15.2	58.8
5.49	8.740	3.46	5.62	14.7	56.9
3.31	8.520	-	5.45	-	55.4
1.48	8.170	3.29	5.33	14.2	-

Figure 2.2.1 - Protodetritiation of 5-X-3- $^{3}\text{H}_1$ -indolin-2-one  
in morpholine buffers at constant pH  
[Cl $^{-}$ ]=0.018 M, Buffer ratio 2:7

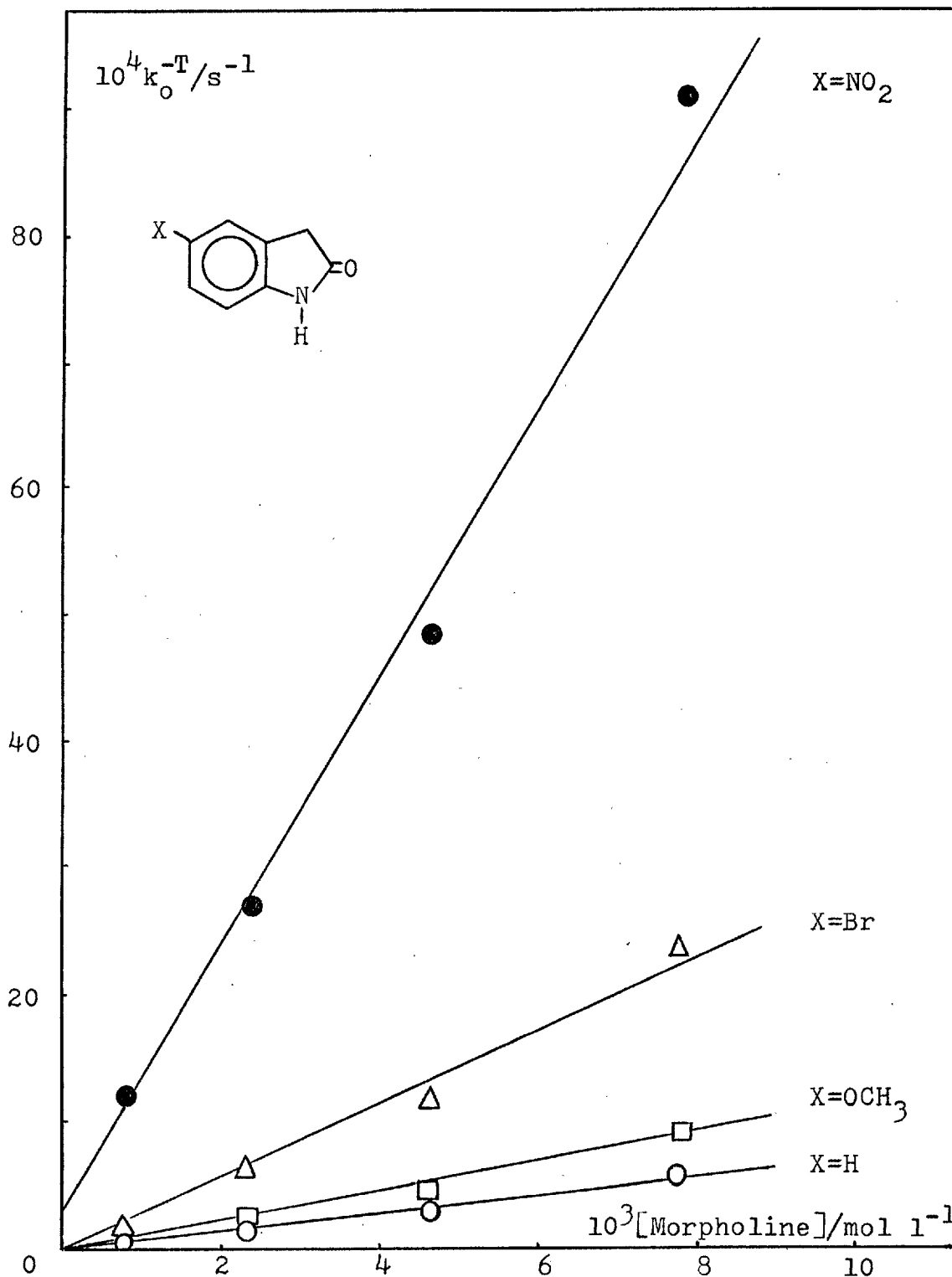




Figure 2.2.2 - Protodetritiation of 5-X-3- $^{3}\text{H}_1$ -indolin-2-ones in morpholine buffers at varying pH

$[\text{Morpholine}] = 5 \times 10^{-3}\text{M}$ ,  $[\text{Cl}^{-}] = 0.018\text{ M}$

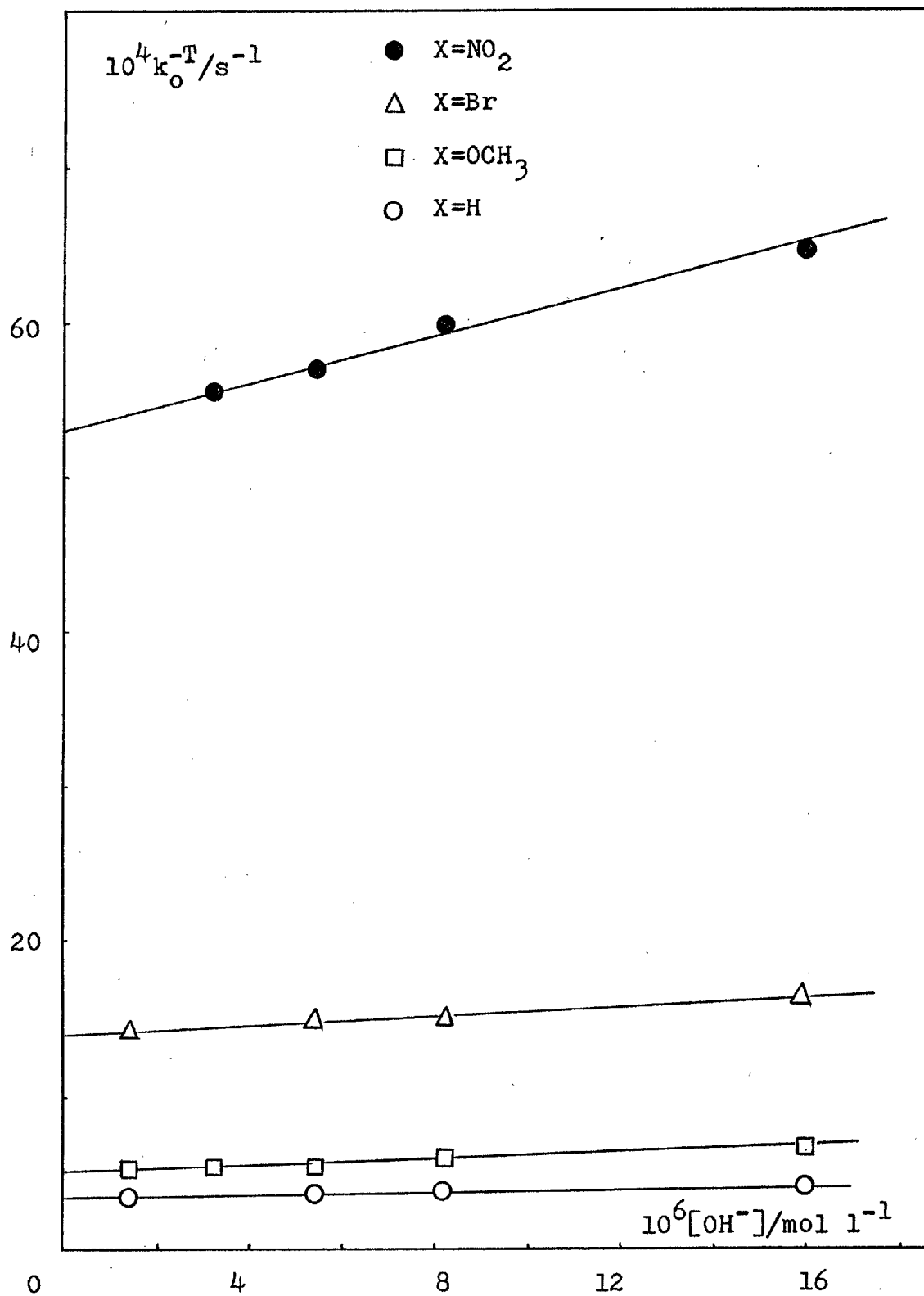


Table 2.2.3 - Protodetritiation of 5-nitro-3- $^{3}\text{H}_1$ -indolin-2-one in phenol buffers

$\mu = 0.002 \text{ M}$ , Buffer ratio 6:1

$10^3[\text{ArO}^-]/\text{mol l}^{-1}$	Experimental pH	$10^4 k_0^{-T}/\text{s}^{-1}$
0.2	9.010	9.27
0.5	9.125	19.0
1.0	9.160	36.9
2.0	9.170	77.5

Table 2.2.4 - Protodetritiation of 5-nitro-3- $^{3}\text{H}_1$ -indolin-2-one in 4-chlorophenol buffers

$\mu = 0.002 \text{ M}$ , Buffer ratio 5:1

$10^3[\text{ArO}^-]/\text{mol l}^{-1}$	Experimental pH	$10^4 k_0^{-T}/\text{s}^{-1}$
0.2	8.620	7.90
0.5	8.650	13.8
1.0	8.675	27.9
2.0	8.685	52.1

Table 2.2.5 - Protodetrition of 5-nitro-3- $[^3\text{H}]$ -indolin-2-one in 4-nitrophenol buffers

$\mu = 0.02 \text{ M}$ , Buffer ratio 1:2

$10^3[\text{ArO}^-]/\text{mol l}^{-1}$	Experimental pH	$10^4 k_{\text{O}}^{-\text{T}}/\text{s}^{-1}$
2	7.365	2.40
5	7.365	5.79
10	7.395	11.2
20	7.415	21.5

Table 2.2.6 - Protodetrition of 5-nitro-3- $[^3\text{H}]$ -indolin-2-one in methylimidazole buffers

$[\text{Cl}^-] = 0.018 \text{ M}$ ,  $\mu = 0.018 \text{ M}$ , Buffer ratio 1:4

$10^3[\text{MeImid.}]/\text{mol l}^{-1}$	Experimental pH	$10^4 k_{\text{O}}^{-\text{T}}/\text{s}^{-1}$
1	7.685	0.48
4	7.700	1.03
8	7.715	1.79
16	7.715	3.15

Table 2.2.7 - Protodetrition of 5-nitro-3-[<sup>3</sup>H<sub>1</sub>]-indolin-2-one in imidazole buffers

[Cl<sup>-</sup>] = 0.05, μ = 0.05, Buffer ratio 1:2

$10^2[\text{Imid.}]/\text{mol l}^{-1}$	Experimental pH	$10^4 k_0^{-T}/\text{s}^{-1}$
10.0	7.415	18.6
7.5	7.415	13.9
5.0	7.420	9.70
1.0	7.420	2.11

Table 2.2.8 - Protodetrition of 5-nitro-3-[<sup>3</sup>H<sub>1</sub>]-indolin-2-one in pyridine buffers at pH 6.08

[Cl<sup>-</sup>] = 0.02 M, μ = 0.02 M, Buffer ratio 1:5

$10^2[\text{Pyrid.}]/\text{mol l}^{-1}$	Experimental pH	$10^4 k_0^{-T}/\text{s}^{-1}$
10.0	6.080	11.1
7.5	6.085	8.20
5.0	6.080	5.50
1.0	6.080	1.15

Table 2.2.9 - Protodetrition of 5-nitro-3-[<sup>3</sup>H<sub>1</sub>]-indolin-2-one in pyridine buffers at pH 6.36

[Cl<sup>-</sup>] = 0.02 M, μ = 0.02 M, Buffer ratio 1:10

$10^2[\text{Pyrid.}]/\text{mol l}^{-1}$	Experimental pH	$10^4 k_0^{-T}/\text{s}^{-1}$
10.0	6.355	11.2
7.5	6.365	8.40
5.0	6.355	5.24

Table 2.2.10 - Protodetrition of 5-nitro-3- $[^3\text{H}]$ -indolin-2-one in acetate buffers at pH 3.83

$\mu = 0.1 \text{ M}$ , Buffer ratio 6:1

$10^2[\text{CH}_3\text{COO}^-]/\text{mol l}^{-1}$	Experimental pH	$10^4 k_0^{-T}/\text{s}^{-1}$
10.0	3.850	1.30
7.5	3.840	0.99
5.0	3.830	0.65
1.0	3.805	0.17

Table 2.2.11 - Protodetrition of 5-nitro-3- $[^3\text{H}]$ -indolin-2-one in acetate buffers at pH 5.33

$\mu = 0.1 \text{ M}$ , Buffer ratio 1:5

$10^2[\text{CH}_3\text{COO}^-]/\text{mol l}^{-1}$	Experimental pH	$10^4 k_0^{-T}/\text{s}^{-1}$
10.0	5.345	1.33
7.5	5.335	1.00
5.0	5.325	0.65
1.0	5.325	0.17

Figure 2.2.3 - Protodetritiation of 5-nitro-3-[<sup>3</sup>H<sub>1</sub>]-indolin-2-one in acetate buffers

$\mu=0.1$  M

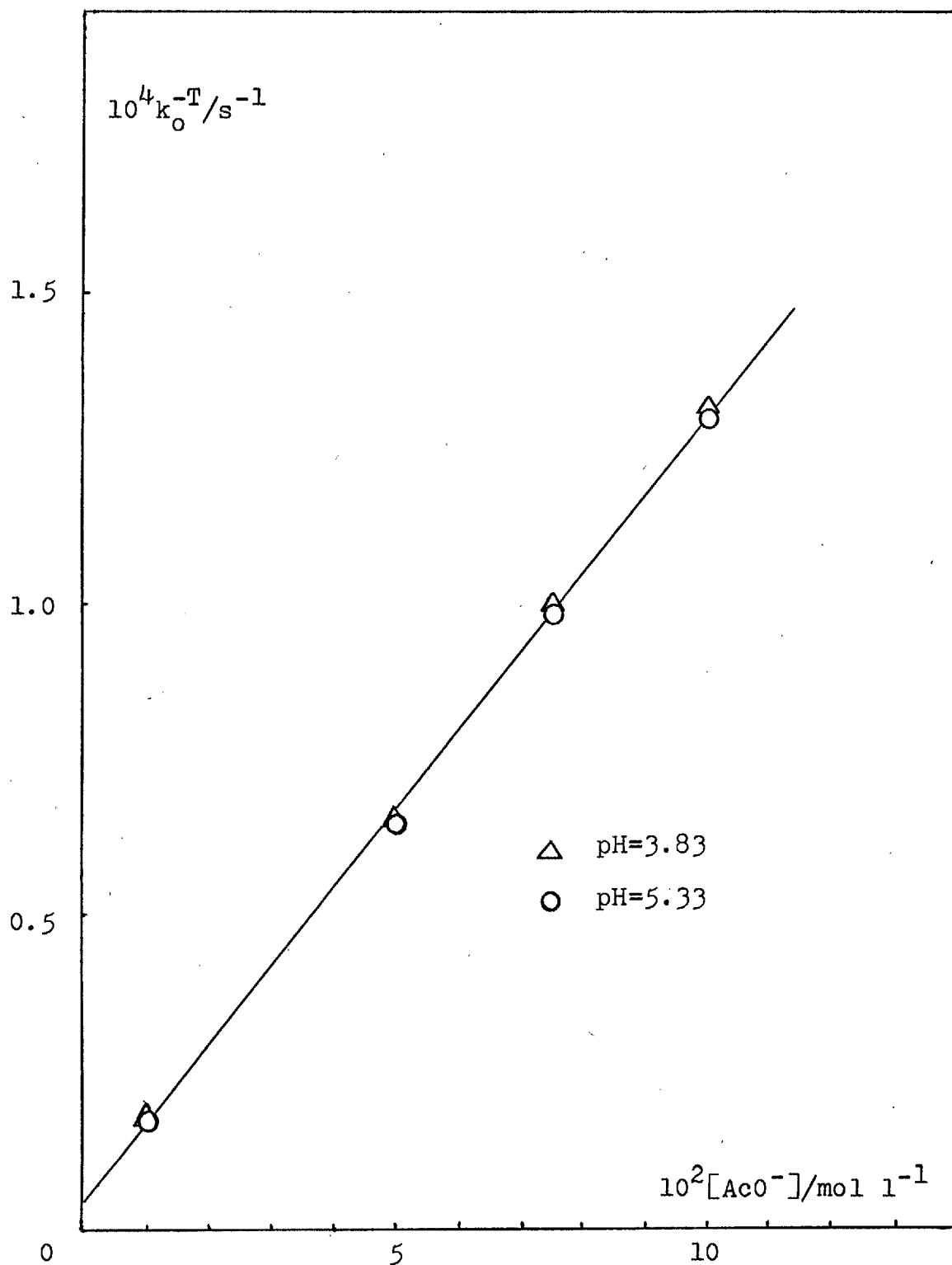
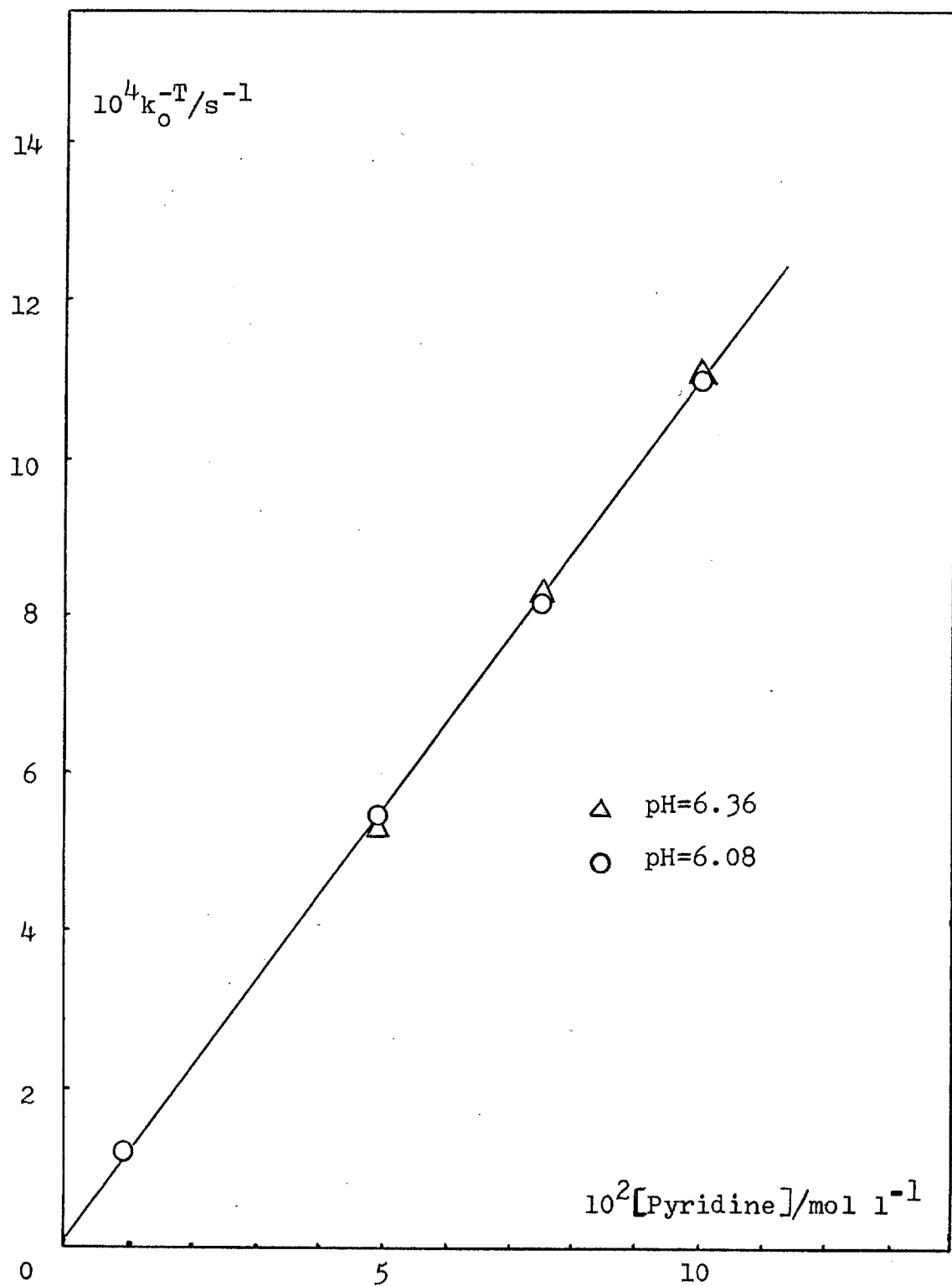


Figure 2.2.4 - Protodetritiation of 5-nitro-3- $[^3\text{H}]$ -indolin-2-one in pyridine buffers

$\mu=0.02 \text{ M}$



2.2.1.2. Protodetritiation in acidic media

It was found that the exchange also follows Equation 2.2.1 and that  $k_0$  depends on the solvent acidity. Results

$$\text{Rate} = k_0 [\text{3-L-indolin-2-one}] \quad (2.2.1)$$

are given in Table 2.2.12 for exchange of 3- $[\text{}^3\text{H}_1]$ -indolin-2-one in HCl and in Table 2.2.13 for exchange of 3- $[\text{}^3\text{H}_1]$ -indolin-2-one, 5-methoxy-3- $[\text{}^3\text{H}_1]$ -indolin-2-one, 5-bromo-3- $[\text{}^3\text{H}_1]$ -indolin-2-one and 5-nitro-3- $[\text{}^3\text{H}_1]$ -indolin-2-one in  $\text{H}_2\text{SO}_4$ . The values of  $k_0$  in  $\text{H}_2\text{SO}_4$  pass through a maximum (Figure 2.2.5). Before the rate maximum,  $k_0$  is linearly dependent on  $[\text{H}_2\text{SO}_4]$  and both the slope of the linear portions of the plots in Figure 2.2.5 and the acidity at which the maxima occur depend slightly on the substituents on the ring (Figure 2.2.5).

Table 2.2.12 - Protodetritiation of 3- $[\text{}^3\text{H}_1]$ -indolin-2-one in hydrochloric acid

$[\text{HCl}] \text{ M}$	$10^4 k_0^{-\text{T}} / \text{s}^{-1}$
0.1	0.042
1	0.46
2	0.96
3	1.37
4	1.90
5	2.21
10	3.07



The presence of methyl groups on the 1,3-positions and of bulky groups on the ring also affects the value of  $k_0$ . The results for the exchange of 1-methyl-3- $^{3}\text{H}_1$ -indolin-2-one, 1,3-dimethyl-3- $^{3}\text{H}_1$ -indolin-2-one, 1,3-dimethyl-5-nitro-3- $^{3}\text{H}_1$ -indolin-2-one, 4,6-di<sup>t</sup>butyl-3- $^{3}\text{H}_1$ -indolin-2-one and 1,3-dimethyl-4,6-di<sup>t</sup>butyl-3- $^{3}\text{H}_1$ -indolin-2-one in  $\text{H}_2\text{SO}_4$  are shown in Table 2.2.14. Since the exchange of 1,3-dimethyl-4,6-di<sup>t</sup>butyl-3- $^{3}\text{H}_1$ -indolin-2-one is very slow, rates in 5.20  $\text{H}_2\text{SO}_4$  M were determined by the differential method<sup>96</sup> (Table 2.2.15, Figure 2.2.6).

The exchange in  $\text{D}_2\text{O}$  is faster than in  $\text{H}_2\text{O}$  except at high acidities. Values of  $k_0^{\text{D}_2\text{O}}$  for the exchange of 3- $^{3}\text{H}_1$ -indolin-2-one in  $\text{D}_2\text{SO}_4/\text{D}_2\text{O}$  are reported in Table 2.2.16 and the variation of the ratio  $k_0^{\text{D}_2\text{O}}/k_0^{\text{H}_2\text{O}}$  with acidity, for the same compound, is shown in Figure 2.2.7.

The energy of activation and the entropy of activation for the exchange of 3- $^{3}\text{H}_1$ -indolin-2-one were determined by measuring  $k_0$  at three different temperatures at the same acidity. The results shown in Table 2.2.17 gave a value of 80.0  $\text{kJ mol}^{-1}$  for  $\Delta H^\ddagger$  and a value of 37.2  $\text{J K}^{-1} \text{mol}^{-1}$  (-8.9 e.u.) for  $\Delta S^\ddagger$ .

Table 2.2.13 - Protodetrition of 5-X-3-[<sup>3</sup>H<sub>1</sub>]-indolin-2-ones in sulphuric acid

	[H <sub>2</sub> SO <sub>4</sub> ] M	10 <sup>4</sup> k <sub>0</sub> <sup>-T</sup> /s <sup>-1</sup>
X=H	0.10	0.08
	0.48	0.35
	1.00	0.74
	1.82	1.49
	2.95	2.54
	3.90	2.87
	4.75	2.99
	5.90	2.97
	6.85	2.30
	7.95	1.53
	9.30	0.74
	10.00	0.43
	10.60	0.19
X=OCH <sub>3</sub>	0.10	0.13
	1.00	1.19
	1.50	1.64
	1.90	2.64
	3.00	3.84
	3.85	4.69
	4.40	4.96
	4.90	4.76
	5.20	4.39
	5.65	4.14
	6.10	3.78
	6.70	3.17
9.95	0.49	

Table 2.2.13 (cont.)

	$[\text{H}_2\text{SO}_4]$ M	$10^4 k_0^{-T}/\text{s}^{-1}$
X=Br	1.00	1.50
	1.90	3.17
	2.05	3.35
	2.85	3.81
	3.90	5.00
	4.85	6.44
	6.10	7.03
	7.85	4.49
	9.80	1.41
X=NO <sub>2</sub>	1.10	1.37
	2.00	2.51
	2.95	4.16
	5.40	7.61
	6.80	9.20
	7.60	9.00
	8.60	8.90
	10.70	7.10

Figure 2.2.5 - Protodetritiation of 5-X-3-[<sup>3</sup>H<sub>1</sub>]-indolin-2-one in sulphuric acid

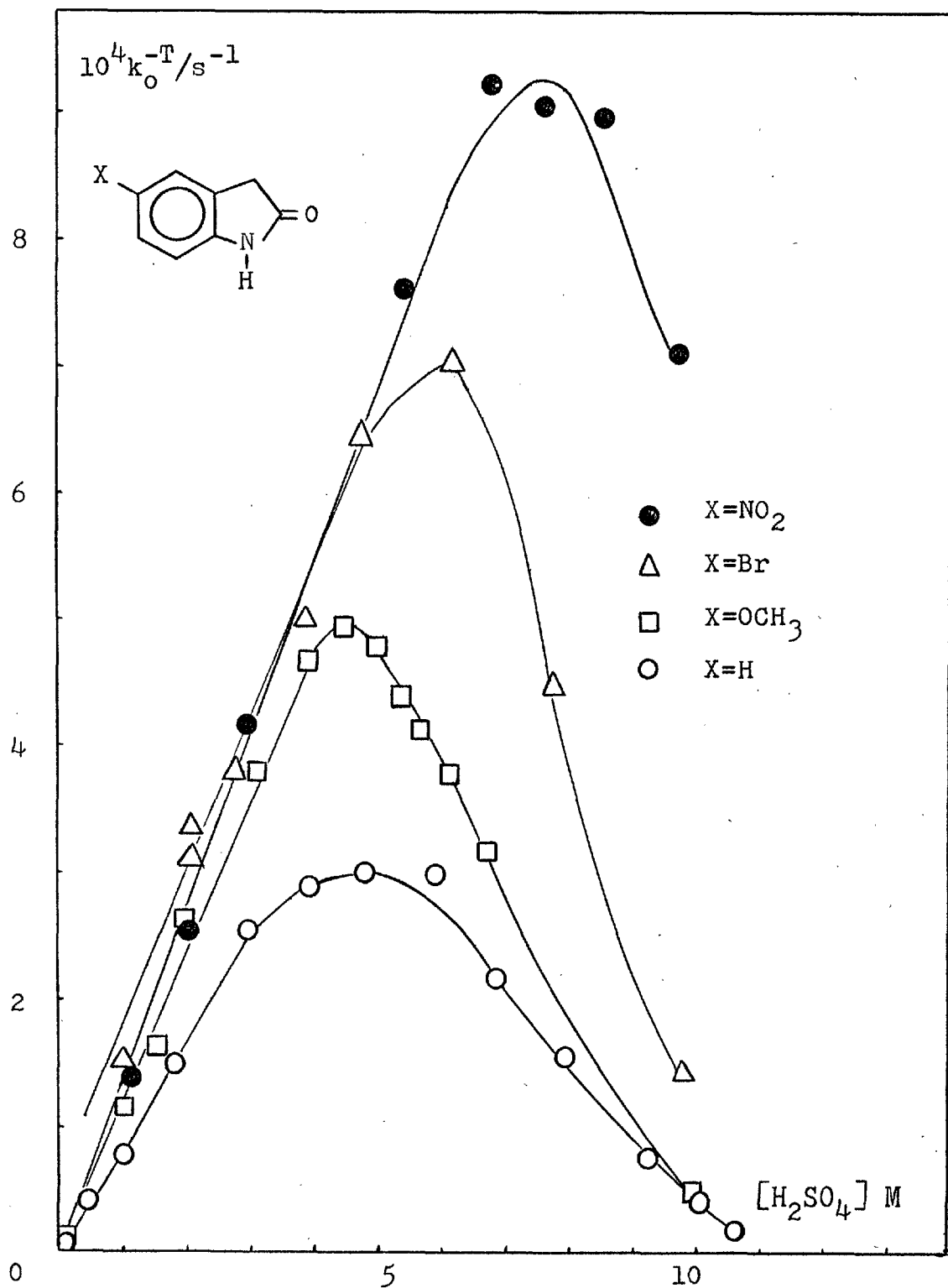
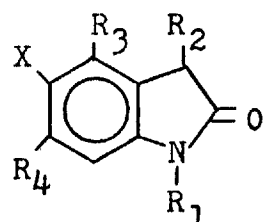


Table 2.2.14 - Protodetritiation of 3-[<sup>3</sup>H<sub>1</sub>]-indolin-2-ones substituted on the 1,3,5- and/or 4,6-positions, in sulphuric acid



	[H <sub>2</sub> SO <sub>4</sub> ] M	10 <sup>4</sup> k <sub>o</sub> <sup>-T</sup> /s <sup>-1</sup>
R <sub>1</sub> =CH <sub>3</sub>	0.95	0.22
R <sub>2</sub> =R <sub>3</sub> =X=R <sub>4</sub> =H	1.90	0.50
	2.95	0.80
	4.40	1.05
	4.90	1.09
	5.65	0.96
	6.70	0.71
<hr/>		
R <sub>1</sub> =R <sub>2</sub> =CH <sub>3</sub>	1.05	0.09
R <sub>2</sub> =X=R <sub>4</sub> =H	1.90	0.15
	3.90	0.47
	4.85	0.56
	5.85	0.58
	7.75	0.45
	8.70	0.27
<hr/>		
R <sub>1</sub> =R <sub>2</sub> =CH <sub>3</sub>	1.10	0.26
R <sub>3</sub> =R <sub>4</sub> =H	2.95	0.51
	5.30	1.20
X=NO <sub>2</sub>	7.05	1.81
	8.10	2.08
	8.90	2.17
	9.50	2.23
	11.65	1.34

Table 2.2.14 (cont.)

	$[\text{H}_2\text{SO}_4]$ M	$10^4 k_0^{-T}/\text{s}^{-1}$
$R_1=R_2=X=\text{H}$	1.05	0.66
$R_3=R_4=\text{}^t\text{Bu}$	2.95	1.90
	4.85	2.33
	5.65	2.22
	6.90	1.40
	7.80	0.99
	9.75	0.20
$R_1=R_2=\text{CH}_3$ $X=\text{H}$ $R_3=R_4=\text{}^t\text{Bu}$	5.20	0.006

Table 2.2.15 - Protodetrition of 1,3-dimethyl-4,6-di<sup>t</sup>butyl-3-[<sup>3</sup>H<sub>1</sub>]-indolin-2-one in 5.20 M sulphuric acid

$10^3$ Initial rate/cpm s <sup>-1</sup>	Initial activity/cpm
8.50	13,150
7.51	11,875
6.77	10,475
6.03	9,135

$$k_o^{-T} = 0.006 \quad 10^{-4} \text{ s}^{-1}$$

Figure 2.2.6 - Protodetrition of 1,3-dimethyl-4,6-di<sup>t</sup>butyl-3-[<sup>3</sup>H<sub>1</sub>]-indolin-2-one in 5.20 M sulphuric acid

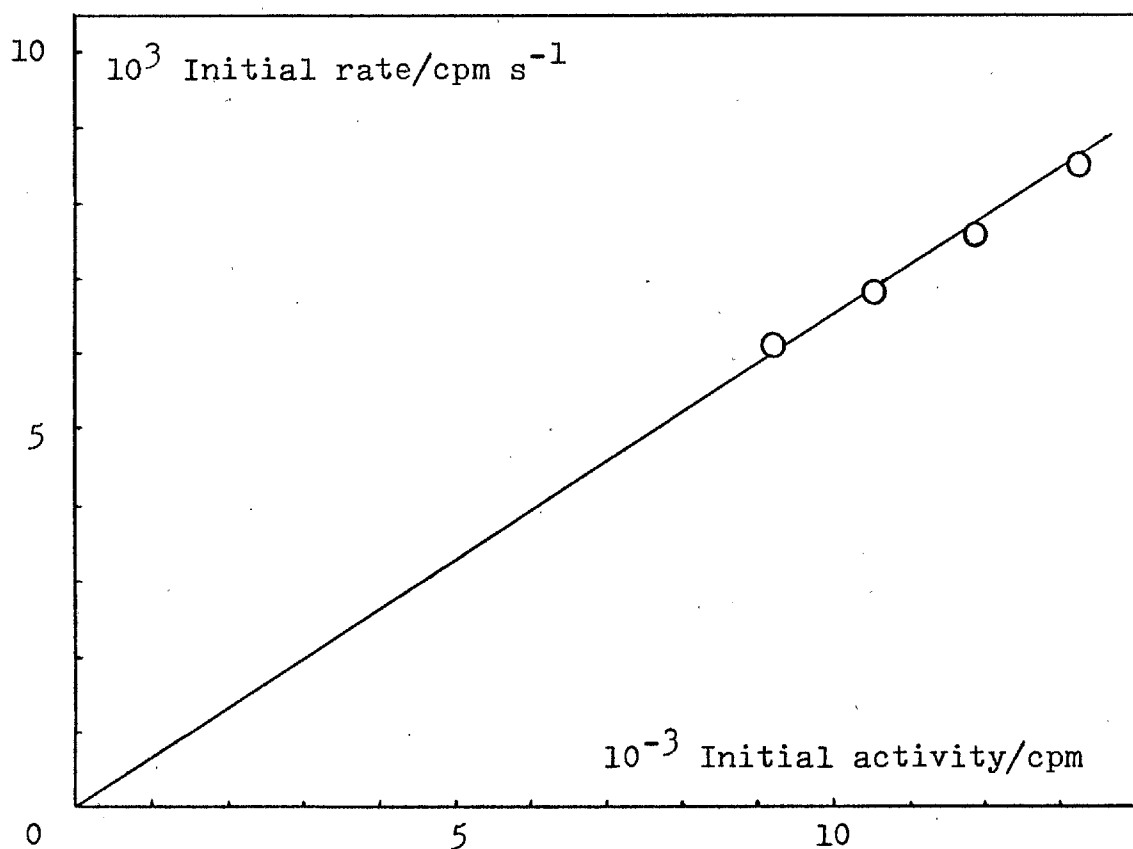


Table 2.2.16 - Deuterodetritionation of 3-[<sup>3</sup>H<sub>1</sub>]-indolin-2-one in deuteriated sulphuric acid

$[D_2SO_4]$ M	$10^4 k_o^{-T}/s^{-1}$
0.11	0.10
0.50	0.46
1.00	1.00
2.05	1.90
3.00	3.02
3.90	3.90
4.95	4.41
6.50	3.71
6.95	2.80
7.90	1.70
9.10	0.78
10.10	0.37

Figure 2.2.7 - Comparison of protodetritionation and deuterodetritionation of 3-[<sup>3</sup>H<sub>1</sub>]-indolin-2-one in H<sub>2</sub>SO<sub>4</sub>/H<sub>2</sub>O and D<sub>2</sub>SO<sub>4</sub>/D<sub>2</sub>O

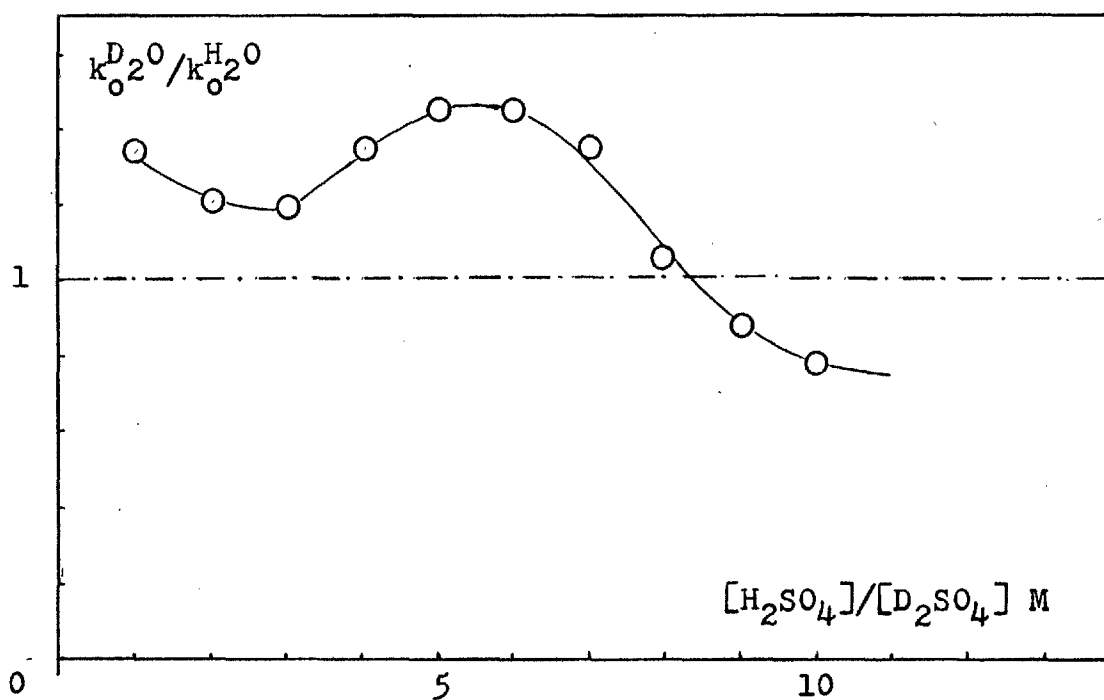




Table 2.2.17 - Temperature dependence of the protodetritiation of 3-[<sup>3</sup>H<sub>1</sub>]-indolin-2-one in 2.45 M sulphuric acid

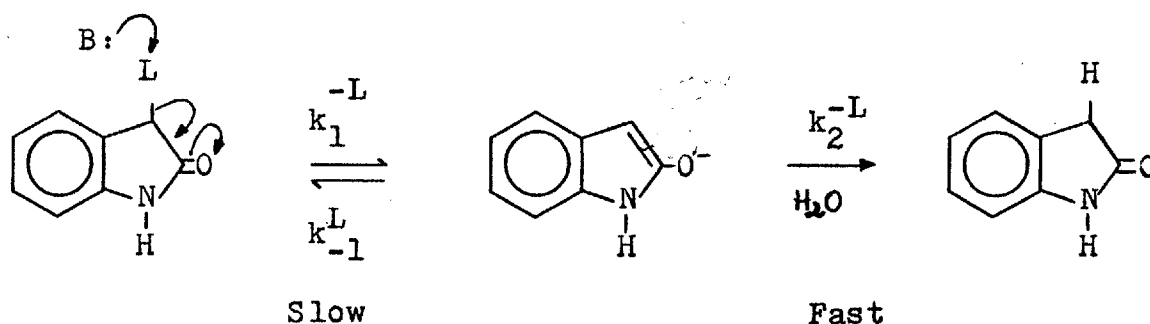
Temperature/°K	$10^4 k_o^{-T}/s^{-1}$
273	0.12
298	1.66
313	8.60

## 2.2.2. DISCUSSION

### 2.2.2.1. Protodetritiation in alkaline media

#### A - General mechanism

The results obtained for the detritiation of indolin-2-ones in alkaline media imply that, as shown before<sup>78,95</sup> and similarly to carbonyl compounds<sup>82</sup>, the exchange reaction must proceed according to Scheme 2.2.1, where B: is any base present in the reaction solution. The steady state treatment



Scheme 2.2.1

applied to this mechanism gives Equation 2.2.4. As the concentration of the labelled substrate is very small, the

$$-d[L]/dt = \frac{k_1^{-L} [B:] [3-L-indolin-2-one]}{1 + k_{-1}^L/k_2^H} \quad (2.2.4)$$

the internal reprotonation ( $k_{-1}^L$ ) is negligible and, therefore, Equation 2.2.4 reduces to Equation 2.2.5 when [B:] is

$$\begin{aligned} -d[L]/dt &= k_1^{-L} [B:] [3-L-indolin-2-one] \\ &= k_0^{-L} [3-L-indolin-2-one] \end{aligned} \quad (2.2.5)$$

$$\therefore k_0^{-L} = k_1^{-L} [B:] \quad (2.2.6)$$

maintained constant. Equation 2.2.6 agrees with Equation 2.2.3 directly deduced from the experimental results.

#### B- Effect of 5-substituents on the rate of exchange

The dependence of  $k_1$  on the 5-substituent is shown both for hydroxide and morpholine in Table 2.2.18.  $k_1^{OH^-}$  and  $k_1^{Morph}$  were derived from the data shown in Tables 2.2.1 and 2.2.2 by calculating the slopes of plots of  $k_0$  against  $[OH^-]$  at constant [Morpholine] and against [Morpholine] at constant pH, respectively.  $k_1^{Morph}$  calculated from the intercepts of the lines in Figure 2.2.2 agree with these within <10%.

Table 2.2.18 and Figures 2.2.1 and 2.2.2 clearly show that the order of reactivity towards hydrogen exchange is

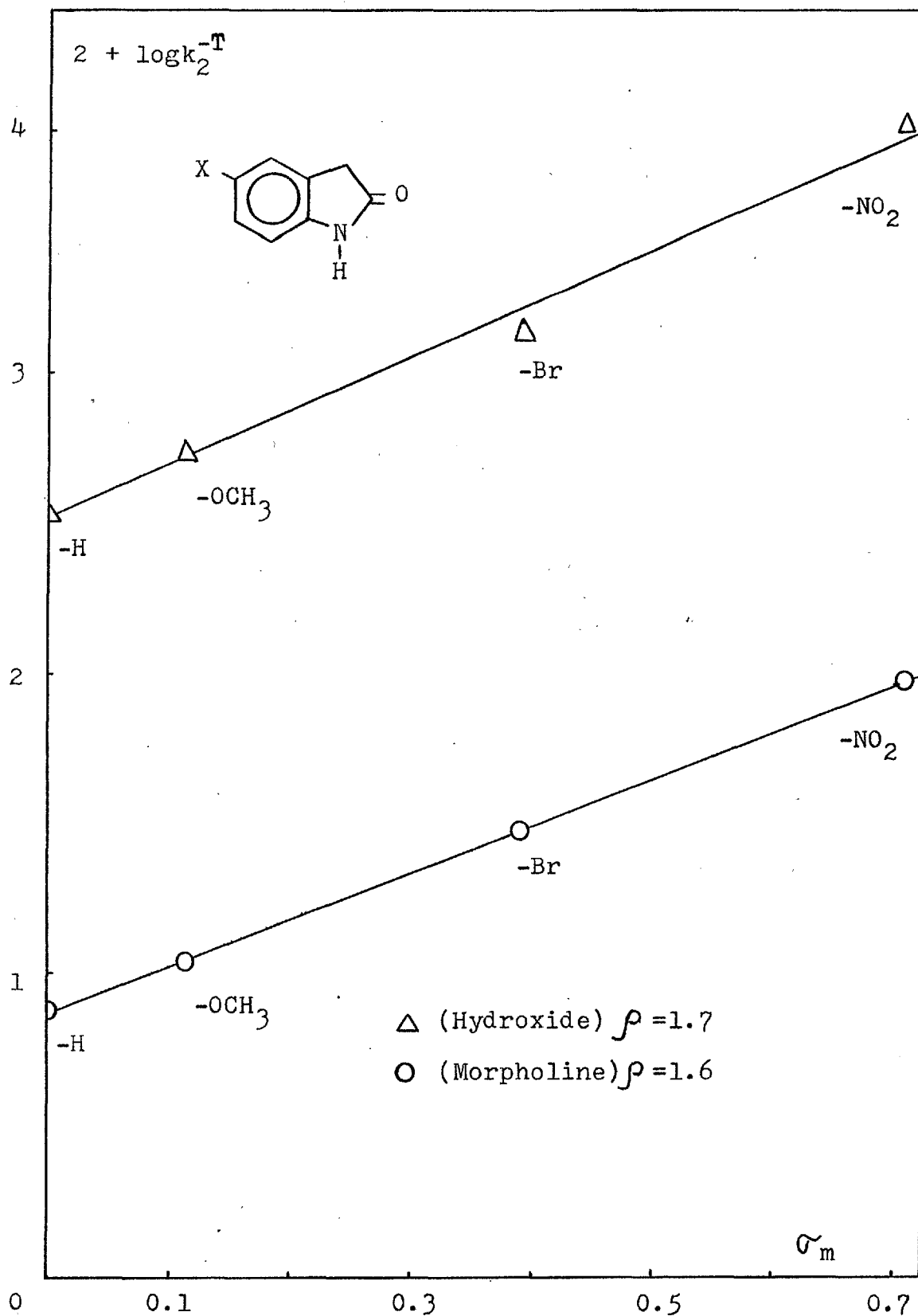
Table 2.2.18 - Dependence of  $k_1^{\text{OH}^-}$  and  $k_1^{\text{Morph}}$  on the 5-substituent for 5-X-indolin-2-ones

X	$k_1^{\text{OH}^-} / \text{l mol}^{-1} \text{s}^{-1}$	$k_1^{\text{Morph}} / \text{l mol}^{-1} \text{s}^{-1}$
H	3.5	0.08
OCH <sub>3</sub>	5.6	0.12
Br	14.4	0.31
NO <sub>2</sub>	68.8	1.11

5-NO<sub>2</sub> > 5-Br > 5-OCH<sub>3</sub> > 5-H in agreement with the results of Daisley and Walker<sup>80</sup> for the base catalysed condensation with benzaldehyde. Figure 2.2.8 shows that  $\log k_1^{\text{Morph}}$  and  $\log k_1^{\text{OH}^-}$  correlate with the  $\sigma_m$  parameter with a positive  $\rho$  (1.6 - 1.7) as expected. In fact, electron withdrawing substituents, by facilitating C-H bond fission, promote the exchange reaction.

Values of  $\rho$  and  $\beta$  will be discussed in Section 2.4 in relation to PKIE and transition state symmetry.

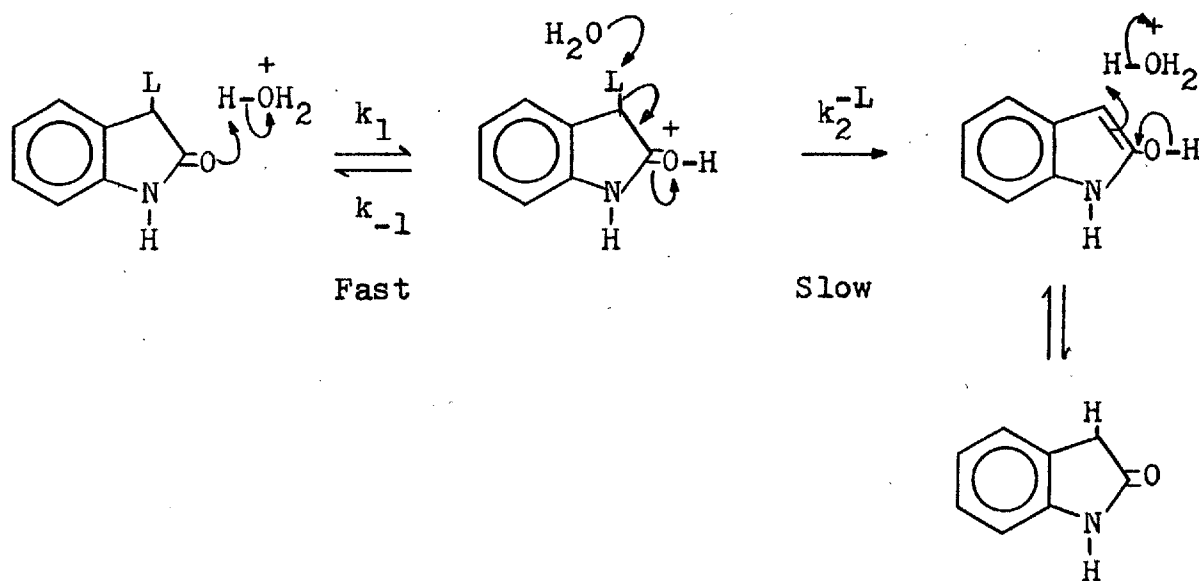
Figure 2.2.8 - Correlation of  $k_1^{\text{OH}^-}$  and  $k_1^{\text{Morph}}$  with  $\sigma_m$



2.2.2.2. Protodetritiation in acidic media

A - General mechanism

The hydrogen exchange of indolin-2-ones in acidic media is expected to involve a conjugate acid intermediate formed in a rapid pre-equilibrium step, followed by rate limiting proton abstraction (Scheme 2.2.2).



Scheme 2.2.2

With tritium at tracer level, protodetritiation is effectively irreversible and the reaction rate will be given by Equation 2.2.7

$$-d[L]/dt = k_2^{-L} [3\text{-L-indolin-2-oneH}^+] \quad (2.2.7)$$

$$= k_2^{-L} [3\text{-L-indolin-2-one}][\text{H}^+]/K_{\text{BH}^+}$$

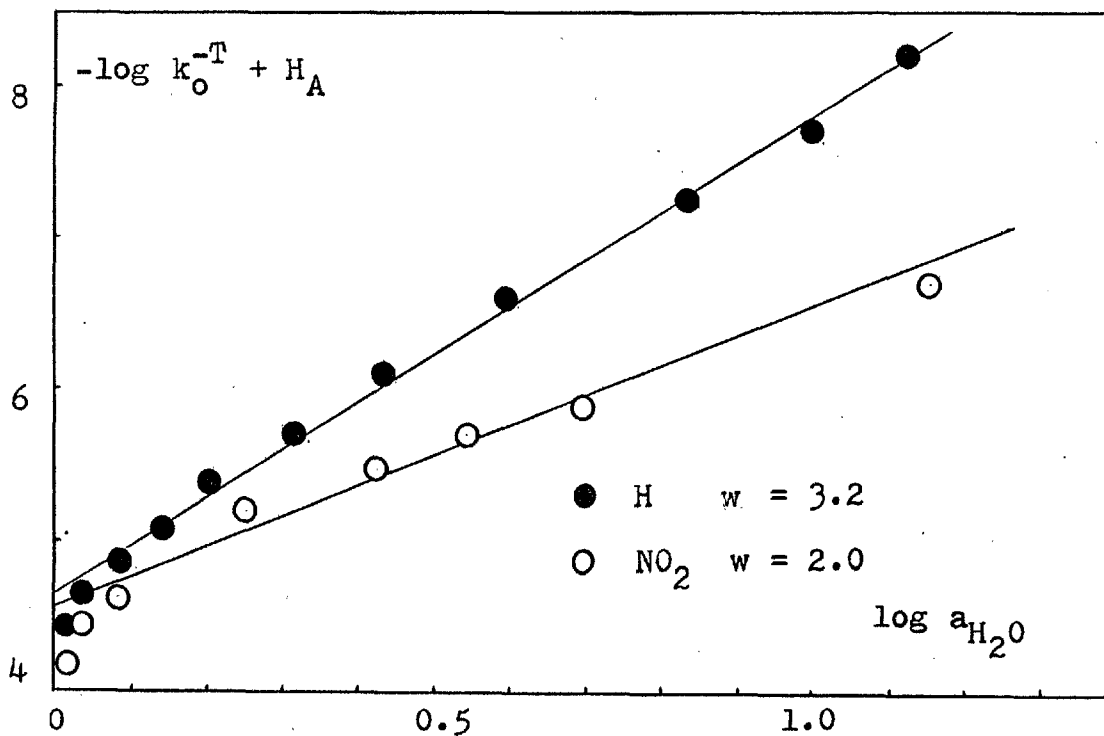
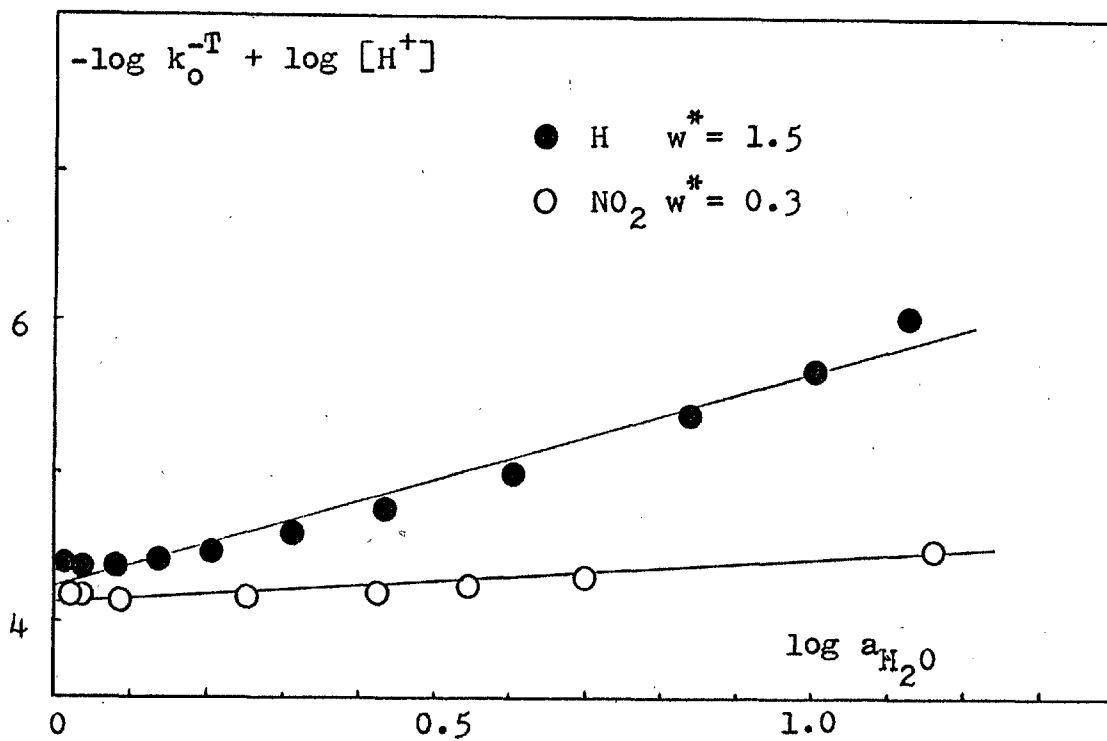
$$= k_0 [3\text{-L-indolin-2-one}] \quad (2.2.8)$$

$$\therefore k_0 = k_2^{-L} [\text{H}^+]/K_{\text{BH}^+} \quad (2.2.9)$$

Good pseudo-first order kinetics in [Substrate] were, in fact, observed. The bell shaped plots for  $k_0$  vs.  $[H^+]$  imply that formation of the conjugate acid of the substrate is substantial at moderate acidities as confirmed by the results for equilibrium protonation. The subsequent decrease in rate results from the reduction in the activity of water with increasing  $[H_2SO_4]$ . The rate maxima occur, for all the indolin-2-ones studied, before half-protonation of the substrate is reached, at still relatively high values of  $a_{H_2O}$ . This suggests that water is extremely important for this reaction. However, the experimental value of  $\Delta S^\ddagger$  for indolin-2-one in 2.45 M  $H_2SO_4$ , although negative, is only  $-37.2 \text{ J K}^{-1} \text{ mol}^{-1}$  (-8.9 e.u.). The value for the acid catalysed enolization of ketones appears to be close to the collision theory value for second order reactions<sup>97</sup>. For example,  $\Delta S^\ddagger$  for the acid catalysed iodination of acetone is  $-12 \text{ e.u.}$ <sup>98</sup>, a value which is not very far from that obtained for the enolization of indolin-2-one.

As shown in Figure 2.2.9, plots of  $\log k_0 + H_A$  vs.  $\log a_{H_2O}$ <sup>99</sup> are not linear. However, if the best straight lines are considered, values of  $w$ <sup>99</sup> in the range 2.0 -- 3.2 are obtained. Values of  $w^*$ <sup>99</sup> were also determined from the slope of graphs of  $\log k_0 - \log [H^+]$  against  $\log a_{H_2O}$  (Figure 2.2.9). It is difficult to determine  $w^*$  values for reactions catalysed in aqueous  $H_2SO_4$  when  $0.5 \text{ M} < [H_2SO_4] < 3 \text{ M}$  because of the uncertainty with which the extent of ionization of  $HSO_4^-$  in these solutions is known<sup>100</sup>. Even if, on basis of this, the first points of the graphs are ignored, the lines still show a slight tendency to curve. Best

Figure 2.2.9 - Bunnett plots for the protodetritiation of 3-[<sup>3</sup>H<sub>1</sub>]-indolin-2-one and 5-nitro-3-[<sup>3</sup>H<sub>1</sub>]-indolin-2-one in H<sub>2</sub>SO<sub>4</sub>



straight lines have slopes in the range 0.3 - 1.5. Better linear graphs are obtained when  $\log k_o + H_A$  is plotted vs.  $H_A + \log [H^+]^{101}$  (Figure 2.2.10). The values of  $\phi$  obtained from the slope of these lines lie in the range 1.1 - 1.5. Only the graphs corresponding to indolin-2-one and 5-nitro-indolin-2-one are shown in Figures 2.2.9 to 2.2.10. 5-Bromo- and 5-methoxyindolin-2-one have values of  $w$ ,  $w^*$  and  $\phi$  lying between those for 5-nitro and unsubstituted compound. Comparison of the values of  $w$ ,  $w^*$  and  $\phi$  calculated above with the values included in Table 2.2.19<sup>102</sup> shows, as with

Table 2.2.19 - Classification of acid-catalysed reactions by the Bunnett criterion<sup>102</sup>

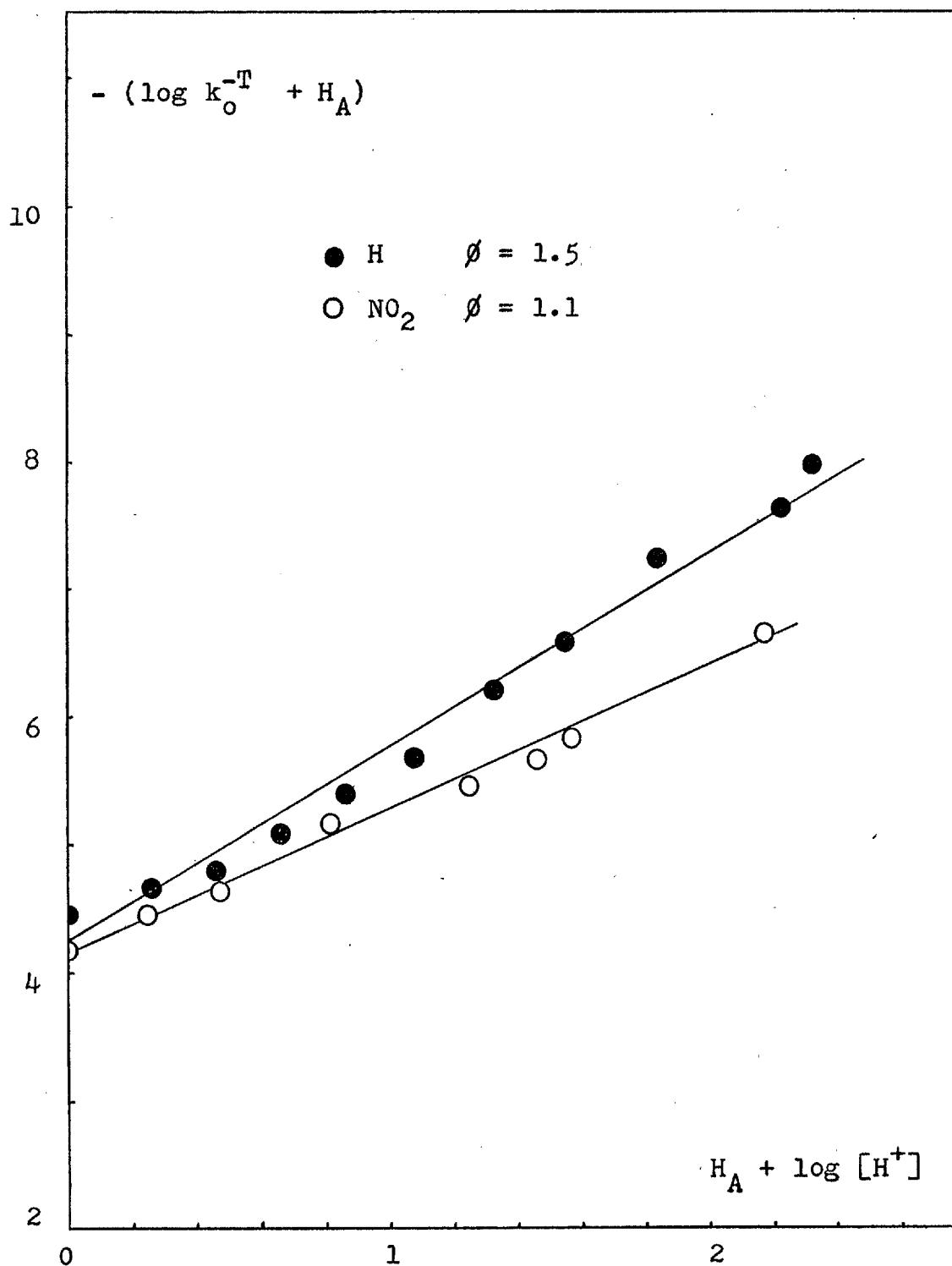
$w$	$w^*$	$\phi$	Mechanism
-2.5 to 0		<0	$A_1$
+1.2 to +3.3	<-2	+0.22 to +0.56	$A_2$ , nucleophilic attack of water
>3.3	>-2	>0.58	$A-S_E2$ or $A_2$ with water as proton acceptor
<u>ca.0</u>			$H^+$ transfer to hydrocarbon bases

carbonyl compounds<sup>82</sup>, that water is involved in the reaction as a proton transfer agent in a typical  $A_2$  mechanism as was, in fact, expected.

The value of  $w$  is usually interpreted as being equal to the difference in hydration between transition state and



Figure 2.2.10 - Bunnett-Olsen plot for the protodetritiation of 3-[<sup>3</sup>H<sub>1</sub>]-indolin-2-one and 5-nitro-3-[<sup>3</sup>H<sub>1</sub>]-indolin-2-one in H<sub>2</sub>SO<sub>4</sub>



initial state. For indolin-2-ones this value lies in the range 2 - 3. Since for each molecule of water involved in the transition state ca. 5 e.u. are lost<sup>97</sup>,  $\Delta S^\ddagger$  for indolin-2-ones (-8.9 e.u.) also indicates that, probably, two molecules of water are gained in the transition state. These probably correspond to an extra molecule needed to solvate the conjugate acid and another acting as a base to abstract the proton (Figure 2.2.11). However, since the exact relation

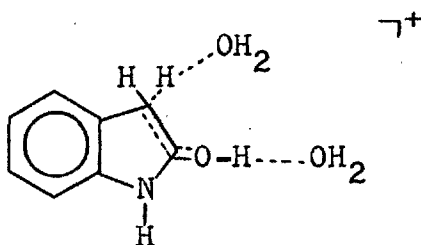


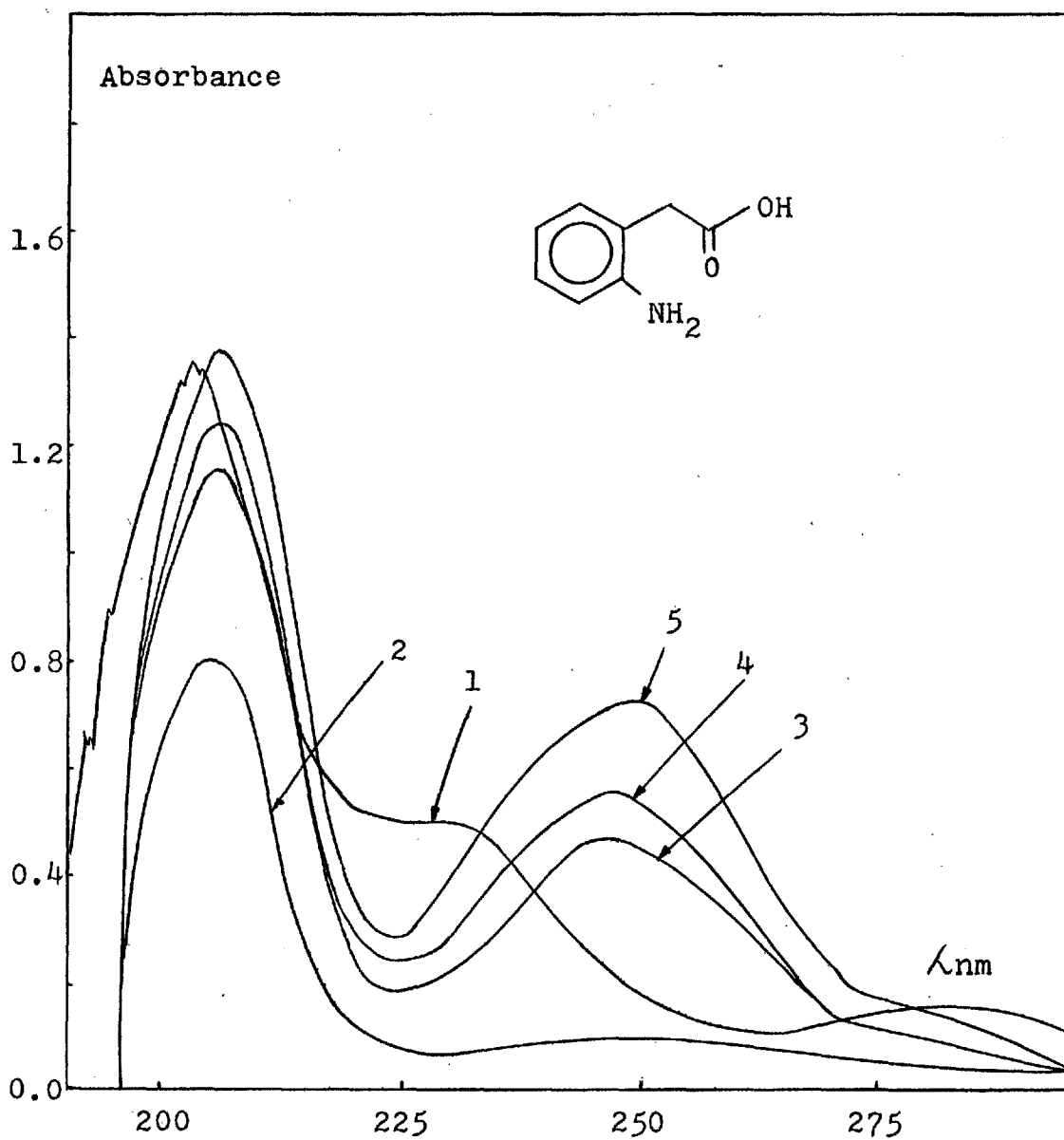
Figure 2.2.11

between  $w$  and/or  $\Delta S^\ddagger$  and transition state solvation is not fully understood, not too much weight should be put into this conclusion.

The decrease in  $k_0$  with increasing acidity could also be explained either by hydrolysis of the substrate or by competitive protonation on the nitrogen. The stability of the substrate was ascertained by UV spectrophotometry. Furthermore, the product of hydrolysis of indolin-2-one, 2'-aminophenylacetic acid, was shown to cyclise in acidic medium at room temperature. Evidence for this is shown in Figure 2.2.12. Also, the first order plots are linear practically until infinity which is a good indication of a clean reaction. Competitive protonation on nitrogen will be discussed in Section 2.2.2.B.

Figure 2.2.12 - Behaviour of 2'-aminophenylacetic acid ( $10^{-4}$  M) in acidic medium

- 1 - In water
- 2 - In 2M  $H_2SO_4$  M ( $t=0$ )
- 3 - In 2M  $H_2SO_4$  M ( $t=22$  hours)
- 4 - In 2M  $H_2SO_4$  M ( $t=46$  hours)
- 5 - Indolin-2-one ( $10^{-4}$  M) in 2M  $H_2SO_4$



The existence of maxima has been observed for other reactions in concentrated sulphuric acid e.g. decarboxylation of aromatic aldehydes<sup>103</sup>, hydrolysis of esters<sup>104</sup>, and amides<sup>105,106</sup> and detritiation of acetophenones<sup>107</sup>. The existence of the rate maxima here is usually interpreted as being due to a combination of substrate protonation and the decrease in water activity.

The pre-equilibrium protonation step is confirmed by the fact that  $k_{\text{O}}^{\text{D}_2\text{O}}/k_{\text{O}}^{\text{H}_2\text{O}} > 1$ . However, at high acidities this ratio decreases until eventually it becomes  $< 1$ . This is due to the fact that, once complete protonation of the substrate is reached, the controlling factor of the rate of exchange is the strength of the base that abstracts the proton. As  $\text{H}_2\text{O}$  is a stronger base than  $\text{D}_2\text{O}$ , the exchange in  $\text{D}_2\text{O}$  becomes slower than in  $\text{H}_2\text{O}$ .

#### B - The site of protonation

The site of protonation in amides has been a controversial subject for many years. Arguments have been advanced to support both O- and N-protonation and these have been reviewed by a number of authors including Katritzky<sup>108</sup>, O'Connor<sup>109</sup>, Hommer and Johnson<sup>90</sup> and Liler<sup>110</sup>. Apparently, there is not a unique answer for the question. Experimental data is very controversial and it seems that both N- and O-protonation is possible depending on the structure of the amide and on the conditions. Theoretical studies on the protonation of formamide<sup>111,112</sup>, urea<sup>113</sup> and peptide bond<sup>114</sup> appear to favour

O-protonation. Nevertheless these calculations refer to the gas phase and do not take into account solvation effects.

In the indolin-2-ones case, the simple fact that isotopic hydrogen exchange is catalysed by acids points to O-protonation (Figure 2.2.13 - I), since N-protonation would provide little additional driving force for the exchange (Figure 2.2.13 - II).

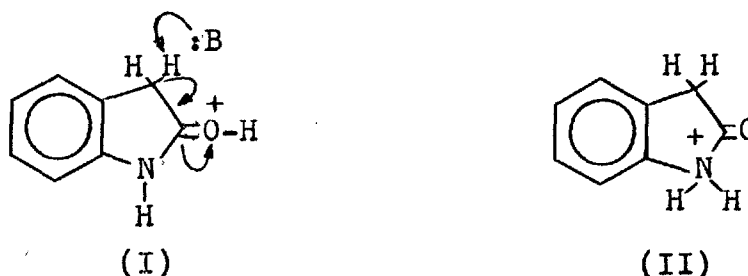
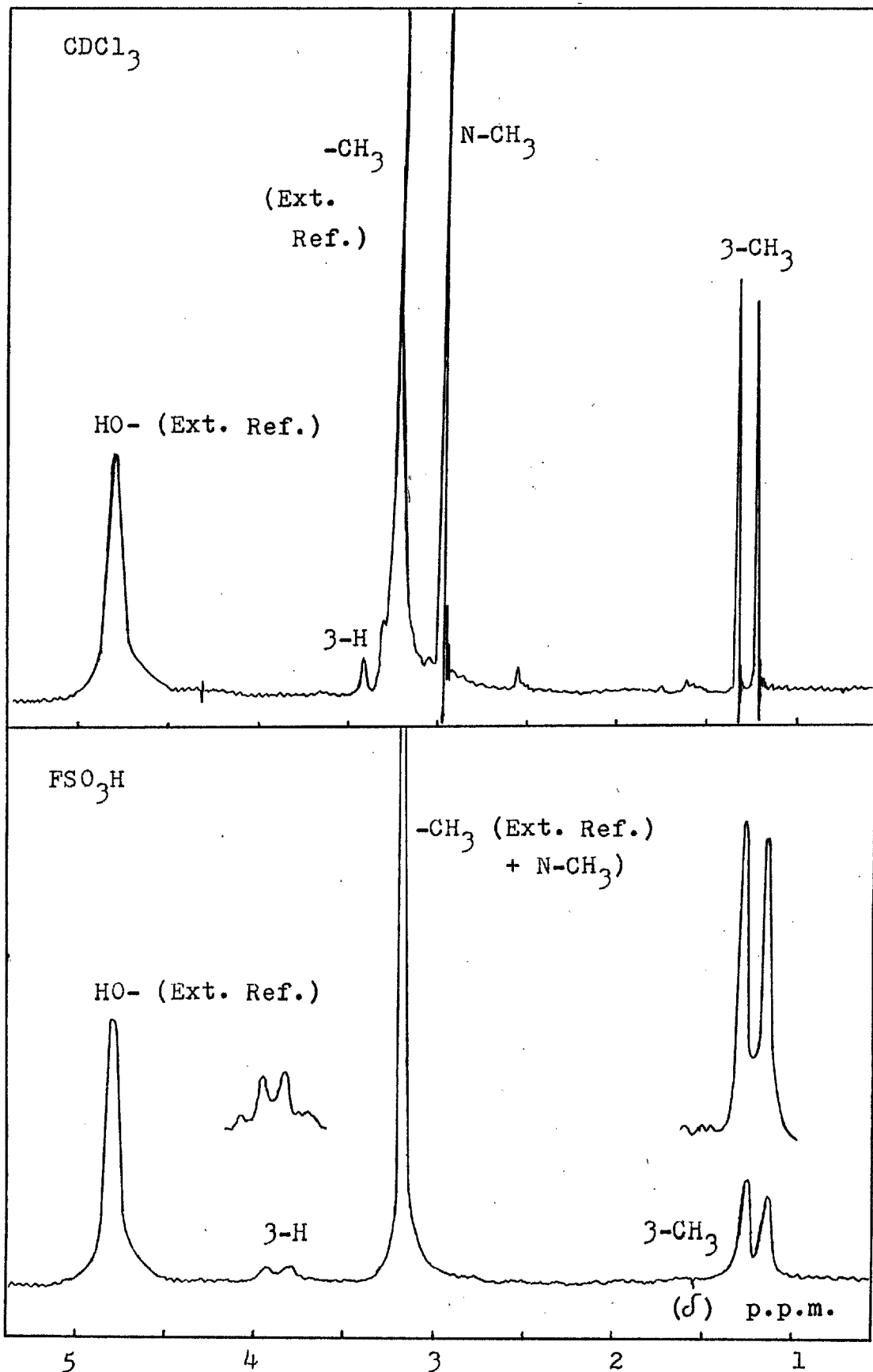


Figure 2.2.13

However, it is possible that O- and N-protonation occur concomitantly, and that the N-conjugate acid is thermodynamically the more stable. One argument against this suggestion is that the  $pK_{BH^+}$  of 5-substituted indolin-2-ones correlate with  $\sigma_m$ . For N-protonation, correlation with  $\sigma_p$  rather than  $\sigma_m$  would be expected.

Comparison of  $^1H$  NMR spectra of 1,3-dimethyl-5-nitro-indolin-2-one in  $CDCl_3$  and in  $FSO_3H$ , as shown in Figure 2.2.14 reveals that, while the N- $CH_3$  peak moves downfield only ca. 0.2 ppm, the 3-H proton shifts downfield by ca. 0.7 ppm. This result can be explained by O-protonation but not by N-protonation, since if the compound were to protonate on nitrogen, as shown in Figure 2.2.15, one would expect the N- $CH_3$  to shift more than the proton on the 3-position. However, if the compound protonates on oxygen, both shifts can be explained by the distribution of charge shown in

Figure 2.2.14 - Proton NMR spectra of 1,3-dimethyl-5-nitroindolin-2-one in  $\text{CDCl}_3$  and in  $\text{FSO}_3\text{H}$  ( $\text{CH}_3\text{OH}$  as external reference)



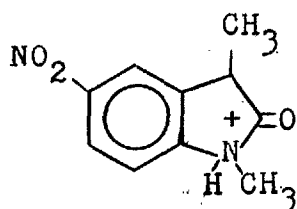


Figure 2.2.15

Figure 2.2.16. Thus, I accounts for the deshielding effect observed for the 3-H and II for the deshielding effect of N-CH<sub>3</sub>.

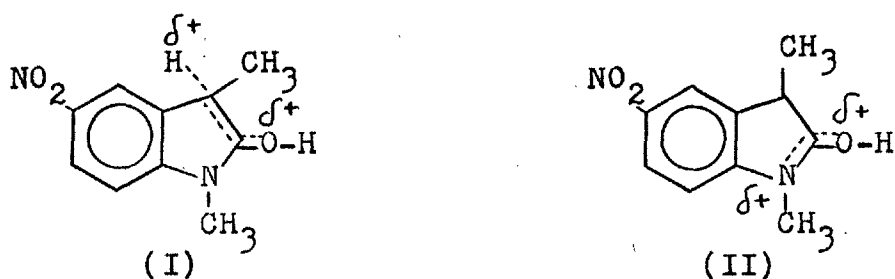
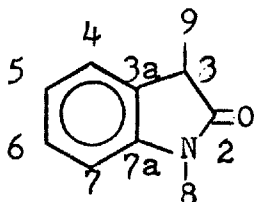


Figure 2.2.16

<sup>13</sup>C NMR spectra of the same compound in the same solvents were also recorded. Chemical shifts are shown in Table 2.2.20. Most carbons undergo a downfield shift as expected. It is difficult to explain the upfield shifts of 7a-C and 9-C on the basis of either O- or N-protonation. Protonation on nitrogen might be expected to provoke the same effect on both 7a-C and 8-C, but, while 7a-C moves upfield, 8-C moves downfield. In addition, 7-C shows a shift of similar order to that of the carbonyl carbon. All these effects are difficult to rationalize and may be caused by solvent interactions other than protonation.

Table 2.2.20 -  $^{13}\text{C}$  NMR of 1,3-dimethyl-5-nitroindolin-2-one in  $\text{CDCl}_3$  and  $\text{FSO}_3\text{H}$



C	$\delta_{\text{CDCl}_3}$	$\delta_{\text{FSO}_3\text{H}}$	$\Delta = \delta_{\text{FSO}_3\text{H}} - \delta_{\text{CDCl}_3}$
2	178.3	185.0	6.7
3	38.9	41.9	3.0
3a	130.9	132.2	1.3
4	118.9	119.9	1.0
5	142.9	145.0	2.1
6	124.9	126.2	1.3
7	107.2	113.3	6.1
7a	149.6	145.6	-4.0
8	25.9	29.0	3.1
9	14.3	11.8	-2.5

(p.p.m. downfield of TMS)

The  $^{13}\text{C}$  NMR spectrum of 1,3-dimethyl-5-nitroindolin-2-one in  $\text{FSO}_3\text{H}$  was also recorded at  $-50^\circ\text{C}$  in order to detect the possible existence of the two isomers that protonation on nitrogen would give rise to (Figure 2.2.17). At this



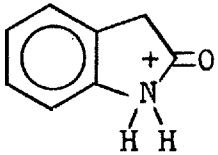
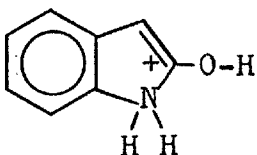
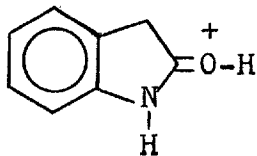
Figure 2.2.17



temperature all the signals still appear as single lines. At  $-70^{\circ}\text{C}$  all the signals became broadened, probably due to the increased viscosity of the solution. This spectral evidence suggests O-protonation rather than N-protonation.

Theoretical calculations to evaluate the relative stability of the O- and N-protonated species were carried out<sup>115</sup> by the MNDO (Modified Neglect of Diatomic overlap)<sup>116</sup> which has been demonstrated to reliably predict the energies and structures of a wide variety of neutral and charged species in the gas phase<sup>117,118,119</sup>. The geometries of the three probable isomers of protonated indolin-2-one were fully optimized using standard methods<sup>116</sup>. The calculated gas phase standard ( $298^{\circ}\text{K}$ ) enthalpies of formation of O- and N-protonated indolin-2-one are shown in Table 2.2.21. These results show

Table 2.2.21 - Enthalpies of formation of the probable isomers of protonated indolin-2-one

	$\Delta H$ kcal/mol
	157.93
	166.50
	144.09

that the O-protonated indolin-2-one is more stable than the N-protonated by ca. 14 kcal/mol in agreement with the interpretation given for the spectral data.

The calculated difference in energy between the keto and enol isomers of N-protonated indolin-2-one (ca. 9 kcal/mol) is similar to the value for acetone in the gas phase (13.9 kcal/mol), obtained by Hehre et al.<sup>120</sup>. Their results suggest that solvation does not change the qualitative order of these equilibria, which gives a degree of credibility to the extrapolation of the present calculations to solution equilibria.

C - Influence of the 5-substituents on the rate of exchange

Second order rate coefficients ( $k_2$ ) were calculated on basis of Equation 2.2.9 derived in Section 2.2.2.2 - A.

$$k_o = k_2 [H^+]/K_{BH^+} \quad (2.2.9)$$

$$\log k_o = \log k_2 + \log [H^+] - \log K_{BH^+}$$

$$\log k_o = \log k_2 + pK_{BH^+} - pH \quad (2.2.10)$$

Since at high acidities the acidity function is a more accurate expression of acidity than the pH, and indolin-2-ones follow  $H_A$  better than  $H_o$ , Equation 2.2.10 is better written under the form of Equation 2.2.11

$$\log k_o = \log k_2 + pK_{BH^+} - H_A \quad (2.2.11)$$

According to Equation 2.2.11,  $\log k_2$  can be derived from the intercepts of the lines obtained when plotting  $\log k_o$  vs.  $pK_{BH^+} - H_A$ , before the maximum, as shown in Figure 2.2.18.

Figure 2.2.19 shows the correlation of  $\log k_2$  with  $\sigma_m$ . A positive value of  $\rho$  (+ 0.66) is expected, since it is understandable that electron withdrawing substituents by facilitating the fission of the C-H bond, decrease, as in alkaline media, the energy of activation of the rate determining step and therefore increase  $k_2$ .

Values of  $\rho$  in alkaline and acidic media will be discussed in Section 2.4.

Figure 2.2.18 - Calculation of second-order rate coefficients for the protodetritiation of 5-X-[<sup>3</sup>H<sub>1</sub>]-indolin-2-ones in H<sub>2</sub>SO<sub>4</sub>

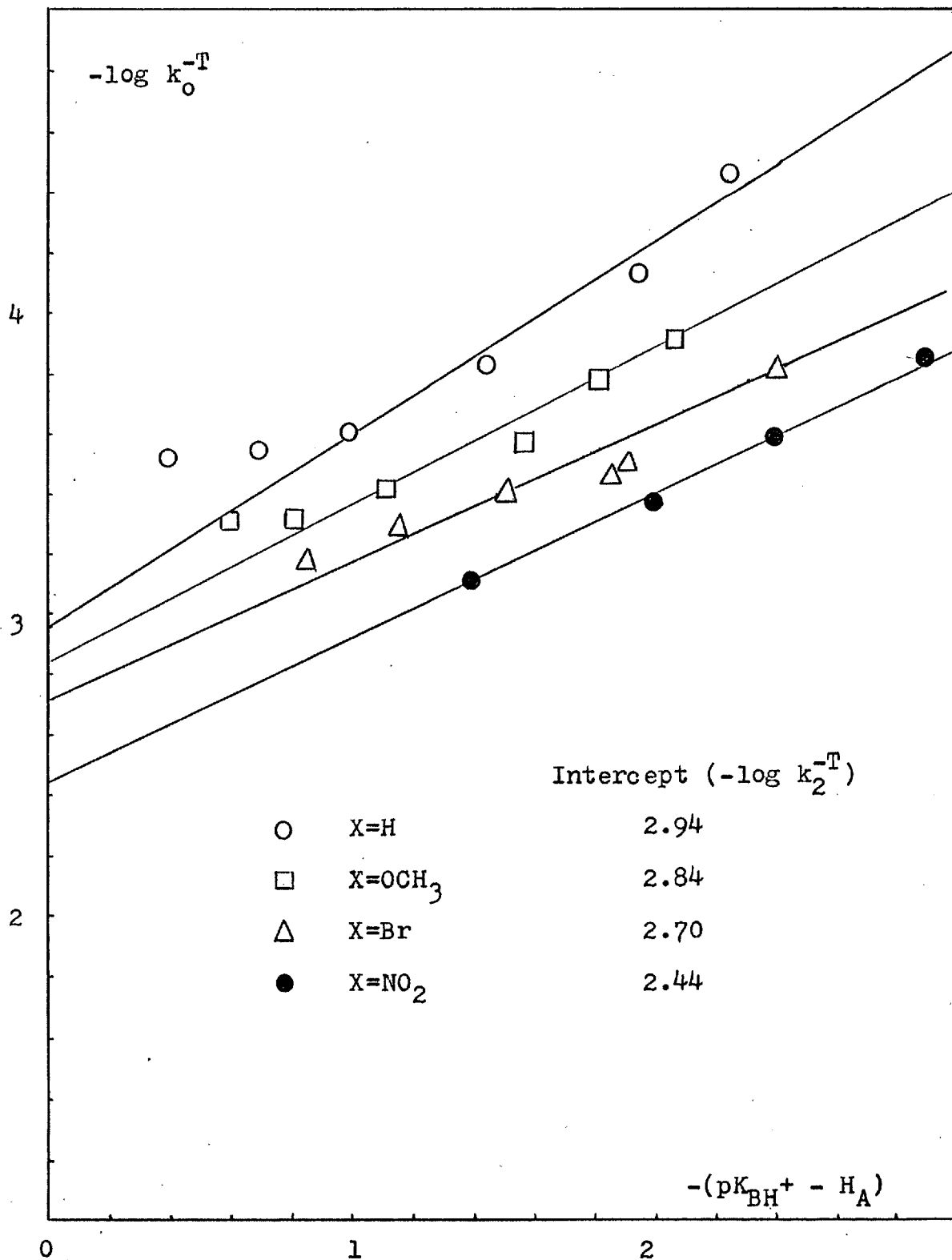


Figure 2.2.19 - Hammett plot for the protodetritiation of 5-X-3-[<sup>3</sup>H]-indolin-2-ones in H<sub>2</sub>SO<sub>4</sub>

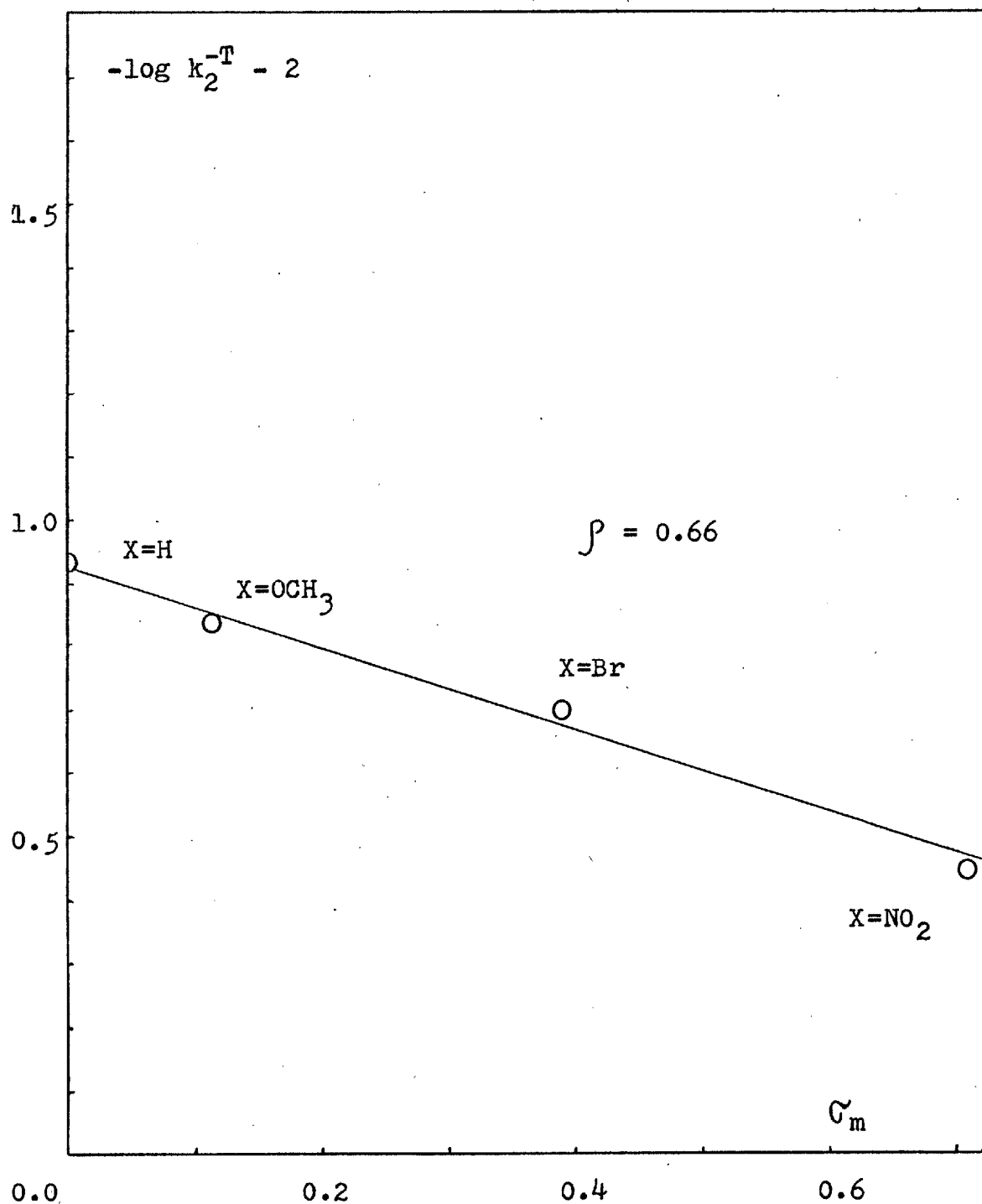
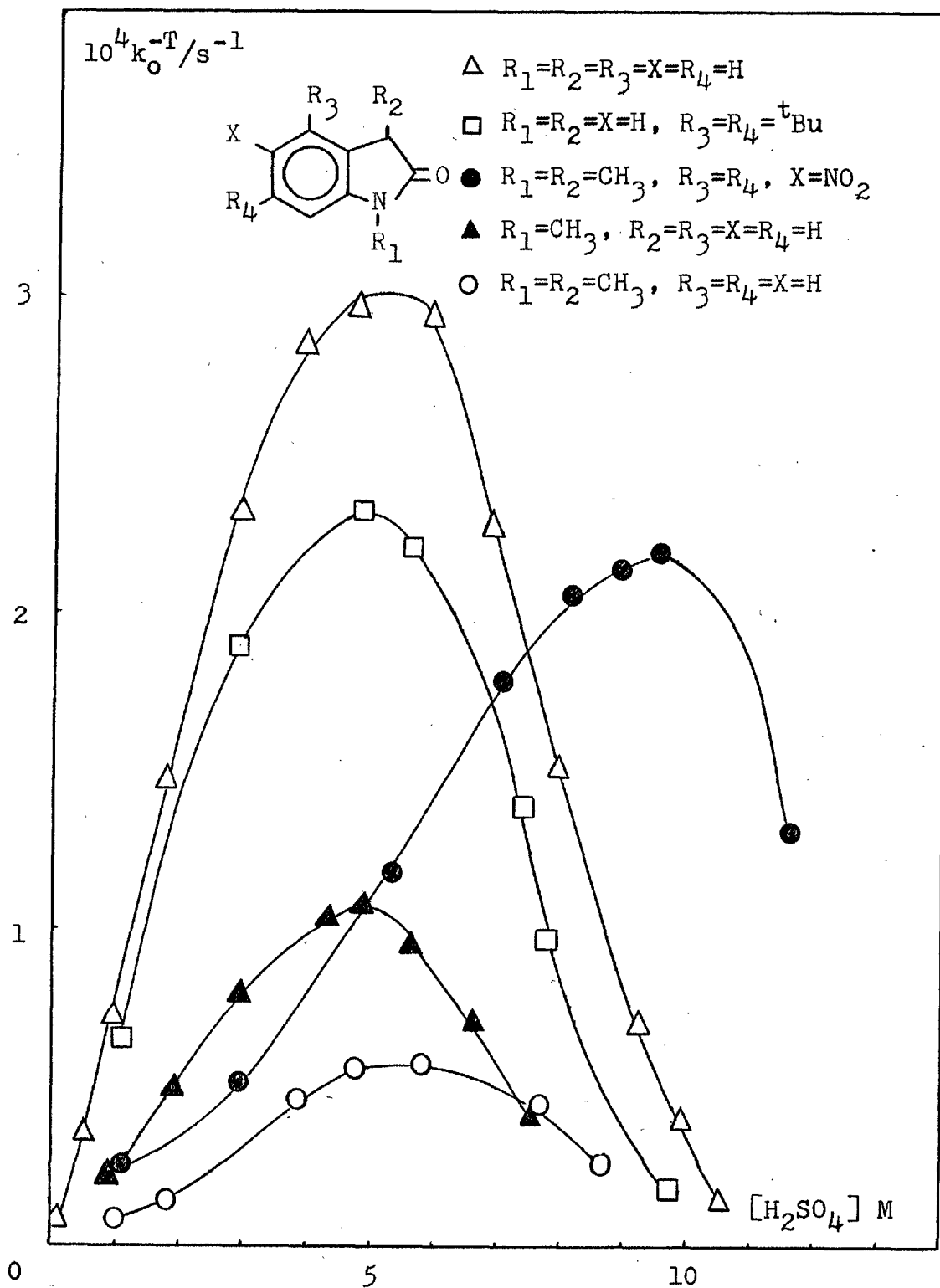


Figure 2.2.20 - Influence of 1,3- and/or 4,6-substituents on the rate of protodetritiation of indolin-2-ones in H<sub>2</sub>SO<sub>4</sub>



D - Influence of the substituents on the 1,3-positions.

Steric effects

The relative influence of substituents on the 1,3-positions and of bulky substituents on the 4-position is shown in Figure 2.2.20 whose numerical data has already been reported in Table 2.2.14. It is apparent that the presence of a methyl group on the nitrogen atom reduces the rate of exchange by a factor of ca. 3. This relative reactivity of indolin-2-one and 1-methylindolin-2-one is similar to that found by Gruda<sup>81</sup> for the addition of the same compounds to methylvinylketone. This reduction in rate can be rationalized in terms of the inductive effect of the methyl group which will increase the relative stability of form (I) relative to form (II) in Figure 2.2.21. In other words, the presence of



Figure 2.2.21

the methyl on the nitrogen atom decreases the ketone character of indolin-2-one by increasing its lactam character. As (I) is inactive towards exchange,  $k_0$  decreases.

The presence of a methyl group on the 3-position also produces a small decrease in the rate, probably due to a slight steric hindrance to the attack of water. The same effect is observed for the relative rates of exchange of

5-nitroindolin-2-one and 1,3-dimethyl-5-nitroindolin-2-one  
(See also Table 2.2.13)

A bulky group on the 4-position, on its own, appears to have only a little effect but, if a methyl group is also present on the 3-position, the rate of exchange in ca. 5M  $H_2SO_4$  decreases by a factor of 500 relative to indolin-2-one and of 100 relative to 1,3-dimethylindolin-2-one. This reduction in rate may be rationalized in terms of an enhanced steric interaction in the intermediate enol and therefore in the transition state that leads to it. In fact, the enol shown in Figure 2.2.22 - I has a planar structure that forces the <sup>t</sup>butyl group and the methyl group on the 3-position to lie in the same plane and therefore to interact more than in the ketonic form of the indolin-2-one (Figure 2.2.22 - II)

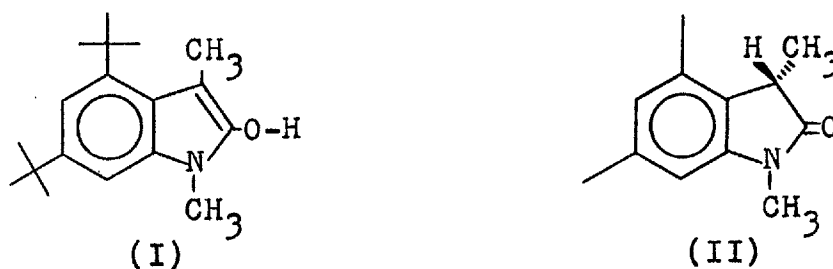


Figure 2.2.22

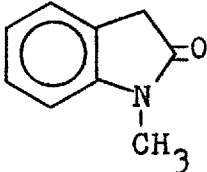
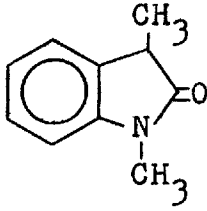
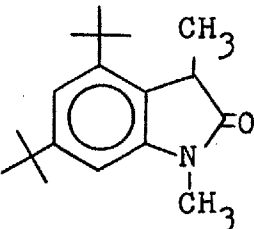
This interaction increases the energy of activation of the rate determining step and therefore the rate decreases substantially.

Steric effects in alkaline media for the same compounds have been established<sup>95</sup> also by measuring rates of protodetritiation. In Table 2.2.20 the steric effects are



compared in both alkaline and acidic media and it is apparent that the steric effect is more important in alkaline than in acidic media. Since the  $pK_{BH^+}$  for those compounds is not available, the comparison in acidic media is done through  $k_0$  on the assumption that the presence of the 3-methyl and <sup>t</sup>butyl groups does not substantially affect their  $pK_{BH^+}$  relative to 1-methylindolin-2-one.

Table 2.2.20 - Comparison of steric effects in acidic and alkaline media

	$10^4 k_0 / s^{-1}$ in <u>ca.</u> 5M $H_2SO_4$	$k_1^{OH^-} / mol^{-1} s^{-1}$
	1.1 (183)	4.95 (696)
	0.6 (100)	1.25 (176)
	0.006 (1)	0.0071 (1)

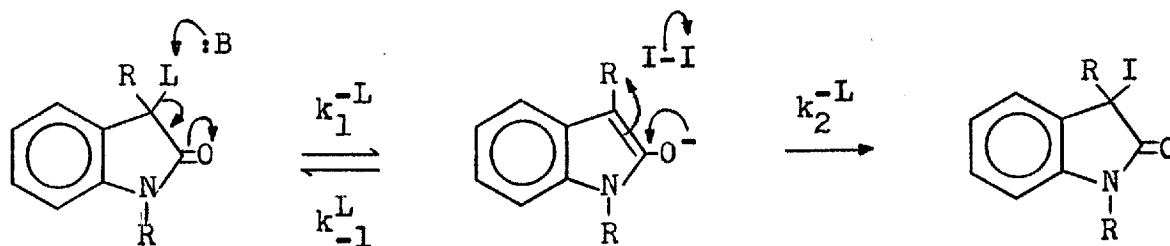
2.3. PRIMARY KINETIC ISOTOPE EFFECTS FOR THE IONIZATION OF INDOLIN-2-ONES

2.3.1. In alkaline media

2.3.1.1. INTRODUCTION

To avoid complications from secondary isotope effects, the rates of hydrogen exchange are best measured in compounds with only one  $\beta$ -H position, such as 1,3-dimethylindolin-2-one.

Indolin-2-ones are liable to air oxidation in alkaline media<sup>63</sup>, but rates of protodetrutiation are not affected because oxidation occurs after ionization<sup>95</sup>. However, rates of protodeuteriation measured by Mass Spectrometry would be affected and, for that reason, the method cannot be used to determine  $k_0^{-D}$ . Of the alternative methods available<sup>19</sup>, the most common and satisfactory one used to measure ionization rates of carbon acids is the halogenation method which involves trapping of the intermediate enolate anion formed by ionization with a molecular halogen, namely iodine, as shown in Scheme 2.3.1. In fact, this method measures the rate of ionization and not the rate of exchange but, as the



Scheme 2.3.1

rate determining step is the same, the rate of exchange is equal to the rate of ionization. The uptake of iodine from the reaction solution, assuming that the steady state approximation applies to the intermediate enolate anion, is expressed by Equation 2.3.1

$$-d[I_2]/dt = \frac{k_1^{-L} [B:] [3-L-indolin-2-one]}{1 + k_{-1}^L / k_2^{-L} [I_2]} \quad (2.3.1)$$

This equation simplifies if special experimental conditions are used:

(i)  $[I^-] \gg [I_2]$

Although  $I_2$  is in equilibrium with  $I_3^-$  ( $I_2 + I^- \rightleftharpoons I_3^-$ ,  $K = [I_3^-]/[I_2][I^-] = 714$  at  $25^\circ C^{19}$ ), the iodide released during the course of the reaction will not affect the total iodine present if  $[I^-] \gg [I_2]$ . Then, the rate of disappearance of  $I_2$  will be equal to the rate of disappearance of  $I_3^-$

$$-d[I_2]/dt = -d[I_3^-]/dt$$

(ii)  $[3-L-indolin-2-one] \gg [I_2]$

This condition allows the substrate concentration to remain practically constant throughout and consequently, Equation 2.3.1, at constant  $[B:]$ , will reduce to Equation 2.3.2, where  $*k_1^{-L} = k_1^{-L} [B:] [3-L-indolin-2-one]$  and

$$-d[I_3^-]/dt = \frac{*k_1^{-L}}{1 + k_{-1}^L / *k_2^{-L} [I_3^-]} \quad (2.3.2)$$

\* $k_2^{-L} = k_2^{-L}/714 [I^-]$ . If \* $k_2^{-L} [I_3^-] \gg k_1^{-L}$ , then Equation 2.3.2 reduces to Equation 2.3.3, and, the rate of disappearance

$$-d[I_3^-]/dt = *k_1^{-L} \quad (2.3.3)$$

of  $I_3^-$  will be zero order in  $[I_3^-]$ . The fact that zero order dependence is usually observed in these reactions<sup>20</sup> suggests that the reprotonation of the intermediate enolate anion is slow as assumed ( i.e., \* $k_2^{-L} [I_3^-] \gg k_{-1}^L$ ). However, if reprotonation is fast, the rate of disappearance of  $I_3^-$  will be first order in  $[I_3^-]$  as observed for phenylacetylene<sup>121</sup>. Intermediate behaviour has been observed for acid-catalysed iodination of acetone<sup>122</sup> and base-catalysed halogenation of ortho-hydroxyacetophenone<sup>123</sup>.

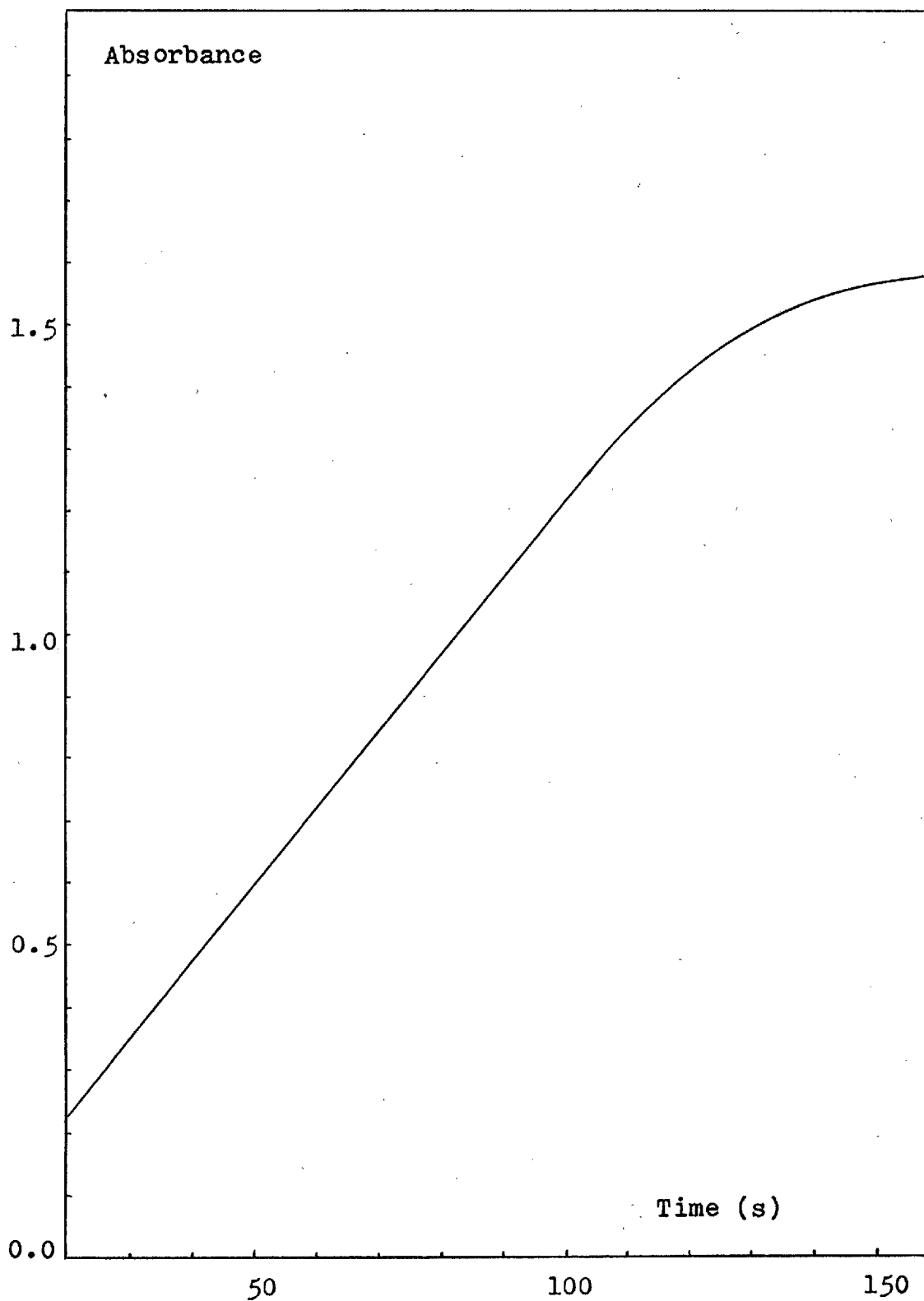
Both protium and deuterium exchange rates of 1,3-dimethyl-indolin-2-one were measured by the halogenation method, following the disappearance of  $I_3^-$  by UV Spectrophotometry as indicated in Section 3.4.3

### 2.3.1.2. RESULTS

Rates of ionization of indolin-2-ones were too fast to be measured in aqueous NaOH so buffers had to be employed. It was found that tris(hydroxymethyl)methylamine (TRIS) is most convenient in terms of pK, rate of exchange and stability of  $I_3^-$ . Under the reaction conditions, excellent zero order kinetics in  $[I_3^-]$  was observed for 1,3-dimethyl-3- $[^1H_1]$ -indolin-2-one as shown in Figure 2.3.1. \* $k_1^{-H}$  were obtained

Figure 2.3.1 - Iododeprotonation of 1,3-dimethyl-3- $[^1\text{H}_1]$ -indolin-2-one in a TRIS buffer

$[\text{TRIS}] = 9 \times 10^{-3}\text{M}$ ,  $[3\text{-H-Indolin-2-one}]_i = 10^{-3}\text{M}$ ,  $\text{pH} = 9.030$



by dividing the slopes of the zero order lines (Absorbance vs. time), recorded by the spectrophotometer at several concentrations of TRIS, by the molecular absorptivity of  $I_3^-$  ( $\epsilon = 2.64 \times 10^4$ )<sup>19</sup>. The values of  $*k_1^{-H}$  listed in Table 2.3.1, together with [TRIS] and the experimental pH measured at the end of each kinetic run, were plotted vs. [TRIS] and  $k_1^{-H}(\text{TRIS})$  and  $k_1^{-H}(\text{OH}^-)$ , derived respectively from the slope and intercept determined by the least squares procedure according to Equations 2.3.4 and 2.3.5.

$$k_1^{-H}(\text{TRIS}) = \text{Slope}/[\text{Indolin-2-one}] \quad (2.3.4)$$

$$k_1^{-H}(\text{OH}^-) = \text{Intercept}/[\text{Indolin-2-one}][\text{OH}^-] \quad (2.3.5)$$

$[\text{OH}^-]$  was calculated from the average experimental pH.

The ionization rates of 1,3-dimethyl-3- $^{2}\text{H}_1$ -indolin-2-one were measured similarly in the presence of TRIS but the variation of  $[I_3^-]$  with time was no longer zero order as shown in Figure 2.3.2. This was interpreted as being an artifact due to the presence of a small amount of 1,3-dimethyl-3- $^1\text{H}_1$ -indolin-2-one ( $2.1 \pm 0.2\%$  analysed by MS) in the deuteriated substrate. Curves of  $dA/dt$  were corrected (see below) for the amount of hydrogenated product present and the corrected values give a satisfactory zero order plot (Figure 2.3.2). The values of  $*k_1^{-D}$  reported in Table 2.3.2 were obtained from the corrected curves of  $dA/dt$ , as indicated for 1,3-dimethyl-3- $^1\text{H}_1$ -indolin-2-one.

The correction of  $dA/dt$  was carried out in the following way. Values of the absorbance at time  $t$  were corrected for

Table 2.3.1 - Rate of ionization of 1,3-dimethyl-3- $[^1\text{H}_1]$ -indolin-2-one in TRIS buffers

$[\text{Indolin-2-one}]_i = 10^{-3}\text{M}$ ,  $[\text{I}_3^-]_i = 6 \times 10^{-5}\text{M}$ ,  $[\text{I}^-] = 0.1\text{M}$   
 $[\text{Cl}^-] = 0.252\text{M}$ ,  $\mu = 0.352$ , Buffer ratio 1:8

$10^3[\text{TRIS}]/\text{mol l}^{-1}$	Experimental pH	$10^8 * k_1^{-\text{H}\ddagger}$
9	9.030	44.3
10	9.030	46.6
11	9.035	49.2
12	9.030	52.5
13	9.040	55.5
14	9.040	57.5
15	9.050	61.2
16	9.060	63.0
17	9.070	65.6
18	9.085	68.3
19	9.080	72.7
20	9.080	74.2
21	9.080	76.5

Mean pH = 9.055    Calculated  $[\text{OH}^-] = 1.14 \times 10^{-5}\text{M}$

$$\ddagger * k_1^{-\text{H}} = d[\text{I}_3^-]/dt \text{ mol l}^{-1}\text{s}^{-1}$$

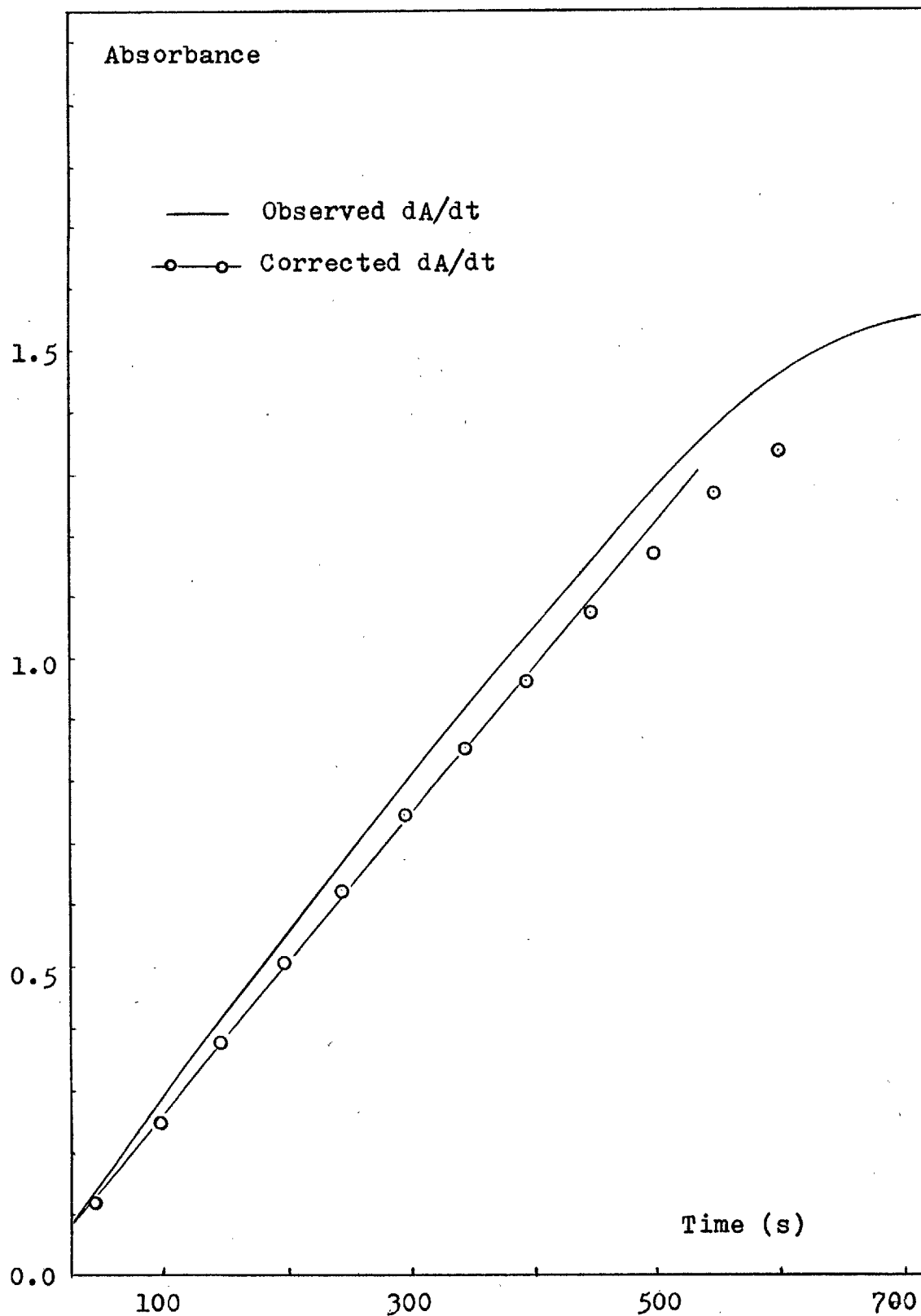
$$k_1^{-\text{H}}(\text{OH}^-) = \frac{\text{Intercept}}{[\text{OH}^-][\text{Indolin-2-one}]} = 17.2 \pm 0.8 \text{ l mol}^{-1}\text{s}^{-1}$$

$$k_1^{-\text{H}}(\text{TRIS}) = \frac{\text{Slope}}{[\text{Indolin-2-one}]} = (2.74 \pm 0.14) \times 10^{-2} \text{ l mol}^{-1}\text{s}^{-1}$$

Figure 2.3.2 - Iododeuteration of 1,3-dimethyl-3-[<sup>2</sup>H<sub>1</sub>]-  
-indolin-2-one in a TRIS buffer

[TRIS] =  $17 \times 10^{-3}$ M, [3-D-Indolin-2-one]<sub>i</sub> =  $0.979 \times 10^{-3}$ M,

[3-H-Indolin-2-one]<sub>i</sub> =  $0.021 \times 10^{-3}$ M, pH = 9.065





the amount of  $I_3^-$  consumed by the unlabelled compound, according to Equation 2.3.6, where  $A_t^c$  is the corrected absorbance,  $A_t$

$$A_t^c = A_t - A_t^H \quad (2.3.6)$$

the observed absorbance and  $A_t^H$  the absorbance corresponding to the amount of  $I_3^-$  consumed by the unlabelled compound at time  $t$ . The value of  $A_t^H$  was calculated by determining the amount of reaction attributable to the unlabelled impurity by means of Equation 2.3.7, where  $[3\text{-I-indolin-2-one}]_t^H$  is the amount of iodinated indolin-2-one at time  $t$ ,  $[3\text{-H-indolin-2-one}]_0$  the initial concentration of unlabelled substrate and  $k_1^{-H} = *k_1^{-H}/[3\text{-H-indolin-2-one}]_i$ .  $*k_1^{-H}$  is the value calculated before for 1,3-dimethyl-3- $[^1H_1]$ -indolin-2-one exactly in the same conditions of dedeuteriation.

$$[3\text{-I-indolin-2-one}]_t^H = [3\text{-H-indolin-2-one}]_0 e^{-k_1^{-H}t} \quad (2.3.7)$$

The concentration of iodinated indolin-2-one at time  $t$  was translated into an absorbance by means of Equation 2.3.8

$$A_t^H = [3\text{-I-indolin-2-one}]_t^H \times \epsilon I_3^- \quad (2.3.8)$$

since, at any time  $t$ ,  $[I_3^-]_t^H = [3\text{-I-indolin-2-one}]_t^H$ .  $[I_3^-]_t$  is the amount of  $I_3^-$  consumed by unlabelled substrate at time  $t$ .  $[3\text{-H-indolin-2-one}]_0$  was determined by Mass Spectrometry by measuring the expanded molecular ion peaks corresponding to the labelled and unlabelled compounds, a special allowance having been made for the intensity of the

M-1 peak which, in general, is of significant height for indolin-2-ones<sup>??</sup> and, in this particular case, is  $4.7 \pm 0.3\%$ .

Values of  $k_1^{-D}(\text{OH}^-)$  and  $k_1^{-D}(\text{TRIS})$  were calculated as for  $k_1^{-H}(\text{OH}^-)$  and  $k_1^{-H}(\text{TRIS})$ , using the data reported in Table 2.3.2

Table 2.3.2 - Rate of ionization of 1,3-dimethyl-3-[<sup>2</sup>H<sub>1</sub>]-indolin-2-one in TRIS buffers

$[\text{Indolin-2-one}]_i = 0.979 \times 10^{-3} \text{M}$ ,  $[\text{I}_3^-]_i = 6 \times 10^{-5} \text{M}$ ,  $[\text{I}^-] = 0.1 \text{M}$   
 $[\text{Cl}^-] = 0.252 \text{M}$ ,  $\mu = 0.352 \text{M}$ , Buffer ratio 1:8

$10^3[\text{TRIS}]/\text{mol l}^{-1}$	Experimental pH	$10^8 * k_1^{-H\dagger}$
9	9.035	6.63
10	9.030	7.00
11	9.030	7.67
13	9.045	8.43
14	9.040	9.09
15	9.045	9.56
17	9.065	10.22
19	9.070	11.11
20	9.085	11.74
21	9.085	12.23

Mean pH = 9.053      Calculated  $[\text{OH}^-] = 1.13 \times 10^{-5} \text{M}$

$\dagger * k_1^{-D} = d[\text{I}_3^-]/dt \text{ mol l}^{-1} \text{s}^{-1}$ , corrected for 2% of 1,3-dimethyl-3-[<sup>1</sup>H<sub>1</sub>]-indolin-2-one

$$k_1^{-D}(\text{OH}^-) = \frac{\text{Intercept}}{[\text{Indolin-2-one}][\text{OH}^-]} = 2.27 \pm 0.11 \text{ l mol}^{-1} \text{s}^{-1}$$

$$k_1^{-D}(\text{TRIS}) = \frac{\text{Slope}}{[\text{Indolin-2-one}]} = (0.47 \pm 0.02) \times 10^{-2} \text{ l mol}^{-1} \text{s}^{-1}$$

The rates of protodetritiation of 1,3-dimethyl-3- $^{3}\text{H}_1$ -indolin-2-one were measured by the general method indicated in Section 3.4.1. Values of  $k_0^{-T}$  are listed in Table 2.3.3, together with [TRIS] and the experimental pH also measured at the end of each kinetic run.

Table 2.3.3 - Protodetritiation of 1,3-dimethyl-3- $^{3}\text{H}_1$ -indolin-2-one in TRIS buffers

$[\text{I}^-] = 0.1 \text{ M}$ ,  $[\text{Cl}^-] = 0.252 \text{ M}$ ,  $\mu = 0.352$ , Buffer ratio 1:8

$10^3[\text{TRIS}]/\text{mol l}^{-1}$	Experimental <sup>‡</sup> pH	$10^4 k_0^{-T}/\text{s}^{-1}$
9	9.125	0.277
12	9.130	0.327
15	9.135	0.377
18	9.145	0.422
21	9.145	0.479

$$k_{1(\text{OH}^-)}^{-T} = 0.92 \pm 0.05 \text{ l mol}^{-1}\text{s}^{-1}$$

$$k_{1(\text{TRIS})}^{-T} = 1.68 \pm 0.08 \text{ l mol}^{-1}\text{s}^{-1}$$

<sup>‡</sup> Although the buffer ratio is the same, the experimental pH of each solution is different from that reported for iodo-deprotonation and iododedeuteriation. This is due to the fact that these buffer solutions were prepared by dilution of a different stock solution.

2.3.1.3. DISCUSSION

Figure 2.3.3 shows the relative rates of ionization ( $k_o$ ) of 1,3-dimethyl-3- $[\text{}^1\text{H}_1]$ -, 1,3-dimethyl-3- $[\text{}^2\text{H}_1]$ - and 1,3-dimethyl-3- $[\text{}^3\text{H}_1]$ -indolin-2-one as a function of [TRIS]. The values of second order rate coefficients,  $k_1^{-L}(\text{TRIS})$  and  $k_1^{-L}(\text{OH}^-)$  (L = H, D, T), are listed in Table 2.3.4. Table 2.3.5 shows the primary kinetic isotope effects calculated from the second order rate coefficients in Table 2.3.4.

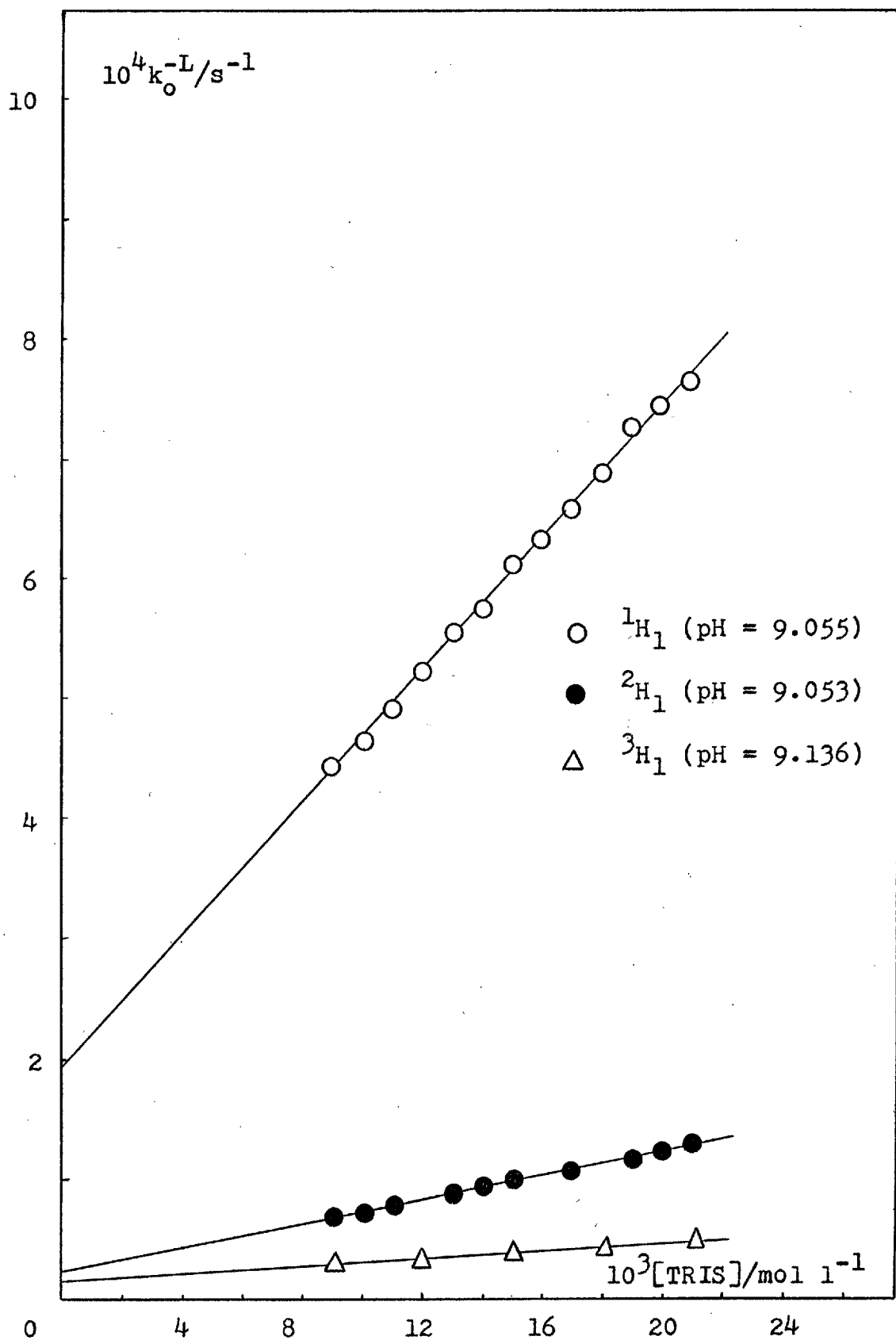
Table 2.3.4 - Second order rate coefficients for the ionization of 1,3-dimethyl-3- $[\text{}^1\text{H}_1]$ -, 1,3-dimethyl-3- $[\text{}^2\text{H}_1]$ - and 1,3-dimethyl-3- $[\text{}^3\text{H}_1]$ -indolin-2-one in TRIS buffers

	$10^3 k_1(\text{TRIS}) / 1 \text{ mol}^{-1} \text{ s}^{-1}$	$k_1(\text{OH}^-) / 1 \text{ mol}^{-1} \text{ s}^{-1}$
$[\text{}^1\text{H}_1]$	$27.4 \pm 1.4$	$17.2 \pm 0.8$
$[\text{}^2\text{H}_1]$	$4.7 \pm 0.2$	$2.27 \pm 0.11$
$[\text{}^3\text{H}_1]$	$1.68 \pm 0.08$	$0.92 \pm 0.05$

Table 2.3.5 - Primary kinetic isotope effects for ionization of 1,3-dimethylindolin-2-one in TRIS buffers

Base	$k_1^{-\text{H}} / k_1^{-\text{D}}$	$k_1^{-\text{H}} / k_1^{-\text{T}}$	$k_1^{-\text{D}} / k_1^{-\text{T}}$
TRIS	$5.8 \pm 0.3$	$16.3 \pm 0.8$	$2.8 \pm 0.1$
$\text{OH}^-$	$7.5 \pm 0.4$	$18.7 \pm 0.9$	$2.5 \pm 0.1$

Figure 2.3.3 - Relative rate of ionization of ( $k_o^{-L}$ ) of 1,3-dimethyl-3- $[^1H_1]$ -, 1,3-dimethyl-3- $[^2H_1]$ - and 1,3-dimethyl-3- $[^3H_1]$ -indolin-2-one in TRIS buffers



Inspection of Tables 2.3.1, 2.3.2 and 2.3.3 shows that the TRIS buffer, under dilution, fails to keep the pH absolutely constant. For that reason there must be an inherent error, on the high side, in the values of the second order rate coefficients due to the variation in  $[\text{OH}^-]$ . Calculations based on the value of  $k_1(\text{OH}^-)$  and on the variation of  $[\text{OH}^-]$  show that the error may be as high as 5%.

The Swain-Schaad exponent calculated from the isotope effects, shown in Table 2.3.5, is 1.587 and 1.455 for TRIS and hydroxide respectively. The value for hydroxide is not very far from the theoretical value (1.442) but 1.587 for TRIS is too high. This may be due to the error that affects  $k_1^{\text{-H}}(\text{TRIS})$ ,  $k_1^{\text{-D}}(\text{TRIS})$  and  $k_1^{\text{-T}}(\text{TRIS})$ . In order to have the value of the Swain-Schaad exponent down to the theoretical value,  $k_1^{\text{-D}}(\text{TRIS})$ , for instance, should be of the order of  $6.7 \times 10^{-3}$ , that is, ca. 40% higher than the experimental value. It is also possible, but very unlikely, that the correction introduced in the calculation of  $k_1^{\text{-D}}(\text{TRIS})$ , based in MS measurements, are affected by errors greater than expected (ca. 0.5%). It is unlikely that the variation in pH could account for the difference in the Swain-Schaad exponent. In fact, although the absolute values of the second order rate coefficients may be affected by errors as high as 5%, as they have all been measured in the same conditions, their ratios and, therefore, the PKIE, would in principle be affected by smaller errors. A possible explanation for the high value of the Swain-Schaad exponent is that, TRIS being a big molecule and, therefore, more susceptible to steric hindrance, the tunnelling component of the isotope effect is more

important than for hydroxide ion. Still, not much weight can be put in this explanation since, on basis of the present results, it is not possible to know how much the values of the second order rate coefficients are affected by the variation in the pH. Furthermore, the ratio  $k_1^{-H}/k_1^{-T}$  is greater for hydroxide than for TRIS, this suggesting tunnelling to be more important for hydroxide.

Values of  $k_1^{-L}(\text{OH}^-)$  in 50% (w/w) aqueous methanol tetraborate buffers have been measured by Challis and Rzepa<sup>78</sup> for the same compound. These values are shown next, together with the isotope effects and the Swain-Schaad exponent ( $r$ ) calculated from them.

$$k_1^{-H}(\text{OH}^-) = 13.74 \pm 0.2 \quad k_1^{-D}(\text{OH}^-) = 2.15 \pm 0.06$$

$$k_1^{-T}(\text{OH}^-) = 1.19 \pm 0.03$$

$$k_1^{-H}/k_1^{-D} = 6.36 \pm 0.21$$

$$k_1^{-H}/k_1^{-T} = 11.48 \pm 0.34$$

$$k_1^{-D}/k_1^{-T} = 1.81 \pm 0.06$$

$$r = 1.32 \pm 0.06$$

These values were derived from plots of absorbance vs. time, which are not zero order in  $[\text{I}_3^-]$ . The non-existence of zero order kinetics has been interpreted as being due to the fact that reprotonation of the intermediate enolate anion is relatively fast compared with its reaction with iodine, this leading to an intermediate order with respect to  $[\text{I}_3^-]$ . The study of the ionization behaviour of 1,3-dimethylindolin-2-one

in aqueous methanol tetraborate buffers was repeated and compared with the ionization in aqueous tetraborate buffers. It was found that it is the presence of methanol which causes the deviation from zero order kinetics.

Comparison of the hydroxide rate coefficients in both aqueous methanol and in water shows that the main difference resides in the value of  $k_1^{-H}$ . In fact,  $k_1^{-H}$  in water is ca. 50% higher than in aqueous methanol. This can be due to the fact that, while in water  $OH^-$  is solvated by only water molecules, in aqueous methanol  $OH^-$  is solvated both with water and methanol molecules which are bigger and heavier. Therefore, the species which effects the abstraction of the proton in the transition state is heavier in methanol-water than in water<sup>124</sup>, this implying that tunnelling could be less important in the former than in the latter medium.

### 2.3.2. In acidic media

Since in acidic media the oxidation of indolin-2-ones is not so facile as in alkaline media, the protodeuteriation of 1,3-dimethyl-3- $[^2H_1]$ -indolin-2-one in  $H_2SO_4$  was followed by Mass Spectrometry.

#### 2.3.2.1. RESULTS

$k_0^{-D}$  were derived from the slopes of the lines obtained when plotting  $\log(\% \text{ deuteriated substrate})$  vs. time. The percentage of deuteriated substrate was calculated from the heights of the expanded molecular ion peaks corresponding to the labelled and unlabelled compounds, according to



Equation 2.3.9, where  $M_D^C = M_D - 0.118 M_H$ .  $M_D$  is the observed

$$\% \text{ Deuteriated substrate} = (M_D^C/M_D^C + M_H) 100 \quad (2.3.9)$$

height of the expanded peak corresponding to the labelled compound,  $M_H$  the observed height of the unlabelled compound,  $0.118 M_H$  the theoretical value of the  $M_H + 1$  peak and  $M_D^C$  the corrected value for  $M_D$ .

Table 2.3.6 shows the value of  $k_o^{-D}$ , measured in aqueous  $H_2SO_4$ , and Figure 2.3.4 compares those values with values obtained for the protodeuteration of the same compound (See Table 2.2.14). The ratio of the slopes of the lines in Figure 2.3.4 give an isotope effect,  $k^{-D}/k^{-T} = 2.4$

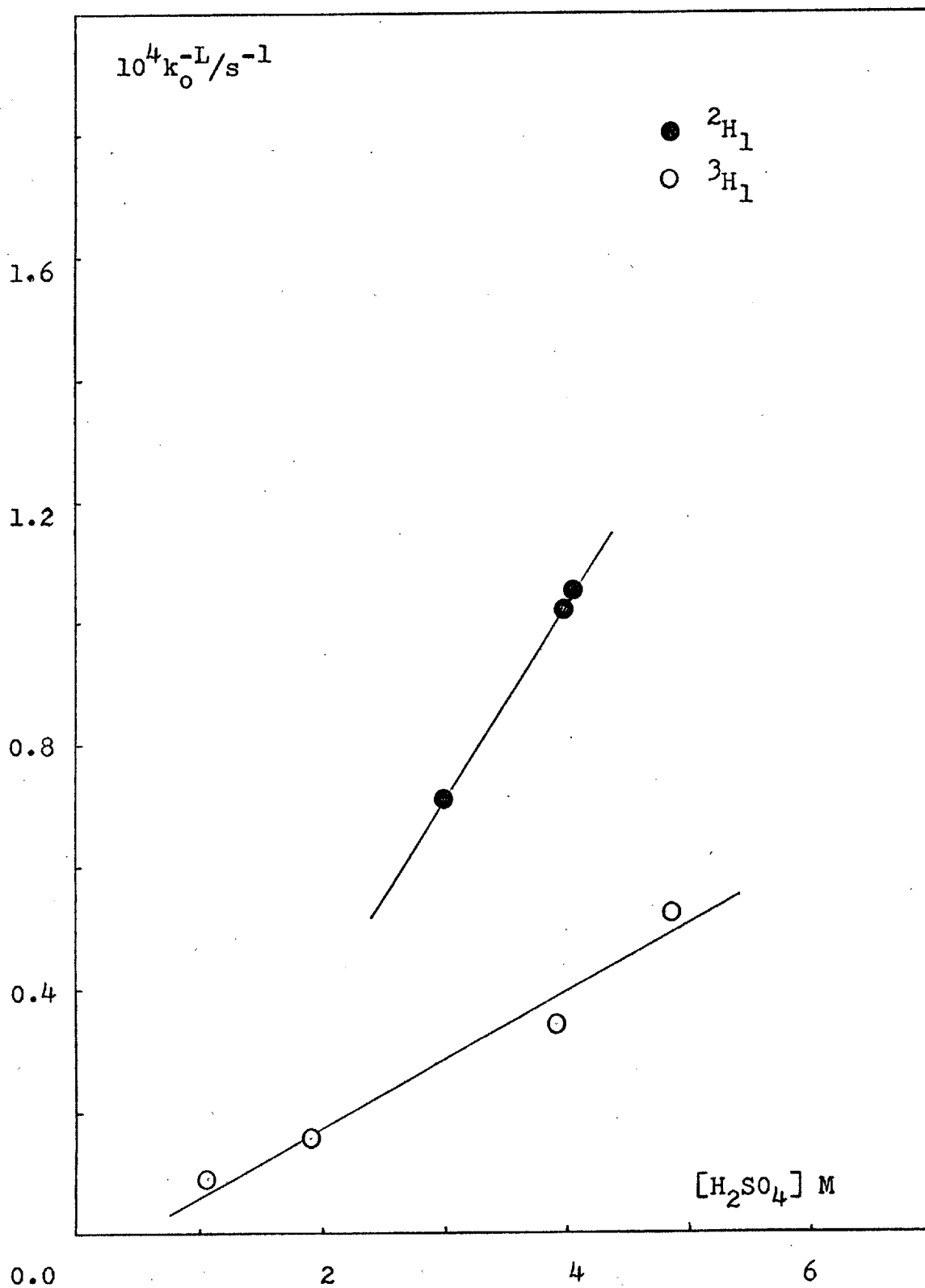
Table 2.3.6 - Protodeuteration of 1,3-dimethyl-3- $[^2H_1]$ -indolin-2-one in sulphuric acid

$[H_2SO_4]$ M	$10^4 k_o^{-D}/s^{-1}$
3.0	0.71
4.0	1.02
4.1	1.05

#### 2.3.2.2. DISCUSSION

The theoretical values of  $k^{-D}/k^{-T}$  calculated from force constants<sup>125</sup> lie in the range 2.26 - 2.34. The experimental value reported in the previous section for the ionization of 1,3-dimethylindolin-2-one is, therefore, very near the

Figure 2.3.4 - Protodetrition and protodeuteriation of 1,3-dimethyl-3- $^{3}\text{H}_1$ -indolin-2-one and 1,3-dimethyl-3- $^{2}\text{H}_1$ -indolin-2-one respectively, in  $\text{H}_2\text{SO}_4$



theoretical values. If the Swain-Schaad relationship is assumed to be valid for the hydrogen exchange in acidic media, a value of 7.2 for  $k^{-H}/k^{-D}$  is calculated.

Since the methods used to follow both the protodetrutiation and protodeuteriation are accurate to less than 1%, the value of the PKIE in acidic media must, therefore, be more accurate than in alkaline media.

#### 2.4. THE GEOMETRY OF THE TRANSITION STATE OF THE HYDROGEN EXCHANGE REACTION OF INDOLIN-2-ONES. BRØNSTED PARAMETERS, HAMMETT VALUES AND PKIE

Table 2.4.1 and Figure 2.4.1 show the correlation between the values of the catalytic rate coefficients,  $k_1^{-T}$ , obtained from the data already reported in Tables 2.2.1 to 2.2.11, with the  $pK_A$  of the catalyst. Oxygen bases, apart from hydroxide, define a good straight line but, nitrogen bases show a greater deviation from the mean. Hydroxide and hydronium ions usually do not conform to the Brønsted relationship. Kresge<sup>45</sup> shows a list of examples in which it can be seen that there is seldom good agreement between observed and calculated hydroxide and hydronium catalytic rate coefficients. The deviation of hydroxide and hydronium ions is explained by the fact that these ions in water are more strongly solvated than most acids and bases<sup>52</sup>. Desolvation of the catalyst will, therefore, require an extra amount of energy and that will make a greater contribution to the

Table 2.4.1 - Brønsted plot for the base-catalysed protodetrutiation of 5-nitro-3-[<sup>3</sup>H<sub>1</sub>]-indolin-2-one

Buffer	pK <sub>A</sub>	10 <sup>2</sup> k <sub>1</sub> <sup>-T</sup> /l mol <sup>-1</sup> s <sup>-1</sup>
Hydroxide	15.95	6810
Phenol	9.89	365
4-Chlorophenol	9.18	246
Morpholine	8.33	111
4-Nitrophenol	7.15	10.6
Methylimidazole	6.95	1.76
Imidazole	6.95	1.83
Pyridine	5.25	1.09
Acetate	4.75	0.136

reaction barrier when the proton transfer involves hydroxide or hydronium ion than when it involves other acids or bases. If the hydroxide ion catalytic rate coefficient is ignored, a value of  $\beta = 0.71$  is calculated. A value of  $\alpha$  can also be generated for the hydrogen exchange in alkaline media if log catalytic rate coefficients for the 5-substituted indolin-2-ones shown in Table 2.2.18 are plotted against the pK<sub>A</sub> of the substrate (Figure 2.4.2). Both values of  $\alpha$  and  $\beta$  indicate that, in alkaline media, the transition state must be product-like.

In acidic media, the value of  $\alpha$  which is obtained by plotting  $\log k_2^{-T}$  vs. pK<sub>A</sub> of the substrate (Figure 2.4.3) is 0.28. This suggests that, in acid, the transition state is reactant-like.

Comparison of the  $\rho$  values both in acidic (0.66, Figure 2.2.19) and in alkaline (1.6 - 1.7, Figure 2.2.8)

Figure 2.4.1 - Brønsted plot for the protodetritiation of 5-nitro-3- $^{3}\text{H}_1$ -indolin-2-one in alkaline media

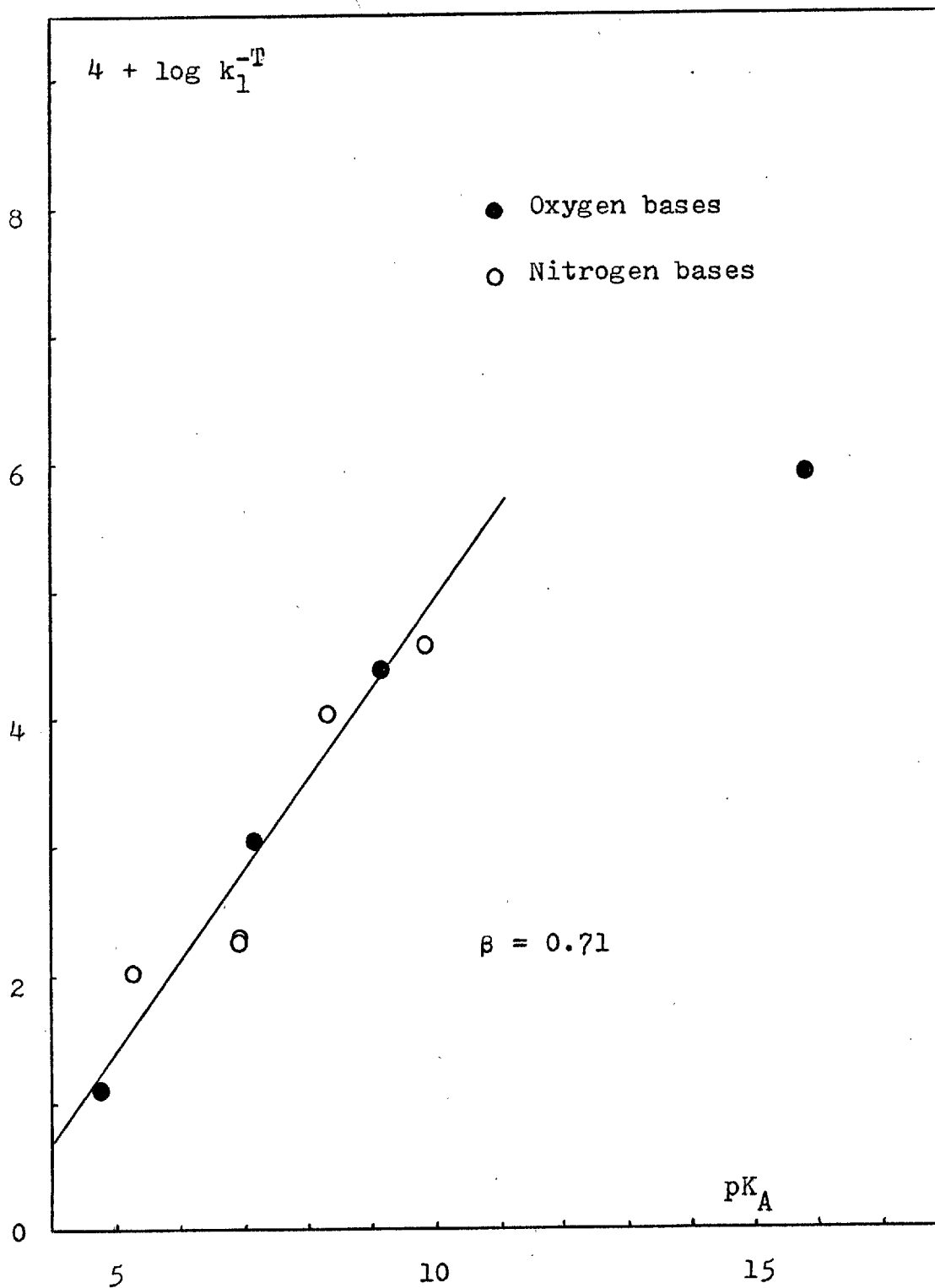


Figure 2.4.3 - Brønsted plot for the protodetrition of 5-X-3- $[^3\text{H}]$ -indolin-2-ones in acidic media ( $\text{H}_2\text{SO}_4$ )

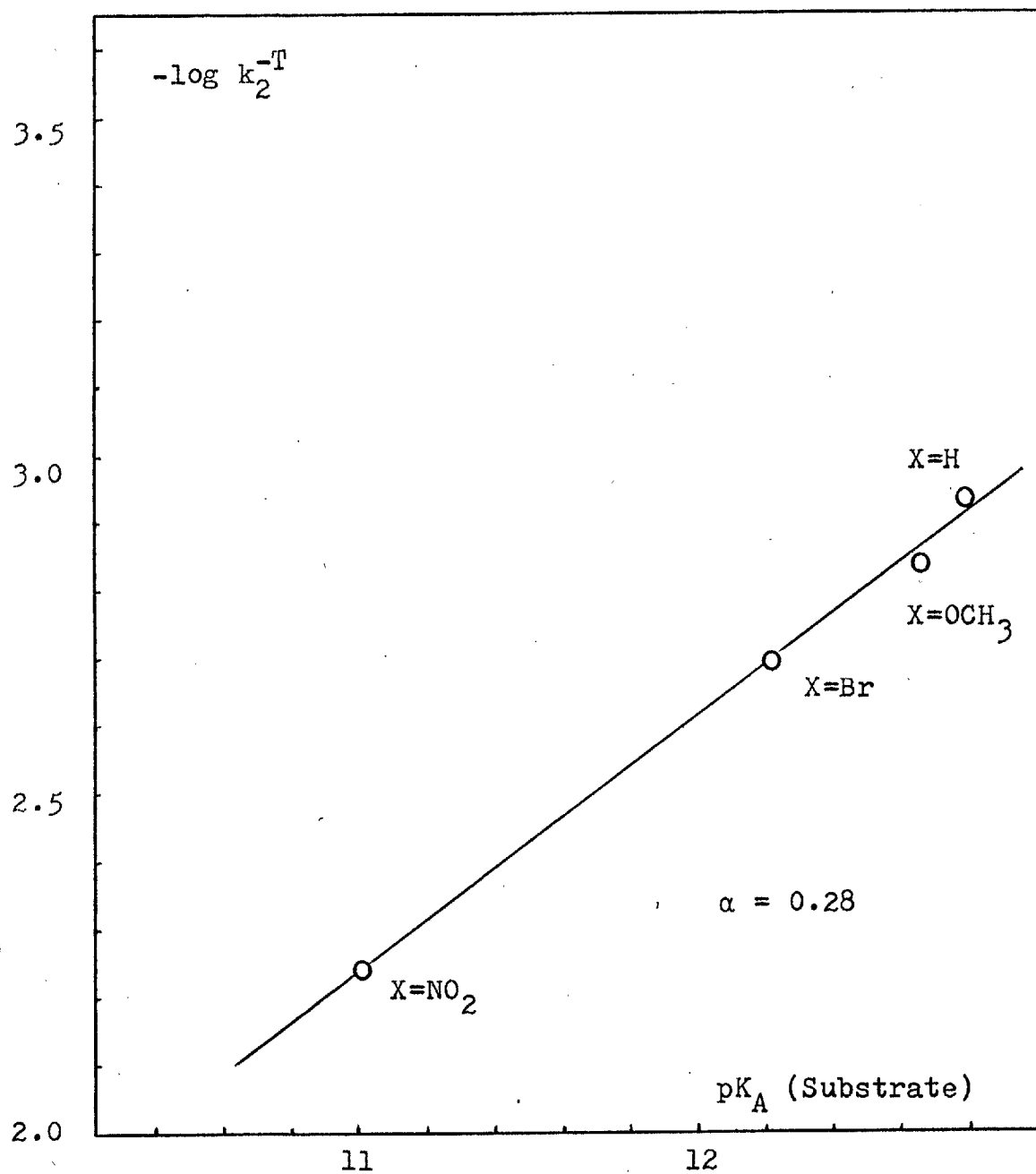
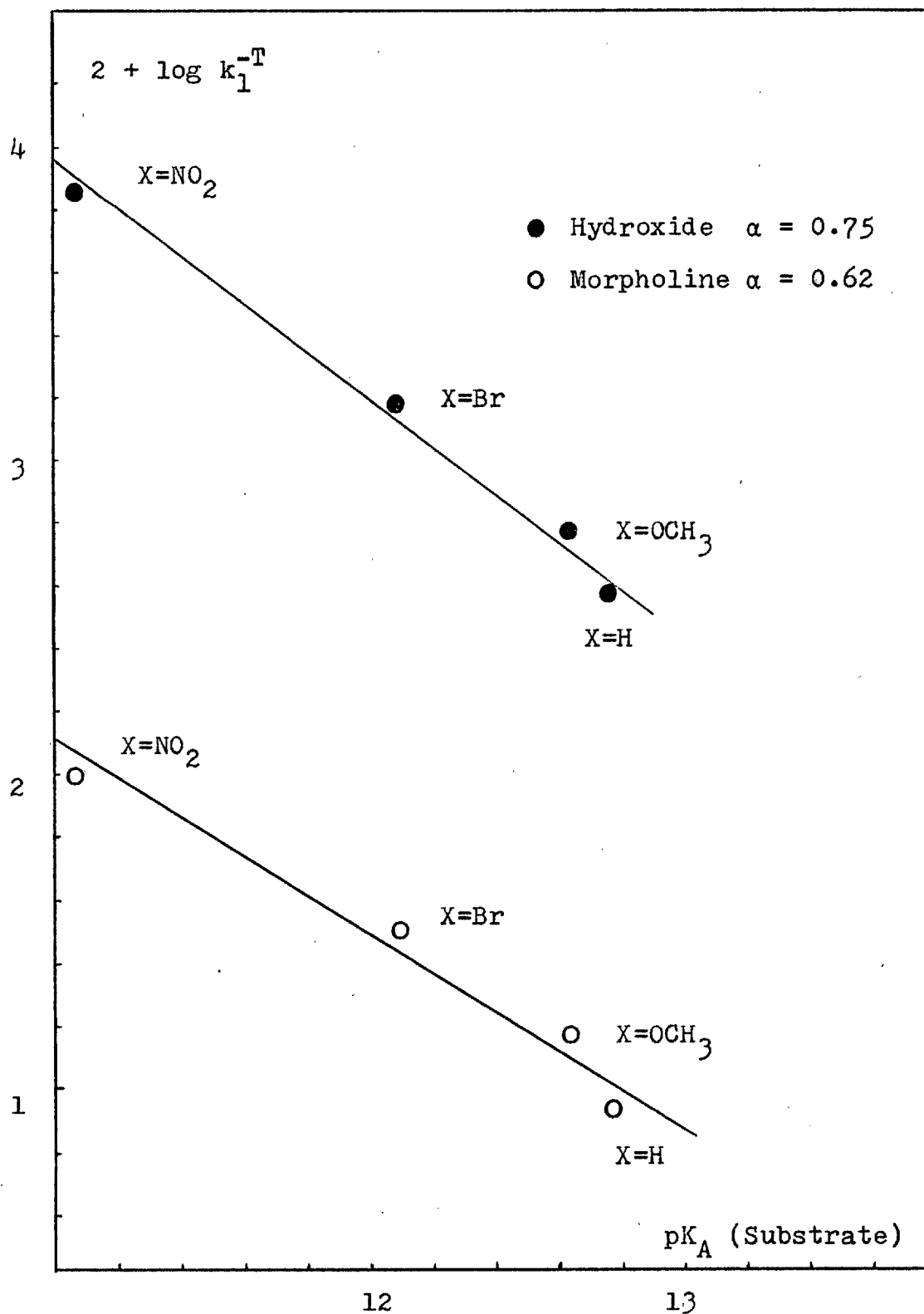


Figure 2.4.2 - Brønsted plots for the protodetrition of 5-X-3-[<sup>3</sup>H<sub>1</sub>]-indolin-2-ones in morpholine buffers



media shows that the amount of negative charge generated in the transition state on the 3-C is smaller in acid. This also implies a later transition state in alkaline media.

Steric effects are greater in alkaline media by a factor of ca. 4. This also points to a more product-like transition state in base, that is, a transition state where the 3-C has a greater  $sp^2$  character. As already considered in Section 2.2.2.2 - D, steric interaction is more important in the planar structure of the intermediate enol/enolate than in the ketonic tautomer. Therefore, the later the transition state, the higher the activation energy for the rate determining step and the more important the steric effects are.

Although experimental evidence seems to indicate transition states with different symmetry in alkaline and acidic media, the primary kinetic isotope effects are of the same order, ca. 7, and suggest a symmetric transition state. Therefore, the present results suggest that there is not a relationship between transition state symmetry and PKIE for the hydrogen exchange reaction of indolin-2-ones.

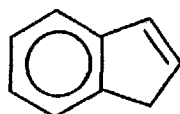


## 2.5. COMPARATIVE HYDROGEN EXCHANGE OF INDOLIN-2-ONES AND RELATED AMIDES

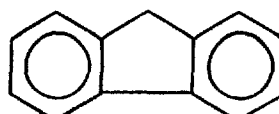
### 2.5.1. INTRODUCTION

Both rate of hydrogen exchange and  $pK_A$  of carbon acids have been qualitatively compared on basis of the relative stability of their conjugate base, a carbanion. Cram<sup>126</sup> has discussed carbanion structure and its stabilization in terms of s-orbital effects, conjugative effects, inductive effects, homoconjugative effects, aromatization effects, negative hyperconjugative effects and d-orbital overlap effects. Of these effects it is the aromatization that appears to be the main cause of the facility of ionization and, therefore, of hydrogen exchange of indolin-2-ones relative to other amides. This effect will be considered briefly.

Molecular orbital symmetry predicts that, of the completely conjugated planar monocyclic polyolefins, those that possess  $(4n + 2)\pi$  electrons ( $n = 0, 1, 2, 3, \dots$ ) will be particularly stable because they have completely filled bonding molecular orbitals with substantial electron delocalization energies<sup>127</sup>. The same should happen with carbocyclic unsaturated anions that fulfil the  $4n + 2$  condition e.g. cyclopentadiene and cyclononatetraene anions. The fact that the  $pK_A$  of the conjugate acids of those anions is considerably lower than the  $pK_A$  of their open-chain analogues <sup>t</sup>at tests the qualitative agreement between theory and experiment<sup>126</sup>. Also, indene



Indene



Fluorene

and fluorene, whose anions are fully conjugated species, exhibit enhanced acidities. The concept that aromaticity is an important factor in stabilizing both neutral molecules and charged species has been extended to transition states. In 1939 Evans<sup>128</sup> suggested that pericyclic reactions that proceed through aromatic transition states are favoured relative to others whose transition states are non-aromatic and Dewar<sup>129</sup> in 1971 discussed the subject in terms of more recent theories applying the theoretical predictions to well known reactions, such as the Claisen and Cope rearrangements. The general conclusion is that, in fact, reactions that go through aromatic transition states are favoured, but, at the same time, it is emphasized that antiaromatic reactions are no less possible than antiaromatic conjugate systems.

In the indolin-2-one case, the intermediates of the exchange reaction in acidic and alkaline media are, respectively, the enol and the enolate anion shown in Figure 2.5.1. Both these species are fully conjugated and fulfill the  $4n + 2$  condition. If one assumes that the structural features that

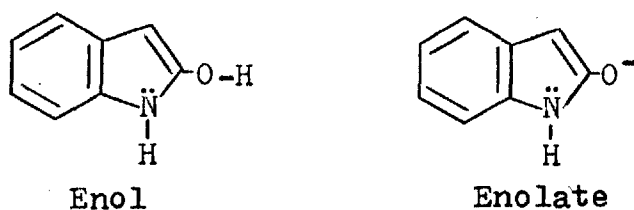
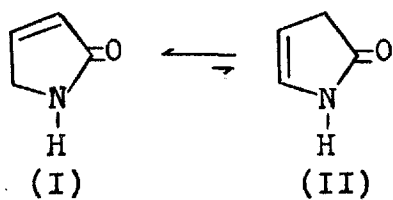


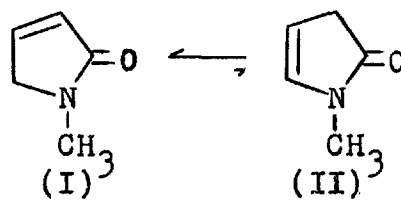
Figure 2.5.1

stabilize the intermediate are also operating in the transition state of the rate determining step, it is understandable that indolin-2-ones show a high rate of exchange when compared with amides and lactams in general.

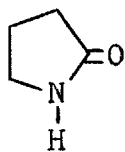
To confirm that the aromaticity of the intermediate is an important factor, the relative rate of exchange of the amides shown in Figure 2.5.2 was studied.



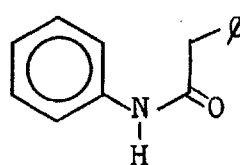
3-Pyrrolin-2-one



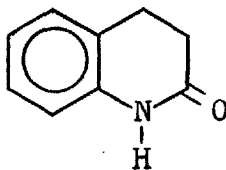
1-Methyl-3-pyrrolin-2-one



2-Pyrrolidone



N-Phenyl phenylacetamide



2-Ketotetrahydroquinoline

Figure 2.5.2

### 2.5.2. RESULTS

3-Pyrrolin-2-one. This compound exists as an equilibrium mixture, as shown in Figure 2.5.2, tautomer (I) being more stable than tautomer (II)<sup>130,131</sup>. The hydrogen exchange reaction was studied by NMR in D<sub>2</sub>O, at 34°C, and, it was found that hydrogen at the 3-position of (II) exchanges rapidly in the absence of base or acid catalyst ( $k_0$  ca.  $1 \times 10^{-4} \text{ s}^{-1}$ ), as shown in Figure 2.5.3. The hydrogens at the 5-position of (I) do not exchange. If DCl (ca. 2%) is added to the solution form (II) exchanges faster ( $k_0$  ca.  $6 \times 10^{-4} \text{ s}^{-1}$ ) and so does form (I) ( $k_0$  ca.  $1 \times 10^{-4} \text{ s}^{-1}$ )

N-Methyl-3-pyrrolin-2-one. The compound also exists as an equilibrium mixture with tautomer (I), where the double-bond is conjugated to the carbonyl as in the previous compound, being more stable than (II). The hydrogen exchange with D<sub>2</sub>O at 34°C was studied both in acid and in alkaline media. In acidic medium (2% DCl) some other reaction becomes dominant and it was not possible to quantify the rate of exchange in these conditions. In alkaline medium (0.1% NaOH) the exchange can be detected by the disappearance of the methylene peak of the 3-position and by the collapsing of the multiplet corresponding to the hydrogen on the 4-position to a singlet. A value of  $3 \times 10^{-2} \text{ s}^{-1}$  was found for  $k_0$ .

2-Pyrrolidone. No appreciable deuteration was detected by NMR in 1M NaOD/D<sub>2</sub>O even after ca. one month at 100°C.

Figure 2.5.3 - Hydrogen exchange of 3-pyrrolidin-2-one in D<sub>2</sub>O followed by NMR

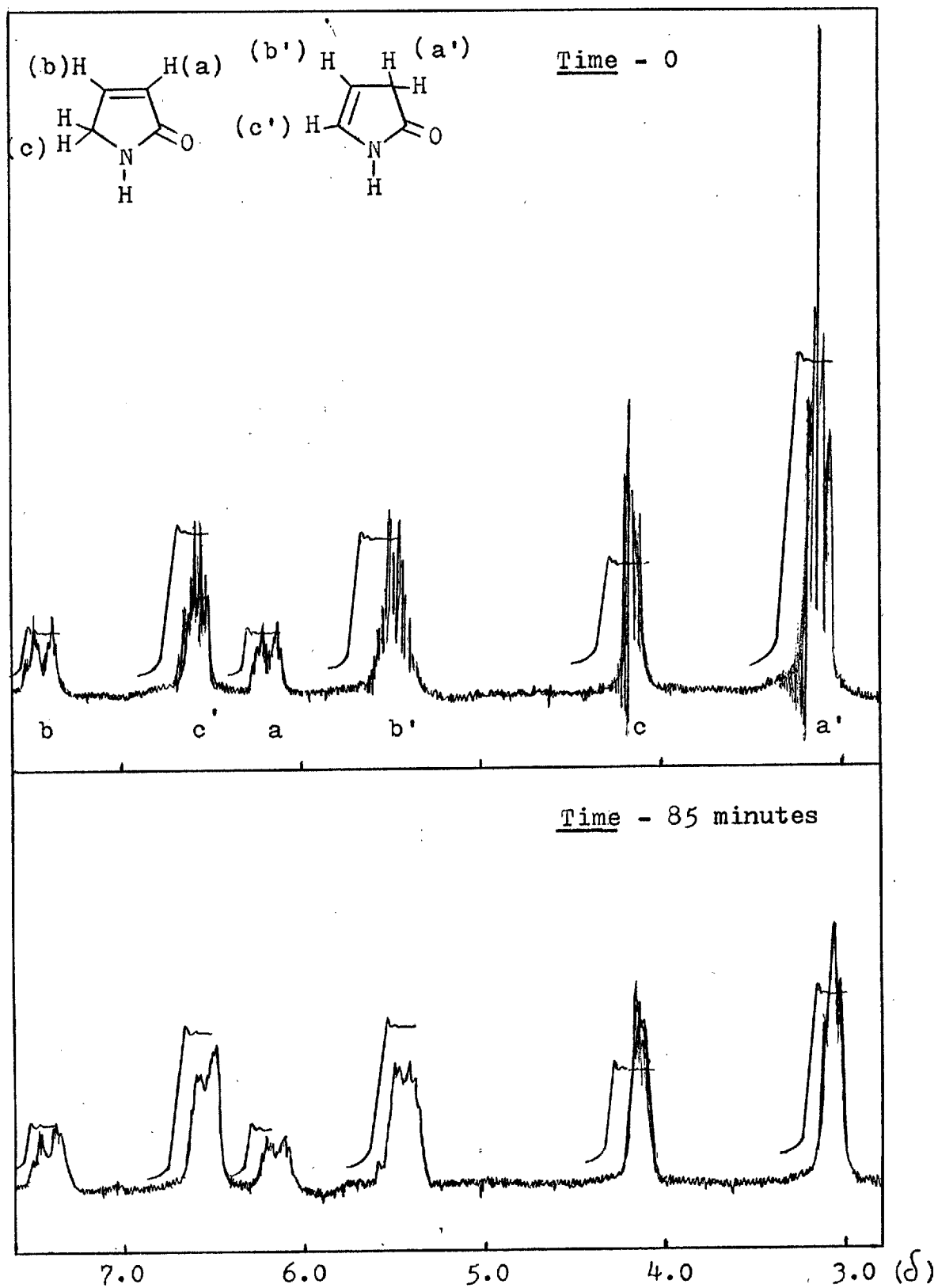
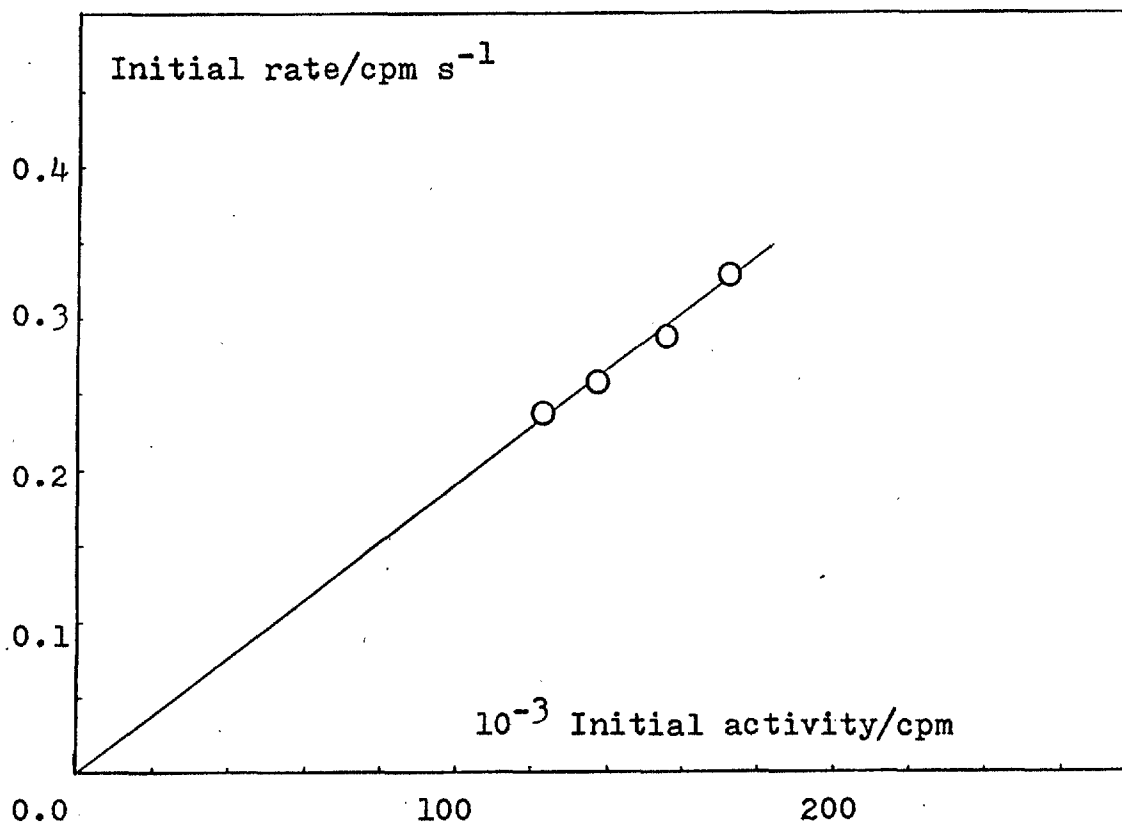


Table 2.5.1 - Protodetrition of N-phenyl phenyl-2-[<sup>3</sup>H<sub>1</sub>]-acetamide in 5.2 M sulphuric acid

<u>Initial rate/cpm s<sup>-1</sup></u>	<u>Initial activity/cpm</u>
0.331	171,000
0.279	155,000
0.260	137,500
0.237	122,500

$$k_o^{-T} = 0.019 \times 10^{-4} \text{ s}^{-1}$$

Figure 2.5.4 - Protodetrition of N-phenyl phenyl-2-[<sup>3</sup>H<sub>1</sub>]-acetamide in 5.2 M sulphuric acid



N-Phenyl phenylacetamide. Rates of protodetrition of N-phenyl phenyl-2- $^{[3}\text{H}_1]$ -acetamide were measured in 0.1 M NaOH ( $k_0 = 0.029 \times 10^{-4} \text{ s}^{-1}$ ) and in 5.2 M  $\text{H}_2\text{SO}_4$  ( $k_0 = 0.018 \times 10^{-4} \text{ s}^{-1}$ ). The rate constant in acid was determined by the differential method<sup>96</sup>, as shown in Table 2.5.1 and Figure 2.5.4.

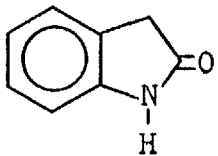
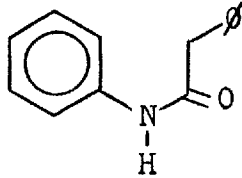
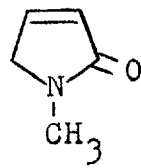
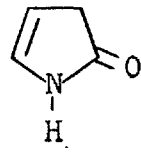
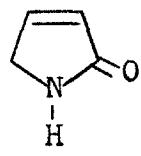
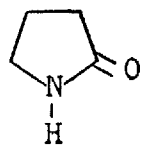
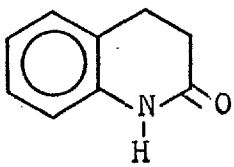
2-Ketotetrahydroquinoline. The reactivity of this compound was directly compared with that of indolin-2-one. It was found that whilst indolin-2-one in ether exchanged heterogeneously with 0.1 M NaOH/ $\text{D}_2\text{O}$  over night, almost completely, and, in  $\text{D}_2\text{SO}_4/\text{D}_2\text{O}$  (1:1) with an approximate rate constant of  $6 \times 10^{-4} \text{ s}^{-1}$ , 2-ketotetrahydroquinoline had not exchanged after a period of three weeks in the same conditions. The exchange in alkaline  $\text{D}_2\text{O}$  could not be directly studied by NMR due to insolubility of the compound in water.

The catalytic rate coefficients for hydroxide and the observed rate constants in acidic media for these amides are compared with the corresponding values obtained for indolin-2-one in Table 2.5.2

### 2.5.3. DISCUSSION

Even if the results obtained by NMR are not so accurate as the protodetrition rates, they still show that exchange only occurs when the enol or enolate anion which forms by hydrogen abstraction is an aromatic entity. However, the hydrogen at the 5-position of 3-pyrrolin-2-one (I) exchanges

Table 2.5.2 - Relative rate of exchange of indolin-2-one and related amides

	$k_0/s^{-1}$ (Aqueous acidic media)	$k_1/l\ mol^{-1}s^{-1}$ (Aqueous NaOH)
	$3 \times 10^{-4*}$ (5M $H_2SO_4$ )	3.58*
	$2 \times 10^{-6*}$ (5.2M $H_2SO_4$ )	$2.9 \times 10^{-5*}$
	-	1.2 <sup>‡</sup>
	$6 \times 10^{-4\dagger}$ (ca. 2% DCl)	-
	$3 \times 10^{-4\dagger}$ (ca. 2% DCl)	-
	-	$< 10^{-8**}$
	$< 10^{-6\dagger}$	$< 10^{-6\dagger}$

\* Protodeuteration rates measured at 25°C

\*\*Deuteration rates measured at 100°C

‡ Deuteration rates measured at 34°C



more slowly than the 3-hydrogens of (II), although they have to go through the same intermediate. This may be explained by the fact that (I) is more stable than (II)<sup>130</sup> and, therefore, requires more energy to form the intermediate, as shown in Figure 2.5.5

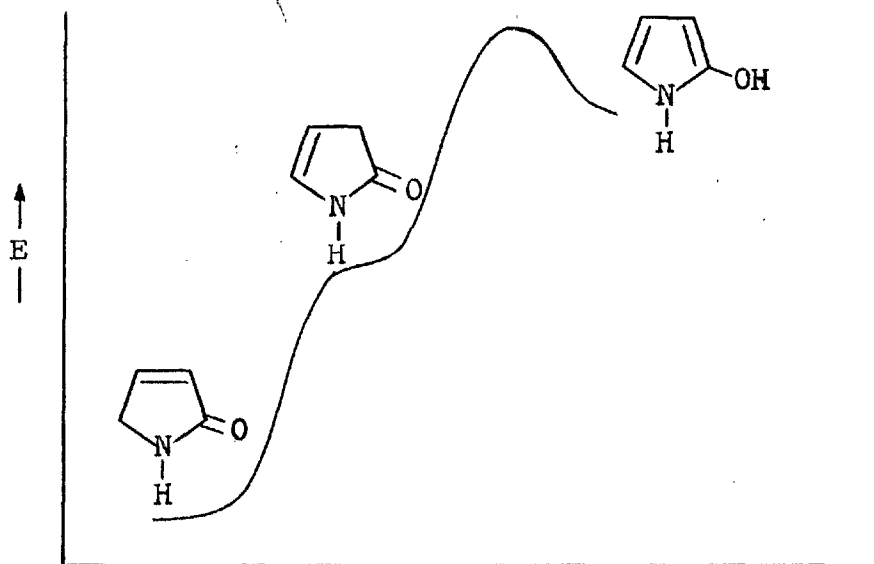


Figure 2.5.5

Both 2-pyrrolidone and 2-ketotetrahydroquinoline are very unreactive towards hydrogen exchange but N-phenyl phenylacetamide exchanges slowly although the intermediate is not an aromatic one. This is due to the fact that, in N-phenyl phenylacetamide, the position of exchange, being  $\alpha$  to both a benzene ring and a carbonyl group, is stabilized by resonance through those two moieties.

3. EXPERIMENTAL

### General procedures

Infrared spectra were recorded as either nujol mulls or liquid films on a Perkin-Elmer 157G Grating Infrared Spectrophotometer. Proton NMR spectra were recorded on a Varian T60 NMR Spectrometer, in the stated solvent, with tetramethylsilane as internal reference. Ultraviolet spectra were recorded on either a Unicam SP1800 or SP800 Spectrophotometer. Mass spectra were recorded on a VG Micromass 7070 Spectrometer.

pH Measurements were made on a Radiometer pHMeter 26, using a G202B glass electrode calibrated with standard aqueous buffers.

Liquid scintillation counting of radioactive samples was performed using a Beckman LS200 Scintillation Counter in a scintillating solution of 2,5-diphenyloxazole (4 g) and 1,4-bis 2-(4-methyl-5-phenyloxazole)benzene (0.1 g) in xylene (1000 ml).

Melting points were determined on a Kofler hot stage apparatus and are uncorrected.

Kinetic runs were carried out at 25°C, except when stated otherwise.

Dissociation constants were measured at 25°C.

### 3.1. PURIFICATION OF REAGENTS AND SOLVENTS

Deuteriated solvents and reagents (Merck, Sharp and Dohme) were used without further purification except for  $D_2SO_4$  which was purified by distillation, b.p.  $143^\circ C / 0.5$  mm.

Sodium chloride, sodium perchlorate, potassium iodide, phenol, tris(hydroxymethyl)methylamine (TRIS), acetic acid, hydrochloric acid and sulphuric acid were all 'Analar' grade reagents and used without further purification. BDH standard volumetric (AVS) solutions of NaOH and HCl were used for volumetric standardisations.

The following amines were dried over NaOH then purified by distillation: piperidine, b.p.  $105-106^\circ C$ ; N-methylimidazole, b.p.  $97^\circ C / 20$  mm; morpholine b.p.  $128-129^\circ C$ ; pyridine, b.p.  $115^\circ C$ . p-Chlorophenol was purified by recrystallization from petroleum ether  $80-100^\circ$ , m.p.  $42-43^\circ C$ ; imidazole from ether/petroleum ether  $80-100^\circ$ , m.p.  $88-89^\circ C$ ; p-nitrophenol from ether/petroleum ether  $60-80^\circ$ , m.p.  $112-114^\circ C$  (purity also checked by TLC and NMR). Iodine was purified by sublimation.

Dioxan and THF were heated under reflux over sodium hydride for 10 hours then fractionally distilled and used immediately. Peroxide free ether was also obtained by heating under reflux over sodium hydride followed by distillation.

### 3.2. SYNTHESIS OF SUBSTRATES

1,3-Dimethylindolin-2-one. N-Methylaniline (67 g, 0.63 moles) was dissolved in dry benzene and 2-bromopropionyl bromide (59 g, 0.28 moles) was added slowly with cooling and stirring over a period of three hours and the mixture was left over night. The amine hydrobromide was separated and washed with dry benzene. The organic solution was washed with 2% HCl, dried and the solvent evaporated. To the residue of the 2-bromo-N-methyl-N-phenylpropionamide, cooled in an ice bath, aluminium trichloride (65 g, 0.48 moles) was added in small portions and the mixture heated at 130-140°C for 20 minutes. After cooling, ice was added and then 2% HCl. The mixture was extracted with ether, the organic fraction washed with 2% HCl, then 5% Na<sub>2</sub>CO<sub>3</sub>, dried and the solvent evaporated. The residue (22 g) was distilled and a yellowish liquid (17.4 g, 40%) b.p. 130-132°C / 11 mm (Lit.<sup>67</sup> 136-138°C / 11 mm) which solidified on cooling was obtained. Two recrystallizations from petroleum ether 60-80° gave white crystals m.p. 55-56°C (Lit.<sup>95</sup> 56°C).

IR (Nujol)  $\nu_{\max}$  3040, 2970, 2940, 1700, 1600 cm<sup>-1</sup>

NMR (CDCl<sub>3</sub>)  $\delta$  1.35 (3H, d, J=7 Hz), 3.1 (3H, s), 3.19 (1H, q, J=7 Hz), 6.9 (4H, m)

MS m/e 161 (M<sup>+</sup>), 146, 118, 91

Found C, 74.37; H, 6.87; N, 8.63 %. Calculated for C<sub>10</sub>H<sub>11</sub>NO:  
C, 74.5; H, 6.87; N, 8.64 %

4,6-Di<sup>t</sup>butylindolin-2-one. A solution of liquid chlorine (2 ml) in dry dichloromethane (10 ml) was added to dichloromethane cooled at  $-68^{\circ}\text{C}$ , under nitrogen. Ethylmercaptoacetate<sup>132</sup> (5.9 g, 0.044 moles) in dichloromethane (20 ml) was added dropwise with stirring, the temperature being maintained under  $-60^{\circ}\text{C}$  and the mixture was stirred for 15 minutes. 3,5-Di<sup>t</sup>butylaniline<sup>133</sup> (17.7 g, 0.088 moles) in dichloromethane (50 ml) was added dropwise over a period of 1 hour with stirring, the temperature still under  $-60^{\circ}\text{C}$ . Stirring was continued for 6 hours at  $-68^{\circ}\text{C}$ . After that period triethylamine (10 ml) was added dropwise and the mixture stirred for 30 minutes further. After having warmed to room temperature, the reaction mixture was washed with water, dried and the solvent evaporated. The oily brown residue was redissolved in ether and poured into sodium ethoxide<sup>134</sup> (5.9 g sodium, 50 ml ethanol) and the mixture stirred at room temperature for 1 hour. The solvent was evaporated, the residue redissolved in ether and the organic solution washed with water, dried and the solvent evaporated (17 g). The oily residue was redissolved in absolute ethanol and  $\text{W}_4$  Raney-Nickel (25 g)<sup>135</sup> was added. The mixture was heated under reflux until TLC (silica, chloroform/methanol 100:1) showed no indication of the sulphurated compound (3 hours). The catalyst was separated, the ethanol evaporated (15 g) and hexane added to the residue. The yellowish solid which precipitated (3.4 g, 10%) was recrystallized twice from dichloromethane/hexane to give a white crystalline compound (1.5 g) m.p.  $205-206^{\circ}\text{C}$  (Lit.<sup>95</sup>  $209-210^{\circ}\text{C}$ ).

IR (Nujol)  $\nu_{\max}$  3120, 1700, 1610, 1575, 875  $\text{cm}^{-1}$

NMR ( $d_6$ -DMSO)  $\delta$  1.10, 1.15 (18H, 2s), 3.5 (2H, s), 6.6, 6.9 (2H, dd,  $J=2$  Hz)

MS m/e 245 ( $M^+$ ), 230, 174

5-Methoxyindolin-2-one. Liquid chlorine (2 ml) in dichloromethane (10 ml) was poured into dichloromethane previously cooled to  $-65^\circ\text{C}$ . Ethylmercaptoacetate<sup>132</sup> (5.9 g, 0.044 moles) in dichloromethane (10 ml) was added dropwise over a period of 25 minutes with stirring, the temperature being maintained at  $-60^\circ\text{C}$ . 4-Methoxyaniline (10.8 g, 0.088 moles) in dichloromethane (30 ml) was added dropwise for 25 minutes maintaining the temperature below  $-60^\circ\text{C}$ , and the mixture was stirred for 1 hour at  $-60^\circ\text{C}$ . Triethylamine (10 ml) was added, the mixture stirred for 30 minutes further and then allowed to warm to room temperature. Water (50 ml) was added and the organic layer washed, separated, dried and the solvent evaporated. The residue was redissolved in ether (150 ml) and stirred over night with 2M HCl (30 ml). The organic layer was separated, washed, dried and the solvent evaporated. The residue, when treated with MeOH, yielded a yellowish solid (4.8 g, 56 %). This material (500 mg) in absolute EtOH (50 ml) was heated under reflux with  $W_{44}$  Raney-Nickel (ca. 1 t. s.) for 2 hours. The catalyst was separated, the alcohol evaporated and the residue recrystallized from dichloromethane/petroleum ether  $40-60^\circ$  to give a white crystalline solid (210 mg, 55 %) m.p.  $152-153^\circ\text{C}$  (Lit.<sup>72</sup>  $152-154^\circ\text{C}$ )

IR (Nujol)  $\nu_{\max}$  3160, 1690, 1140, 1040  $\text{cm}^{-1}$

NMR ( $\text{CDCl}_3$ )  $\delta$  3.55 (2H, s), 3.8 (3H, s), 6.8 (3H, m)

5-Nitroindolin-2-one. Indolin-2-one (1 g) in concentrated sulphuric acid (10 ml) was cooled to  $-5^\circ\text{C}$ . Fuming nitric acid (ca. 0.9 ml) was added dropwise with stirring and cooling. After 30 minutes at  $0^\circ\text{C}$ , the mixture was poured into ice and the precipitate separated. The crude product was recrystallized from acetic acid, sublimed and recrystallized again from dioxane/water to give pale yellow crystals (0.64 g, 48 %) m.p.  $240-241^\circ$  (Lit.<sup>69</sup>  $240-241^\circ\text{C}$ ).

IR (Nujol)  $\nu_{\max}$  3180, 1710, 1610, 1600, 1510, 1340  $\text{cm}^{-1}$

NMR ( $d_6$ -DMSO)  $\delta$  3.58 (2H, s), 6.95 (1H, d,  $J=8$  Hz), 11.50 (1H, broad s, exch.)

MS m/e 178 ( $\text{M}^+$ ), 132, 104

1,3-Dimethyl-5-nitroindolin-2-one. The nitration of 1,3-dimethylindolin-2-one (820 mg) was carried out by the above procedure. The crude product was recrystallized from EtOH yielding yellow needles (530 mg, 51 %) m.p.  $149-150^\circ\text{C}$ .

IR (Nujol)  $\nu_{\max}$  1715, 1600, 1505, 1400, 1315  $\text{cm}^{-1}$

NMR ( $\text{CDCl}_3$ )  $\delta$  1.35 (3H, d,  $J=7$  Hz), 3.1 (3H, s), 3.3 (1H, q,  $J=7$  Hz), 7.1 (1H, d,  $J=8$  Hz), 8.10-8.15 (2H, s and d,  $J=8$  Hz)



MS m/e 206 ( $M^+$ ), 191, 176, 160, 148

Found C, 58.27; H, 4.86; N, 13.59 %.  $C_{10}H_{10}N_2O_3$  requires  
C, 58.27; H, 4.84; N, 13.51 %

5-Bromoindolin-2-one. Bromine (1.6 g, 0.01 moles) and potassium bromide (2.4 g, 0.01 moles) in water (5 ml) were added slowly with stirring to a hot solution of indolin-2-one (1.33 g, 0.01 moles) in water (40 ml). The precipitate was separated and recrystallized twice from EtOH to give white crystals (1.05 g, 50 %) m.p. 220-221°C (Lit.<sup>70</sup> 220°C).

IR (Nujol)  $\nu_{max}$  3150, 1730, 1695, 1610  $cm^{-1}$

NMR ( $d_6$ -DMSO)  $\delta$  3.55 (2H, s), 7.4-6.8 (3H, dd, J=8 Hz)  
10.5 (1H, broad, s, exch.)

1,3-Dimethyl-4,6-di<sup>t</sup>butylindolin-2-one. Sodium hydride (250 mg, 80 % dispersion in oil) previously washed with petroleum ether was mixed with a solution of 4,6-di<sup>t</sup>butylindolin-2-one (940 mg, 3.84 mmoles) in dry benzene (30 ml). Methyl iodide (2.2 g, 15 mmoles) was then added and the solution heated under reflux until TLC (silica, chloroform/MeOH 100:1) showed no signs of starting material (3 hours). The mixture was poured into ice, the organic layer separated, washed twice with water, dried and the organic solvent evaporated. The residue was dissolved in toluene (50 ml) and added to sodium hydride (1 g, 80 % dispersion in oil) previously washed with

petroleum ether. After the addition of methyl iodide (45 mmoles), the solution was heated under reflux until no appreciable amount of starting material was evident by NMR (6 hours). The mixture was poured into ice, the organic layer separated, washed with water, dried and the solvent evaporated. The residue was chromatographed on neutral alumina with petroleum ether 60-80°/chloroform and the middle fraction recrystallized from petroleum ether 40-60° to give white crystals (381 mg, 36 %) m.p. 105-106°C (Lit.<sup>95</sup> 101-102°C).

IR (Nujol)  $\nu_{\max}$  1104, 1615, 1580, 1005, 860  $\text{cm}^{-1}$

NMR ( $\text{CDCl}_3$ )  $\delta$  1.32, 1.42 (18H, 2s), 1.55 (3H, d,  $J=7$  Hz)  
3.2 (3H, s), 3.65 (1H, qu,  $J=7$  Hz), 6.73, 7.2 (2H, dd,  $J=2$  Hz)

MS m/e 273 ( $\text{M}^+$ ), 258, 202, 91

1-Methylindolin-2-one. Indolin-2-one (1.33 g, 0.01 moles) in dry benzene (30 ml) was added to sodium hydride (0.24 g, 0.01 moles) in dry benzene (30 ml) and the mixture was heated under reflux for three hours. Methyl iodide (2.8 g, 0.02 moles) in dry benzene (15 ml) was added dropwise and the mixture heated under reflux (using a dry ice condenser) for 6 hours and then left over night. The precipitate of NaI was separated off and the benzene solution was washed with water and dried. Evaporation of the solvent yielded a brownish oil, (1.50 g) which solidified on cooling. After purification by column chromatography (alumina, mixtures of petroleum ether 60-80°/chloroform of increasing polarity), sublimation

and recrystallization from hexane white crystals (0.6 g, 40 %), m.p. 87-88°C (Lit.<sup>132</sup> 88-90°C, Lit.<sup>95</sup> 87-88°C), were obtained.

IR (Nujol)  $\nu$  max 1700, 1609, 1490, 1350, 750  $\text{cm}^{-1}$

NMR ( $\text{CDCl}_3$ )  $\delta$  3.20 (3H, s), 3.50 (2H, s), 6.7-7.4 (4H, m)

2-Aminophenylacetic acid. Palladium on charcoal (5 mg) was added to a solution of 2-nitrophenylacetic acid (100 mg) in MeOH (10 ml) and the mixture was exhaustively hydrogenated at atmospheric pressure and room temperature. The catalyst was filtered off and the solvent removed under vacuum, at room temperature. The crystalline residue (85 mg, 96 %) m.p. 117-119°C (Lit.<sup>136</sup> 119°C) showed no traces of starting material by TLC (silica, chloroform/MeOH 100:1) but a small amount of an impurity identified as indolin-2-one. Further purification by recrystallization or sublimation increased the percentage of indolin-2-one which suggests that the 2-aminophenylacetic acid spontaneously cyclized.

IR (Nujol)  $\nu$  max 2550, 2150 (both weak and broad), 1730 (weak), 1640, 1600  $\text{cm}^{-1}$

NMR ( $d_6$ -DMSO)  $\delta$  3.3 (2H, s), 5.7 (3H, broad s, exch.), 6.4-7.2 (4H, m)

N-Phenyl phenylacetamide. Aniline (9.3 g, 0.1 moles) and triethylamine (10.1 g, 0.1 moles) in dichloromethane (150 ml) were cooled to -5°C. Phenylacetylchloride (15.45 g, 0.1 moles) in dichloromethane (20 ml) was added dropwise with stirring

while the temperature was maintained below 0°C. The mixture was then left over night. The organic solution was washed with 5% HCl (100 ml), 5 % aqueous Na<sub>2</sub>CO<sub>3</sub> (100 ml), again with water (100 ml), dried and the solvent evaporated. The crude product (15 g) was recrystallized from acetone/petroleum ether 40-60° to yield bright white crystals (13 g, 60 %) m.p. 116-117°C (Lit.<sup>137</sup> 117-118°C).

IR (Nujol)  $\nu_{\max}$  3280, 3250, 1660, 1600, 1500, 760, 725 cm<sup>-1</sup>  
NMR (d<sub>6</sub>-DMSO)  $\delta$  3.70 (2H, s), 7-8 (10H, m), 10.1 (1H, broad s, exch.). In CDCl<sub>3</sub> the N-H is concealed by the aromatic multiplet.

2-Ketotetrahydroquinoline. Aniline (18.6 g, 0.2 moles) in acetone (20 ml) was heated under reflux and 3-chloropropionyl chloride (12.8 g, 0.1 moles) in acetone (20 ml) was added slowly over a period of 45 minutes. The mixture was then heated under reflux for 60 minutes. After cooling, dilute HCl (100 ml, 5 %) was added and the precipitated N-phenyl 3-chloropropionamide separated and dried (13 g, 71 %). The crude amide, m.p. 110-113°, IR  $\nu_{\max}$  3260, 1660 cm<sup>-1</sup> (12 g), was melted and aluminium trichloride (30 g) was added in small portions while the temperature was kept at 140°C. After the addition, the mixture was heated for 1 hour at 130-140°C. Ice and water were then added and the precipitate that formed was collected and recrystallized from MeOH/water to give white crystals (6 g, 63 %) m.p. 163-164°C (Lit.<sup>138</sup> 163°C)

IR (Nujol)  $\nu_{\max}$  3140, 1680, 1590, 815, 750 cm<sup>-1</sup>

NMR ( $\text{CDCl}_3$ )  $\delta$  2.3-3.2 (4H, m), 6.75-7.4 (4H, m), 9.65 (1H, broad s, exch.)

3-Pyrrolin-2-one. Pyrrole (10 g, purified by distillation), hydrogen peroxide (14 ml, 36%) and barium carbonate (3 g) in water (900 ml) were heated under reflux for 4 hours. Lead dioxide (3 g) was then added in small portions. The solution was filtered and the water evaporated under reduced pressure at  $50^\circ\text{C}$ . The residue was treated with peroxide free dioxan, the mixture filtered and the filtrate dried over anhydrous magnesium sulphate. After removal of the organic solvent, the residue was purified by vacuum distillation to yield a yellowish liquid (2.5 g, 20%) b.p.  $82-84^\circ\text{C}/0.5$  mm (Lit.<sup>131</sup>  $90-92^\circ\text{C}/0.5$  mm).

IR (Film)  $\nu_{\text{max}}$  3250, 1680, 1455, 1250, 1160, 810, 700  $\text{cm}^{-1}$

NMR ( $\text{D}_2\text{O}$ ) shows that the compound exists as an equilibrium mixture of 2 tautomers as indicated in section 2.5 :  $\delta$  4.10 (2H, m), 6.10 (1H, m), 7.35 (1H, m) (Tautomer I);  $\delta$  3.05 (2H, m), 5.40 (1H, m), 6.50 (1H, m) (Tautomer II)

MS m/e 83 ( $\text{M}^+$ ), 55

1-Methyl-3-pyrrolin-2-one was synthesized in the same way using N-methylpyrrole in place of pyrrole. After purification, a yellowish liquid (2 g, 14%), b.p.  $60^\circ\text{C}/1$  mm, was obtained.

IR (Film)  $\nu_{\text{max}}$  3440, 2880, 1660, 1380, 1240, 790, 700  $\text{cm}^{-1}$

NMR ( $\text{D}_2\text{O}$ ) also shows the presence of 2 tautomers, but tautomer

II was present in a very small proportion. For tautomer I:  $\delta$  2.95 (3H, s), 4.10 (2H, m), 6.10 (1H, m), 7.25 (1H, m)

MS m/e 97 ( $M^+$ ), 69

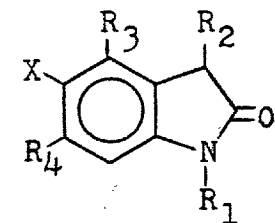
### 3.3. LABELLING OF SUBSTRATES

#### 3.3.1. [ $^3H_1$ ]-Compounds

3-[ $^3H_1$ ]-Indolin-2-ones were prepared by shaking a solution of the unlabelled compound dissolved in a suitable solvent with tritiated water (THO) under alkaline, acidic or neutral conditions for varying lengths of time according to the reactivity of the compound (Table 3.3.1). Whenever ether was employed, the organic solution was separated from the tritiated water, dried and the solvent evaporated. The crude compound was then purified (Table 3.3.1) and its purity checked by the melting point and TLC. In the case of dioxan and THF, the labelled compounds were precipitated by addition of water and both the melting point and TLC indicated that no further purification was required.

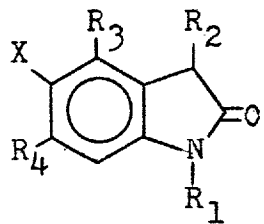
The hydrogen atoms  $\alpha$  to the carbonyl group in N-phenyl phenylacetamide are very unreactive so a different procedure using n-buylithium as base catalyst was employed. The lithium salt of the amide was then quenched with THO and the labelled compound purified by recrystallization with acetone/petroleum ether 60-80°.

Table 3.3.1 - Labelling of indolin-2-ones



	Solvent	Time of reaction	Catalyst	[THO] mCi/ml	m.p. (°C)	Purification
$R_1=R_2=R_3=X$ $=R_4=H$	Ether	over night	NaOH (0.5 M)	10	125-126	Sublimation
$R_1=R_2=CH_3$ $R_3=X=R_4=H$	Ether	over night	NaOH (0.5 M)	10	55-56	Sublimation + recrystallization (Petroleum ether 40-60°)
$R_1=CH_3$ $R_2=R_3=X=R_4=H$	Ether	over night	NaOH (0.2 M)	10	87-88	Sublimation
$R_1=R_2=X=H$ $R_3=R_4=^tBu$	Ether	over night	NaOH (0.5 M)	10	205-206	Recrystallization (Hexane)
$R_1=R_2=R_3=R_4=H$ $X=OCH_3$	Ether	over night	NaOH (0.5 M)	10	152-153	Recrystallization (CH <sub>2</sub> Cl <sub>2</sub> /petroleum ether 40-60°)
$R_1=R_2=R_3=R_4=H$ $X=NO_2$	Dioxan	over night	-	0.4	240-241	-

Table 3.3.1 - Labelling of indolin-2-ones (cont.)



	Solvent	Time of reaction	Catalyst	[THO] mCi/ml	m.p. (°C)	Purification
$R_3=R_4=H, X=NO_2$ $R_1=R_2=CH_3$	Ether	over night	NaOH (0.01 M)	10	149-150	Sublimation + recrystallization ( $CH_2Cl_2$ /petroleum ether 40-60°)
$R_1=R_2=R_3=R_4=H$ $X=Br$	THF	19 hours	$H_2SO_4$ (pH 1-2)	0.15	220-221	-
$R_1=R_2=CH_3$ $R_3=R_4=tBu, X=H$	Ether/ Alcohol	48 hours	NaOH (0.5 M)	10	105-106	Recrystallization (Petroleum ether 40-60°)



3. .2. [ $^2\text{H}_1$ ]-Compounds

1,3-Dimethyl-3- $^2\text{H}_1$ -indolin-2-one was prepared by the following procedure: a solution of sodium in deuterium oxide (20 ml, ca. 1M NaOD) degassed for 60 minutes with oxygen-free nitrogen was added to a solution of 1,3-dimethylindolin-2-one (954 mg) in dry degassed ether (30 ml). This mixture, kept under nitrogen, was stirred over night. The aqueous phase of NaOD in deuterium oxide was renewed twice and the stirring continued for a total of 36 hours, always under nitrogen. The ethereal phase was then separated, dried and the solvent evaporated under reduced pressure. The residue was purified by sublimation yielding white crystals m.p.  $56^\circ\text{C}$ . The labelling procedure was carried out under anaerobic conditions to minimise oxidation of the substrate. TLC and MS showed no signs of the oxidation product.

Found C, 74.12; H, 7.01; N, 8.64 %. Calculated for  $\text{C}_{10}\text{H}_{10}\text{DNO}$ :  
C, 74.05; H, 6.83; N, 8.64 %

### 3.4. KINETIC PROCEDURES

#### 3.4.1. Protodetritiation reactions

The exchange of  $^3\text{H}_1$  was always followed by monitoring the decrease in radioactivity of the labelled substrate with time. In a typical experiment the reaction solution, contained in a 50 ml volumetric flask, was placed in a thermostatted bath and allowed to thermally equilibrate. The exchange reaction was then initiated by addition of a small volume (0.5 ml) of a stock solution of the labelled substrate. The stock solutions were made up in ethanol except in the case of 5-bromo and 5-nitroindolin-2-one where, for reasons of solubility, THF and dioxan, respectively, were used. Aliquots of the reaction solution (5 ml) were removed at timed intervals and extracted by shaking for ca. 30 seconds with xylene (10 ml). The xylene phase (5 ml) was then added to the liquid scintillation mixture (5 ml) in a counting vial. The radioactivity of this solution was then determined in the liquid scintillation counter. The rate of the reaction was usually measured for more than 4 half-lives and an infinity value determined from an aliquot taken at a time greater than 10 half-lives. The infinity did not normally exceed the background count (ca. 30 cpm) by more than 10-20 cpm.

When the concentration of the acid in the solution exceeded 5 M, the aliquots from the reaction were first cooled in dry ice/acetone and partially neutralized with standard NaOH (5 M, 5 ml) before being extracted with xylene.

The acidic reaction solutions were titrated against

standard alkali at the end of each run. For reactions in buffers the pH of the reaction solution was determined at the conclusion of the kinetic experiment.

Typical kinetic experiments are shown in Tables 3.4.1 to 3.4.6 and in Figures 3.4.1 and 3.4.2. Results are reproducible to less than 1%.

Table 3.4.1 - Protodetrition of 5-methoxy-3-[<sup>3</sup>H<sub>1</sub>]-indolin-2-one in 1.90 M H<sub>2</sub>SO<sub>4</sub>

Time (Min.)	Activity (cpm)	% Reaction
0	5,439	0
11	4,600	15.5
20	4,044	25.8
30	3,407	37.6
55	2,364	56.8
82	1,516	72.5
126	803	85.7
213	222	96.5
∞	30	100

$$k_0^{-T} = 3.17 \times 10^{-4} \text{ s}^{-1}$$

Table 3.4.2 - Protodetritiation of 5-bromo-3-[<sup>3</sup>H<sub>1</sub>]-indolin-2-one in 2 M H<sub>2</sub>SO<sub>4</sub>

Time (Min.)	Activity (cpm)	% Reaction
0	4,577	0
5	4,147	9.5
16	3,402	25.9
30	2,641	42.7
60	1,459	68.8
91	846	82.3
120	508	89.8
200	157	97.6
∞	46	100

$$k_0^{-T} = 2.64 \times 10^{-4} \text{ s}^{-1}$$

Table 3.4.3 - Protodetritiation of 1-methyl-3-[<sup>3</sup>H<sub>1</sub>]-indolin-2-one in 0.95 M H<sub>2</sub>SO<sub>4</sub>

Time (Min.)	Activity (cpm)	% Reaction
0	12,996	0
83	11,825	9.0
203	10,102	22.3
372	8,072	38.0
1,431	2,027	84.7
1,642	1,514	88.6
1,808	1,195	91.0
2,184	725	94.7
∞	40	100

$$k_0^{-T} = 0.22 \times 10^{-4} \text{ s}^{-1}$$

Table 3.4.4 - Protodetrition of 3- $^{3}\text{H}_1$ -indolin-2-one in piperidine buffer.  $[\text{Piperidine}] = 2.5 \times 10^{-3}$ , Buffer ratio 6:1

Time (Sec.)	Activity (cpm)	% Reaction
0	6,741	0
70	5,715	15.3
140	4,744	29.8
210	3,860	43.0
300	3,064	54.9
600	1,383	80.0
900	565	92.2
1,200	291	96.4
$\infty$	46	100

$$k_0^{-T} = 26.8 \times 10^{-4} \text{ s}^{-1}$$

Table 3.4.5 - Protodetrition of 5-nitro-3- $^{3}\text{H}_1$ -indolin-2-one in acetate buffer.  $[\text{AcO}^-] = 10 \times 10^{-2} \text{ M}$ , Buffer ratio 6:1

Time (Min.)	Activity (cpm)	% Reaction
0	6,514	0
20	5,635	13.6
111	2,848	56.5
143	2,179	66.9
196	1,458	78.0
256	929	86.2
327	540	92.2
376	372	94.8
$\infty$	36	100

$$k_0^{-T} = 1.30 \times 10^{-4} \text{ s}^{-1}$$

Figure 3.4.1 - Protodetrition of 1-methyl-3-[ $^3\text{H}_1$ ]-indolin-2-one in 0.95 M  $\text{H}_2\text{SO}_4$

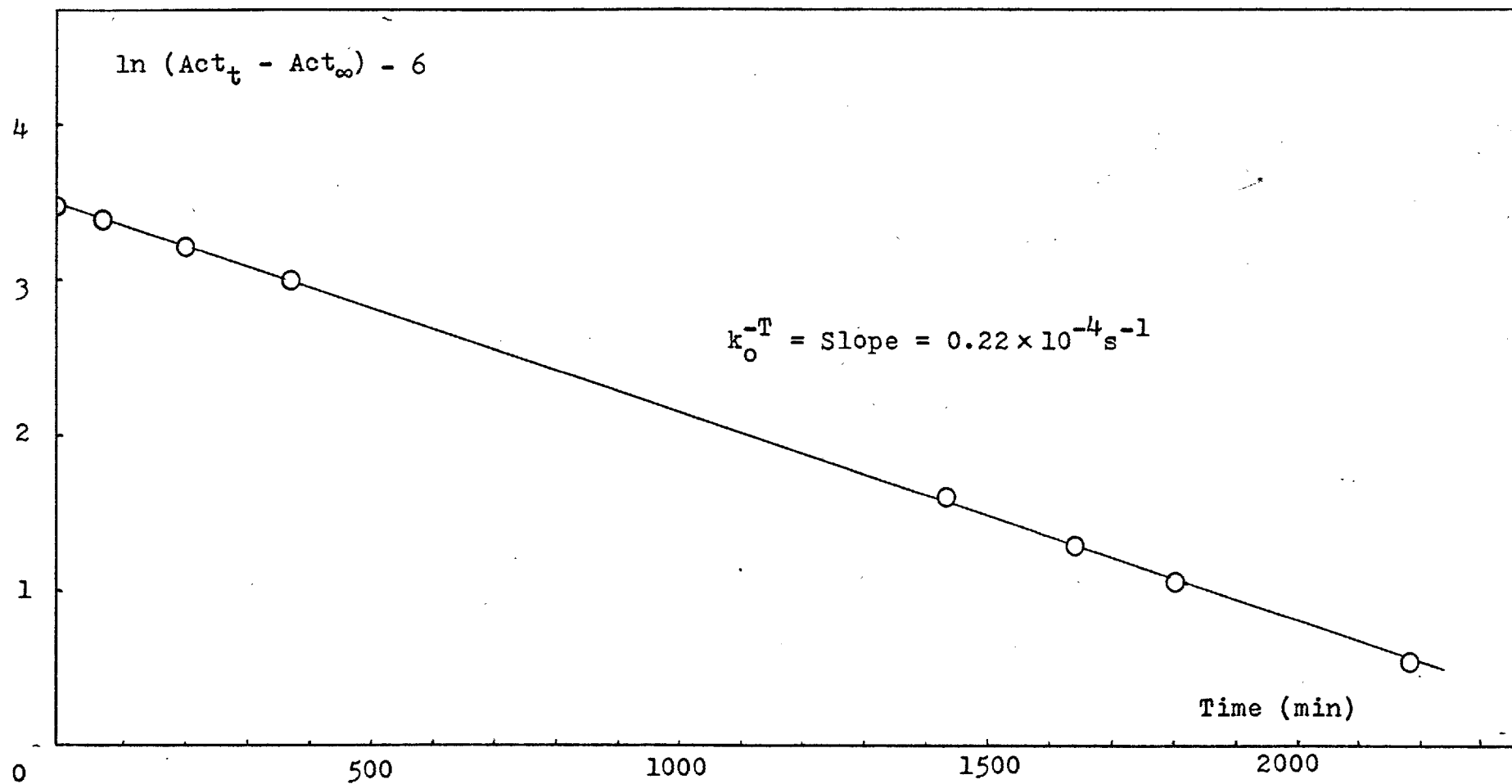


Figure 3.4.2 - Protodetrition of 3-[<sup>3</sup>H]-indolin-2-one in a piperidine buffer

[Piperidine] =  $2.5 \times 10^{-4}$  M, Buffer ratio 6:1

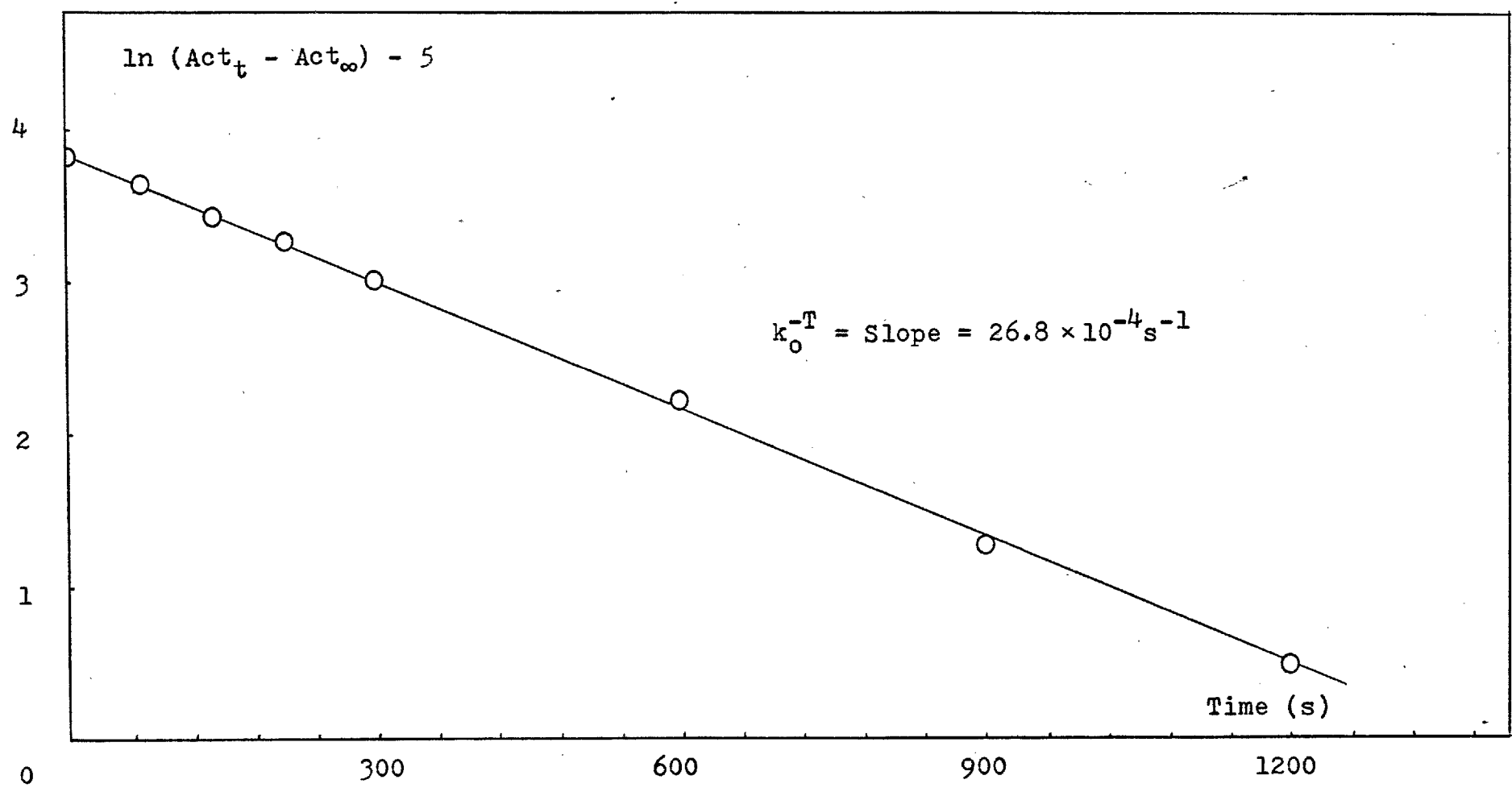


Table 3.4.6 - Protodetritionation of 5-nitro-3-[<sup>3</sup>H<sub>1</sub>]-indolin-2-one in 4-nitrophenol buffer. [ArO<sup>-</sup>] = 10 × 10<sup>-3</sup>M, Buffer ratio 1:2

Time (Min.)	Activity (cpm)	% Reaction
0	5,341	0
2	4,726	11.6
5	3,889	27.3
10	2,740	49.0
15	2,024	62.4
20	1,447	73.3
25	1,040	81.0
40	369	93.6
∞	29	100

$$k_0^{-T} = 11.2 \times 10^{-4} \text{ s}^{-1}$$

3.4.2. Protodeuteriation reactions (Mass spectral analysis)

A solution of 1,3-dimethyl-3-[<sup>2</sup>H<sub>1</sub>]-indolin-2-one (30 mg) in ethanol (5 ml) was made up to 50 ml with previously prepared acidic solutions and placed in a thermostatted bath. Aliquots of this solution (5 ml), taken at timed intervals, were extracted with petroleum ether 40-60° (5 ml). This extract was evaporated to dryness under reduced pressure at room temperature. The residues obtained were then analysed by Mass Spectrometry. The intensities of the signals corresponding to M<sup>+</sup> for the deuteriated substrate and unlabelled product



were compared. Usually an average of 8 determinations of the ratio  $[^2\text{H}_1]/[^1\text{H}_1]$  were taken for each aliquot of reaction solution. The referred ratio for each sample is reproducible to  $< 0.5\%$ .

Typical experiments are shown in Tables 3.4.7 and 3.4.8 and Figures 3.4.3 and 3.4.4.

Table 3.4.7 - Protodeuteriation of 1,3-dimethyl-3- $[^2\text{H}_1]$ -indolin-2-one in 3.0 M  $\text{H}_2\text{SO}_4$

Time (Min.)	$[^2\text{H}_1]/[^1\text{H}_1]$ % <sup>*</sup>
0	93.4
78	60.5
144	47.6
216	36.2
276	29.7
337	24.2
480	12.5

$$k_0^{-D} = 0.71 \cdot 10^{-4} \text{s}^{-1}$$

\* For calculation details see Section 2.3.2.1

Table 3.4.8 - Protodeuteration of 1,3-dimethyl-3-[<sup>2</sup>H<sub>1</sub>]-  
-indolin-2-one in 4.1 M H<sub>2</sub>SO<sub>4</sub>

Time (Min.)	[ <sup>2</sup> H <sub>1</sub> ]/[ <sup>1</sup> H <sub>1</sub> ] % *
0	95.0
30	81.6
52	71.6
93	56.4
155	38.4
258	20.0
330	15.3
451	7.7

$$k_0^{-D} = 1.03 \cdot 10^{-4} \text{ s}^{-1}$$

\* For calculation details see Section 2.3.2.1

Figure 3.4.3 - Protodeuteriation of 1,3-dimethyl-3-[<sup>2</sup>H<sub>1</sub>]-indolin-2-one in 3.0 M H<sub>2</sub>SO<sub>4</sub>

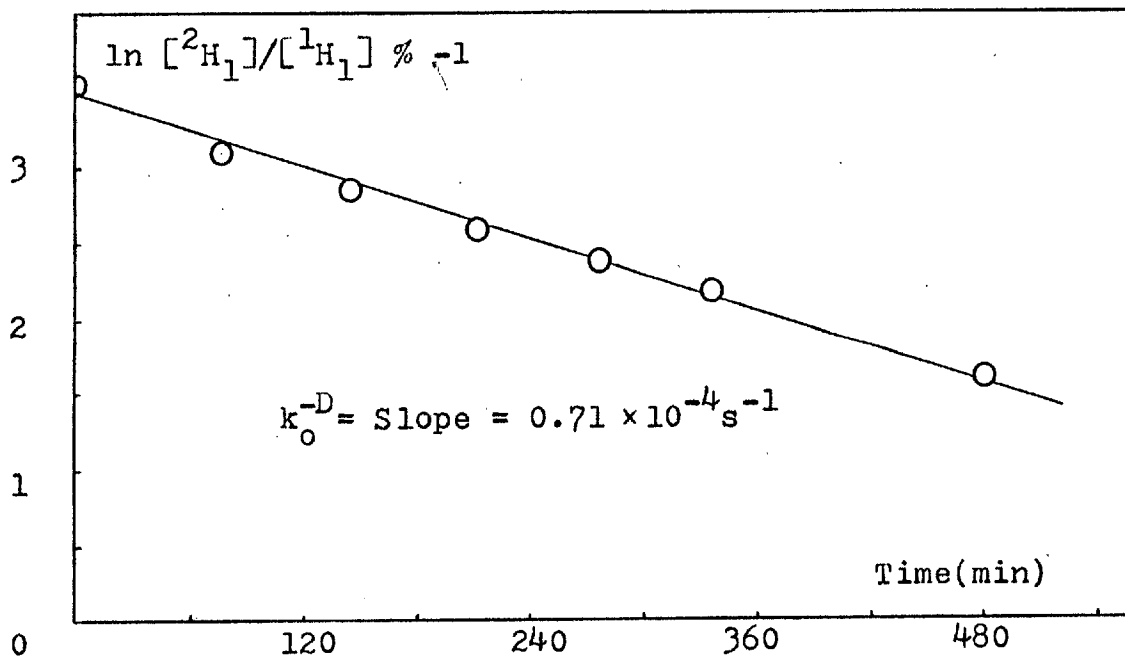
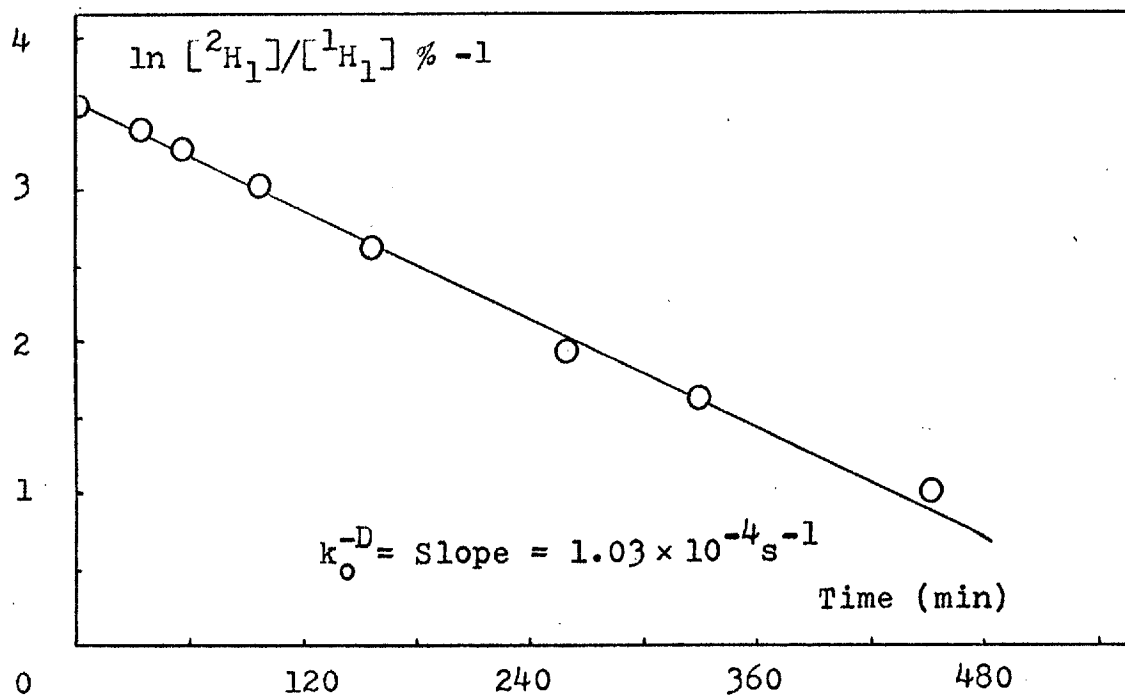


Figure 3.4.4 - Protodeuteriation of 1,3-dimethyl-3-[<sup>2</sup>H<sub>1</sub>]-indolin-2-one in 4.1 M H<sub>2</sub>SO<sub>4</sub>



### 3.4.3. Iododeprotonation and iododedeuteriation reactions.

(Iodometric analysis)

Each kinetic run was started by adding a stock solution of the substrate (0.25 ml,  $10^{-2}$ M) in methanol to a solution of iodine ( $6 \times 10^{-5}$ M) and iodide (0.12 M) in a TRIS buffer (25 ml), already thermally equilibrated at  $25^{\circ}$ . A sample of the reaction solution was then placed in a UV cell and the decrease in  $[I_3^-]$  monitored at 352 nm in the thermostatted compartment of a Unicam SP1800 Spectrophotometer. To overcome errors introduced by the slight spontaneous decomposition of  $I_3^-$ , an identical solution of  $I_3^-$  in the same buffer to which 0.25 ml of methanol had been added was placed in the sample cell of the spectrophotometer. The reaction solution was placed in the reference beam and the apparent increase in optical density monitored at the above wavelength.

The pH of the reaction solution was measured at the end of the kinetic experiment.

Figures 3.4.5 and 3.4.6 show the variation of absorbance with time for the iododeprotonation of 1,3-dimethyl-3- $[^1H_1]$ -indolin-2-one and Figures 3.4.7 and 3.4.8 show the same variation for the iododedeuteriation of 1,3-dimethyl-3- $[^2H_1]$ -indolin-2-one as typical examples of the kinetic experiments. The correction for iododedeuteriation due to the presence of 2.1% of unlabelled substrate is outlined in Tables 3.4.9 and 3.4.10. The corrected and observed variation of absorbance vs. time are compared in Figures 3.4.7 and 3.4.8.

Results are reproducible to less than 1%.

Figure 3.4.5 - Iododeprotonation of 1,3-dimethyl-3-<sup>1</sup>H<sub>1</sub>-indolin-2-one in a TRIS buffer

[TRIS] =  $11 \times 10^{-3}$ M, [3-H-Indolin-2-one]<sub>i</sub> =  $10^{-3}$ M, pH = 9.035

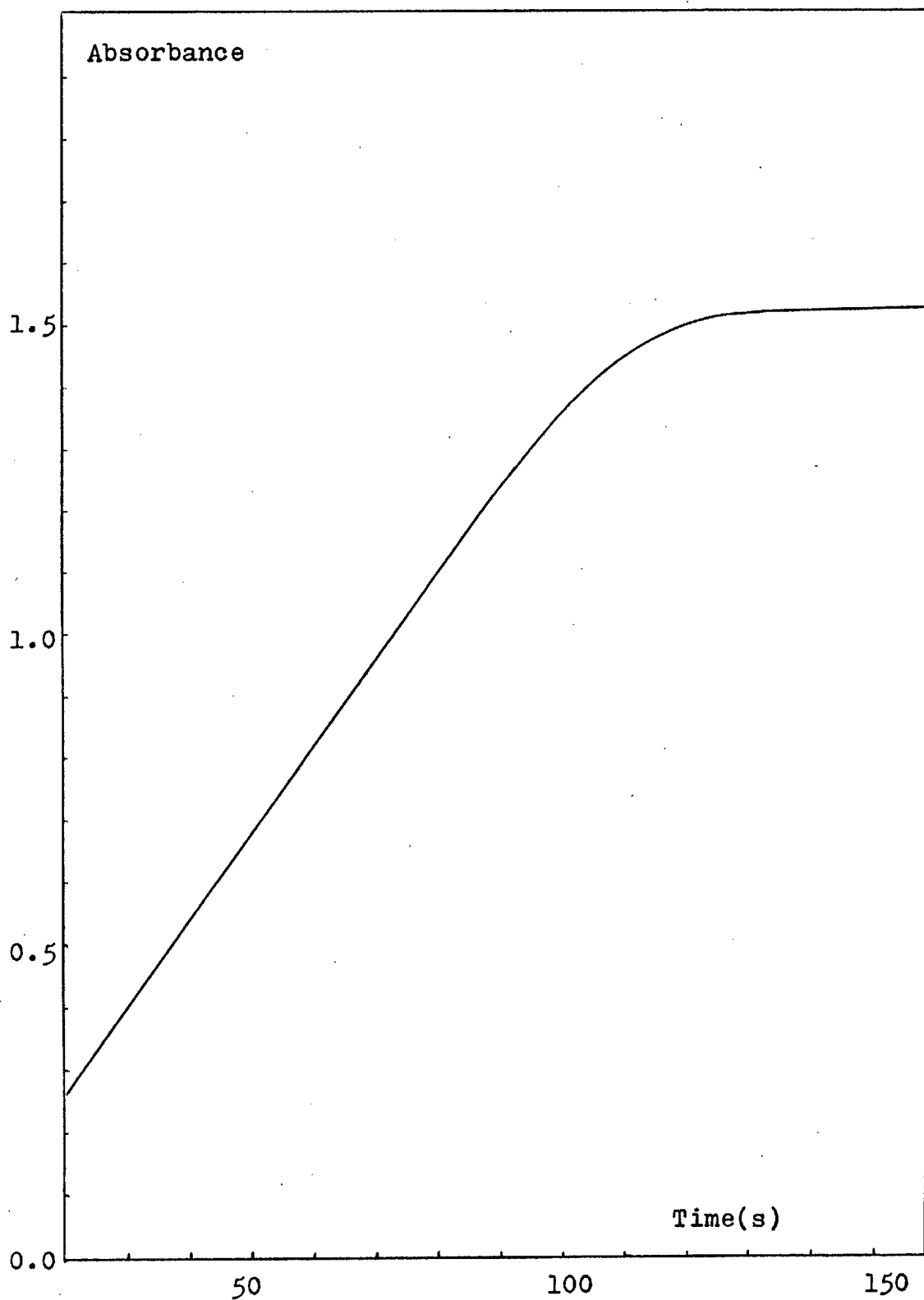


Figure 3.4.6 - Iododeprotonation of 1,3-dimethyl-3- $[^1\text{H}_1]$ -indolin-2-one in a TRIS buffer

$[\text{TRIS}] = 13 \times 10^{-3}\text{M}$ ,  $[\text{3-H-Indolin-2-one}]_i = 10^{-3}\text{M}$ ,  $\text{pH} = 9.040$

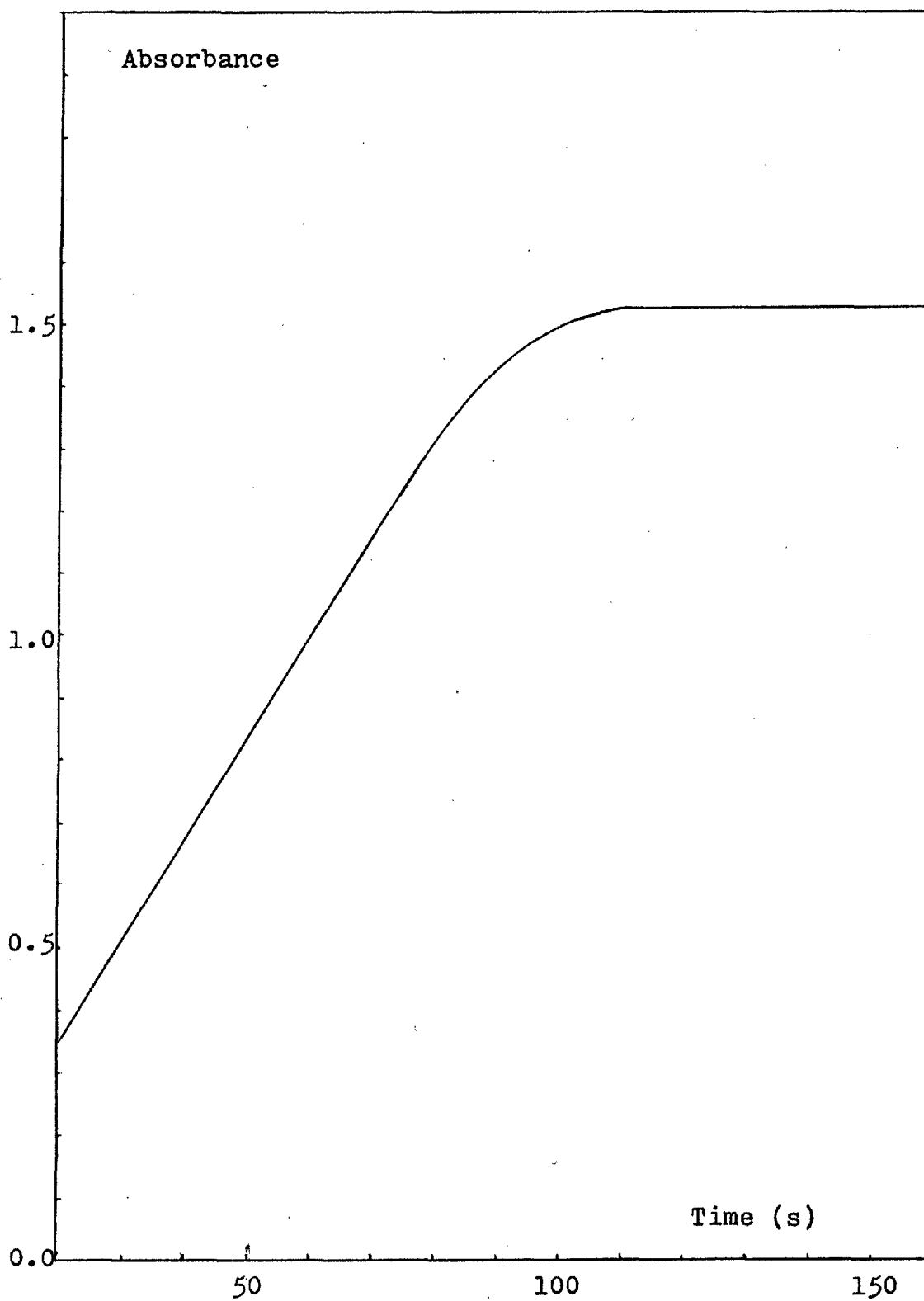


Figure 3.4.7 - Iododeuteriation of 1,3-dimethyl-3- $^{2}\text{H}_1$ -indolin-2-one in a TRIS buffer

$[\text{TRIS}] = 11 \times 10^{-3}\text{M}$ ,  $[\text{3-D-Indolin-2-one}]_i = 0.979 \times 10^{-3}\text{M}$ ,

$[\text{3-H-Indolin-2-one}]_i = 0.021 \times 10^{-3}\text{M}$ ,  $\text{pH} = 9.030$

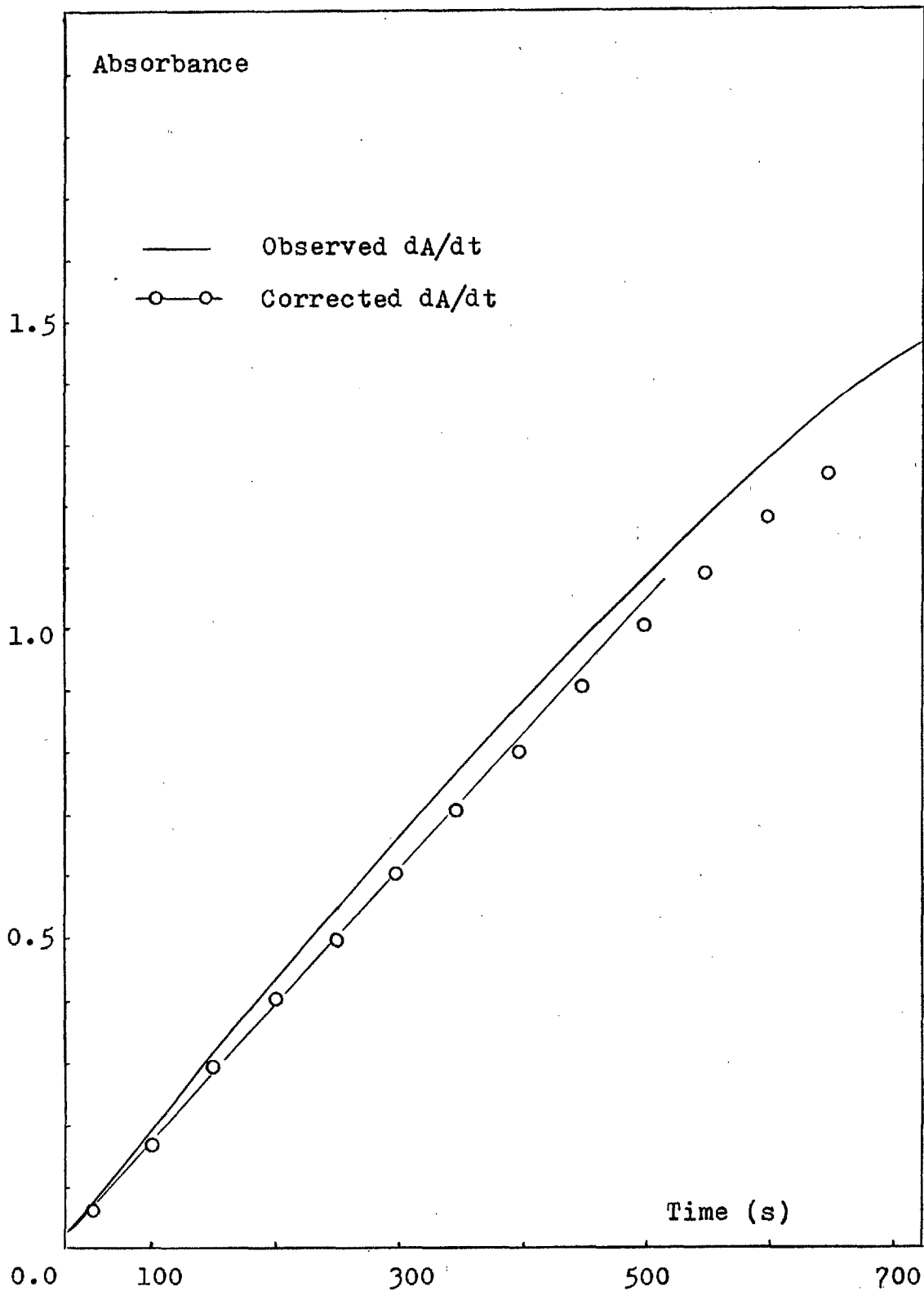


Figure 3.4.8 - Iododeuteration of 1,3-dimethyl-3- $^{2}\text{H}_1$ -indolin-2-one in a TRIS buffer

$[\text{TRIS}] = 21 \times 10^{-3}\text{M}$ ,  $[\text{3-D-Indolin-2-one}]_i = 0.979 \times 10^{-3}\text{M}$ ,

$[\text{3-H-Indolin-2-one}]_i = 0.021 \times 10^{-3}\text{M}$ ,  $\text{pH} = 9.085$

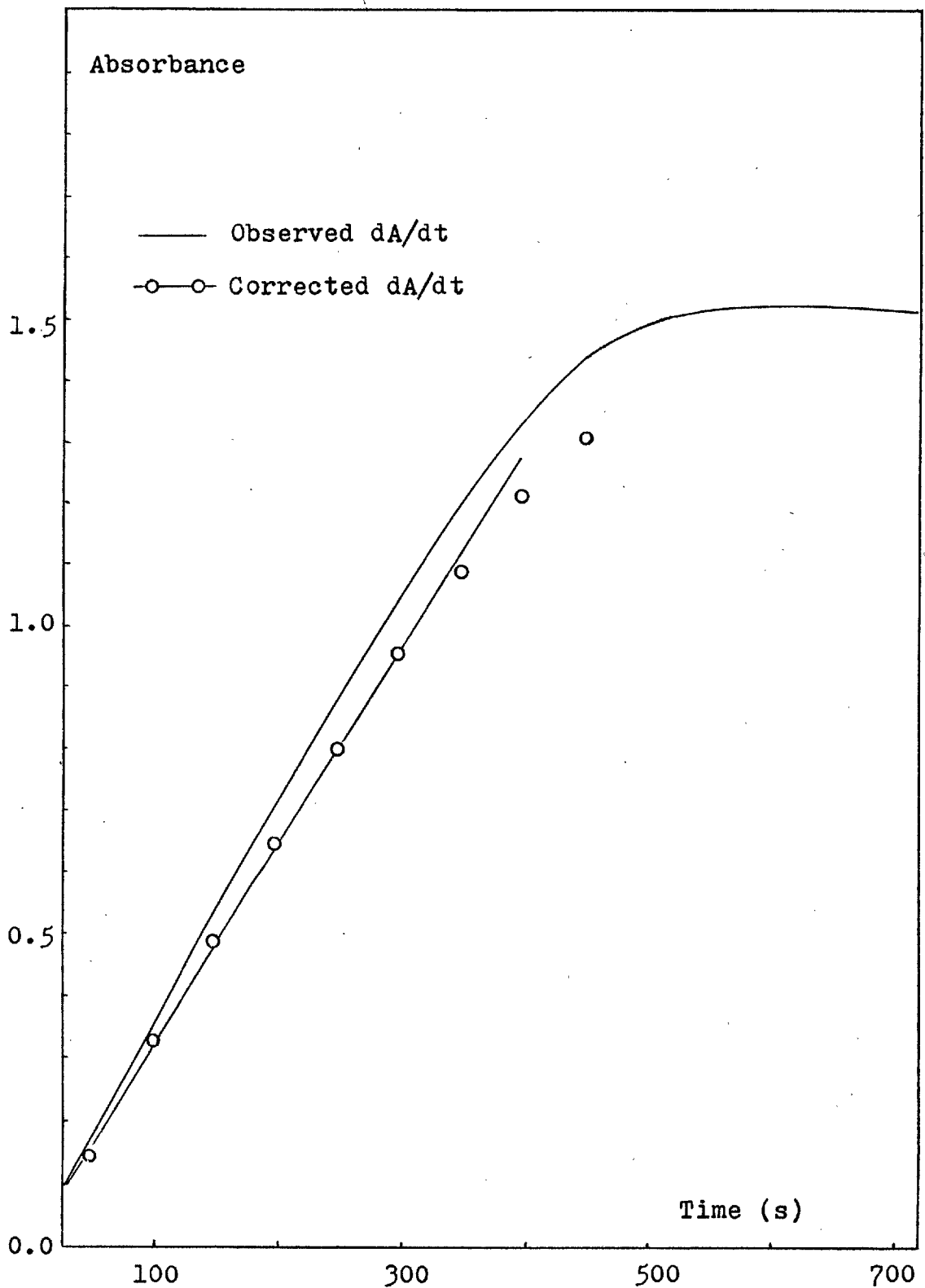




Table 3.4.9 - Correction of dA/dt for the iododeuteriation of 1,3-dimethyl-3-[<sup>2</sup>H<sub>1</sub>]-indolin-2-one in a TRIS buffer ‡  
 [TRIS] =  $11 \times 10^{-3} \text{M}$ , [3-D-Indolin-2-one]<sub>i</sub> =  $0.979 \times 10^{-3} \text{M}$ ,  
 [3-H-Indolin-2-one]<sub>i</sub> =  $0.021 \times 10^{-3} \text{M}$

Time (sec.)	A <sub>t</sub>	A <sub>t</sub> <sup>H</sup>	A <sub>t</sub> <sup>C</sup>
0	0	0	0
100	0.20	0.019	0.18
200	0.44	0.037	0.40
300	0.66	0.055	0.60
400	0.88	0.071	0.81
500	1.08	0.087	0.99
600	1.28	0.105	1.18
700	1.44	0.122	1.32

Table 3.4.10 - Correction of dA/dt for the iododeuteriation of 1,3-dimethyl-3-[<sup>2</sup>H<sub>1</sub>]-indolin-2-one in a TRIS buffer ‡  
 [TRIS] =  $21 \times 10^{-3} \text{M}$ , [3-D-Indolin-2-one]<sub>i</sub> =  $0.979 \times 10^{-3} \text{M}$ ,  
 [3-H-Indolin-2-one]<sub>i</sub> =  $0.021 \times 10^{-3} \text{M}$

Time (sec.)	A <sub>t</sub>	A <sub>t</sub> <sup>H</sup>	A <sub>t</sub> <sup>C</sup>
0	0	0	0
50	0.15	0.015	0.14
100	0.33	0.029	0.30
150	0.50	0.043	0.46
200	0.66	0.056	0.60
250	0.83	0.069	0.76
300	0.99	0.081	0.91
350	1.13	0.093	1.04

‡ For correction details see Section 2.3.1.2

### 3.5. pK MEASUREMENTS

A - Substrates were purified by recrystallization to constant melting point and their purity was also checked both mass spectrometrically and by TIC.

B - Sulphuric acids. The acid solutions were prepared by dilution of Analar 98% (w/w) sulphuric acid with distilled water. Their concentration was determined by titration against sodium hydroxide using methyl orange as indicator.

C- Alkaline solutions were prepared by diluting standard sodium hydroxide with deionized water. These solutions were used and titrated immediately after preparation, against standard hydrochloric acid using bromophenol blue as indicator. The pH was calculated from the experimental  $[\text{OH}^-]$ .

Buffers were prepared according to Section 3.5 and their pH was measured at the end of the experiment.

D - Choice of wavelength. The best wavelength for the measurement of ionization ratios is either the wavelength of the maximum absorbance of the anion/cation or of the maximum absorbance of the neutral molecule. Of the two possible wavelengths, that which gave greater differences in absorbance when changing the concentration of acid or base was used.

E - Measurement of UV spectra. The substrate solutions ( $10^{-4}\text{M}$ ) were prepared by adding aliquots of stock solutions (0.25 ml,  $10^{-2}\text{M}$ ) to 25 ml of the acidic or alkaline solution previously equilibrated at  $25^{\circ}\text{C}$ . The spectra of the acidic solutions

were recorded against a blank of the same acid on a Unicam SP800 Spectrophotometer and their absorbances determined at constant wavelength, against the same blank, on a Unicam SP1800 Spectrophotometer in thermostatted cells at 25°.

As indolin-2-ones alter slightly in alkaline medium, the absorbances here were measured at constant wavelength over a period of ca. 10 minutes. The initial absorbance was determined by extrapolation to zero time.

### 3.6. PREPARATION OF BUFFER SOLUTIONS

Buffer solutions were prepared by addition of the calculated amount of standard HCl or NaOH to the required volume of a stock solution of the appropriate base or acid. Buffers of constant pH were prepared by making a concentrated buffer and diluting it in order to give the required concentration of base. The ionic strength was maintained constant by addition of the required amount of Analar NaCl or, in some cases, Analar NaClO<sub>4</sub>. These were calculated according to expression  $\mu = 1/2 \sum c_i z_i^2$  where,  $\mu$  is the ionic strength of the solution,  $c_i$  the concentration of a particular ion and  $z_i$  the charge associated with that ion.

3.7.  $^{13}\text{C}$  NMR spectra

$^{13}\text{C}$  NMR spectra were recorded at 25.16 MHz on a Varian XL-100-12 Spectrometer, with 8K sampling points before Fourier transformation. The spectra were recorded of solutions in  $\text{CDCl}_3$  and  $\text{FSO}_3\text{H}$  in a 10 mm tube, with a 5 mm  $\text{D}_2\text{O}$  insert as external lock. Assignments were made according to other work<sup>139</sup> and of-resonance spectra.

BIBLIOGRAPHY

- (1) K. B. Wiberg, Chem. Rev., 1955, 55, 713
- (2) R. A. More O'Ferrall, 'Substrate Isotope Effects', in 'Proton Transfer Reactions', eds. E. F. Caldin and V. Gold, Chapman and Hall, London, 1975, ch. 8.
- (3) A. J. Kresge, Disc. Faraday Soc., 1965, 39, 48
- (4) A. F. Cockerill, J. Chem. Soc. (B), 1967, 964
- (5) R. P. Bell and D. M. Goodall, Proc. Roy. Soc. (A), 1967, 294, 273
- (6) J. L. Longridge and F. A. Long, J. Am. Chem. Soc., 1967, 89, 1292
- (7) A. J. Kresge, D. S. Sagatys and H. L. Cheng, J. Am. Chem. Soc., 1968, 90, 4174
- (8) R. P. Bell and B. G. Cox, J. Chem. Soc. (B), 1970, 194
- (9) D. J. Barnes and R. P. Bell, Proc. Roy. Soc. (A), 1970, 318, 421
- (10) F. H. Westheimer, Chem. Rev., 1961, 61, 265
- (11) R. A. More O'Ferrall and J. Kouba, J. Chem. Soc. (B), 1967, 985
- (12) R. A. More O'Ferrall, J. Chem. Soc. (B), 1970, 785
- (13) R. P. Bell, W. S. Sachs and R. L. Tranter, Trans. Faraday Soc., 1971, 67, 1995
- (14) R. P. Bell, Chem. Soc. Rev., 1974, 3, 513
- (15) W.H. Saunders, 'Kinetic Isotope effects', in 'Techniques of Chemistry', ed. E. S. Lewis, Wiley-Interscience, New

- York, 1974, vol. 6 - Part I, ch. 5
- (16) B.C. Challis and E. M. Millar, J.C.S. Perkin II, 1972, 1111, 1116, 1618, 1625
- (17) F. G. Bordwell and W. J. Boyle Jr., J. Am. Chem. Soc., 1971, 93, 511, 512
- (18) E. F. Caldin, Chem. Rev., 1969, 69, 135
- (19) J. R. Jones, 'The Ionization of Carbon Acids', Academic Press, London, 1973
- (20) E.S. Lewis, 'Tunnelling in Hydrogen Transfer Reactions', in 'Proton Transfer Reactions', eds. E. F. Caldin and V. Gold, Chapman and Hall, London, 1975, ch. 10
- (21) R. P. Bell, Trans. Faraday Soc., 1959, 55, 1
- (22) R. P., 'The Proton in Chemistry', Chapman and Hall, London, 1973
- (23) C. G. Swain, E. C. Stivers, J. F. Reuwer and L. J. Schaad, J. Am. Chem. Soc., 1958, 80, 5885
- (24) J. Bigleisen, in 'Tritium in the Physical and Biological Sciences', IAEA, Vienna, 1962, vol. 1, p. 161
- (25) J. R. Hulett, Quart. Rev. (London), 1964, 18, 227
- (26) E. S. Lewis and J. K. Robinson, J. Am. Chem. Soc., 1968, 90, 4337
- (27) J. R. Jones, Trans. Faraday Soc., 1969, 65, 2138
- (28) N. S. Isaacs, K. Javaid and E. Rannala, Nature (London), 1977, 268 (5618), 372
- (29) D. J. Underwood and J. H. Bowie, J.C.S. Perkin II, 1977, 1670
- (30) M. Simonyi, I. Fitos, J. Kardos, I. Kovacs and I. Lucovits, J.C.S. Faraday I, 1977, 73, 1286
- (31) K. Toriyama, K. Nunome and M. Iwasaki, J. Am. Chem. Soc., 1977, 99, 5823

- (32) E. S. Lewis and M. M. Butler, J. Am. Chem. Soc., 1976, 98, 2257
- (33) G. Brunton, D. Griller, L. R. C. Barclay and K. U. Ingold, J. Am. Chem. Soc., 1976, 98, 6803
- (34) J. A. Elvidge, D. K. Jaiswal, J. R. Jones and R. Thomas, J.C.S. Perkin II, 1976, 353
- (35) L. F. Blackwell and J. L. Woodhead, J.C.S. Perkin II, 1975, 234
- (36) J. R. Jones and T. G. Rumney, J.C.S. Chem. Commun., 1975, 995
- (37) D. J. McLennan, J.C.S. Perkin II, 1977, 1753
- (38) R. Srinivasan and R. Stewart, J. Am. Chem. Soc., 1976, 98, 7648
- (39) J. N. Brønsted and K. Pedersen, Z. Phys. Chem., 1924, 108, 185
- (40) A. J. Kresge, 'The Brønsted Relation: Significance of the Exponent' in 'Proton Transfer Reactions', eds. E. F. Caldin and V. Gold, Chapman and Hall, London, 1975, ch. 7
- (41) F. Hibbert, 'Proton Transfer to and from Carbon' in 'Comprehensive Chemical Kinetics-Proton Transfer', eds. C. H. Bamford and C. F. H. Tipper, Elsevier, Oxford, 1977, vol. 8, ch. 2
- (42) F. G. Bordwell, W. J. Boyle, Jr., J. A. Hautala and K. C. Yee, J. Am. Chem. Soc., 1969, 91, 4002
- (43) M. Fukuyama, P. W. Flanagan, F.T. Williams, Jr., L. Frainier, S.A. Miller and H. Schechter, J. Am. Chem. Soc., 1970, 92, 4689
- (44) F. G. Bordwell and W. J. Boyle, Jr., J. Am. Chem. Soc., 1972, 94, 3907

- (45) A. J. Kresge, Chem. Soc. Rev., 1973, 2, 475
- (46) W. P. Jenks and J. M. Sayer, Faraday Symp. Chem. Soc., 1975, 10, 41
- (47) M. Eigen, Angew. Chem. Internat. Edn., 1964, 3, 1
- (48) E. A. Walkers and F. A. Long, J. Am. Chem. Soc., 1969, 91, 3733
- (49) F. Hibbert, F. A. Long and E. A. Walkers, J. Am. Chem. Soc., 1971, 93, 2829
- (50) F. Hibbert and F. A. Long, J. Am. Chem. Soc., 1972, 94, 2647
- (51) Z. Margolin and F. A. Long, J. Am. Chem. Soc., 1972, 94, 5108; 1973, 95, 2757
- (52) A. J. Kresge and A. C. Lin, J.C.S. Chem. Commun., 1973, 761
- (53) A. J. Kresge, Acc. Chem. Res., 1975, 8, 354
- (54) R. A. Marcus, J. Phys. Chem., 1968, 72, 891
- (55) A. O. Cohen and R. A. Marcus, J. Phys. Chem., 1968, 72, 4249
- (56) G. W. Koeppl and A. J. Kresge, J.C.S. Chem. Commun., 1973, 371
- (57) R. J. Thomas and F. A. Long, J. Am. Chem. Soc., 1964, 86, 4770
- (58) A. J. Kresge and Y. Chiang, J. Am. Chem. Soc., 1973, 95, 803
- (59) W. J. Albery, A. N. Campbell Crawford and J. S. Curran, J.C.S. Perkin II, 1972, 2206
- (60) A. R. Katritzky and J. M. Lagowski, Advan. Heterocyclic Chem., 1963, 2, 1
- (61) A. E. Kellie, D. G. O'Sullivan and P. W. Sadler, J. Chem. Soc., 1956, 3809



- (62) W. C. Sumpter, Chem. Rev., 1945, 37, 443
- (63) R. J. Sundberg, 'The Chemistry of Indoles', Academic Press, New York, 1970
- (64) P. G. Gassman and T. J. van Bergen, J. Am. Chem. Soc., 1974, 96, 5508
- (65) A. S. Bailey and P. H. Bogle, J. Chem. Res., 1977, 227
- (66) M. Mori and Y. Ban, Tet. Letters, 1976, 1807
- (67) P. L. Julian, J. Pikl and D. Boggess, J. Am. Chem. Soc., 1934, 56, 1797
- (68) A. W. Beckett, R. W. Daisley and J. Walker, Tetrahedron, 1968, 24, 6093
- (69) W. C. Sumpter, M. Miller and M. E. Magan, J. Am. Chem. Soc., 1945, 67, 499
- (70) W. C. Sumpter, M. Miller and L. N. Hendrick, J. Am. Chem. Soc., 1945, 67, 1656
- (71) P. G. Gassman, U. S. Pat. 3,972,894, Chem. Abs., 1976, 85, 177251 p
- (72) P. G. Gassman, G. Gruetzmacher and T. J. van Bergen, J. Am. Chem. Soc., 1974, 96, 5512
- (73) R. G. Pearson and R. L. Dillon, J. Am. Chem. Soc., 1953, 75, 2439
- (74) K. F. Bonhoeffer, K.H. Geib and O. Reitz, J. Chem. Phys., 1939, 7, 664
- (75) D. J. Cram, B. Rickborn, C. A. Kingsbury and P. Haberfield, J. Am. Chem. Soc., 1961, 83, 3678
- (76) H. Matsuo, Y. Kawasoe, M. Sato, O. Ohnishi and T. Tatsuno, Chem. Pharm. Bull., 1967, 15, 391
- (77) T. Hino, M. Nakagawa, K. Tsuneoka, S. Misawa and S. Akaboshi, Chem. Pharm. Bull., 1969, 17, 1651

- (78) B. C. Challis and H. S. Rzepa, J.C.S. Perkin II, 1975, 1822
- (79) W. S. O'Sullivan, Clin. Chim. Acta, 1975, 62, 181
- (80) R. W. Daisley and J. Walker, J. Chem. Soc. (B), 1969, 146
- (81) I. Gruda, Tet. Letters, 1973, 457
- (82) G. Lamaty, 'Deuterium Exchange in Carbonyl Compounds' in 'Isotopes in Organic Chemistry', eds. E. Buncl and C. C. Lee, Elsevier, Oxford, 1976, vol. 2, ch. 2
- (83) E. Hardegger and H. Corrodi, Helv. Chim. Acta, 1956, 39, 514
- (84) H. Romeo, H. Corrodi and E. Hardegger, Helv. Chim. Acta, 1955, 38, 463
- (85) K. J. Arora, M. K. M. Dirania and J. Hill, J. Chem. Soc. (C), 1971, 2865
- (86) A. Albert and E. P. Serjeant, 'Ionization Constants of Acids and Bases', Methuen, London, 1962, ch. 4
- (87) Handbook of Chemistry and Physics, ed. R. C. Weast, CRC Press, Cleveland, 1974
- (88) L.P. Hammett, J. Am. Chem. Soc., 1937, 59, 96
- (89) K. Yates and J. B. Stevens, Canad. J. Chem., 1964, 42, 1957
- (90) R. B. Homer and C.D. Johnson, 'Acid-base and Complexing Properties of Amides' in 'The Chemistry of Amides' ed. J. Zabicky, Interscience, London, 1970, ch. 3
- (91) L. P. Hammett, 'Physical Organic Chemistry', McGraw-Hill, New York, 1940
- (92) A. R. Katritzky, A. J. Waring and K. Yates, Tetrahedron, 1963, 19, 465
- (93) R. Stewart and M. R. Granger, Canad. J. Chem., 1961, 39, 2508

- (94) R. Huisgen, I. Ugi, H. Brade and E. Rauenbusch, Ann. Chem., 1954, 586, 30
- (95) H. S. Rzepa, Ph. D. Thesis, 1974
- (96) K. J. Laidler, 'Chemical Kinetics', McGraw-Hill, New York, 1965
- (97) L. L. Schaleger and F. A. Long, Adv. Phys. Org. Chem., 1963, 1, 1
- (98) F. O. Rice and M. Kilpatrick, Jr., J. Am. Chem. Soc., 1923, 45, 1401
- (99) J. F. Bunnett, J. Am. Chem. Soc., 1961, 83, 4956, 4968, 4973, 4978
- (100) C. H. Rochester, 'Acidity Functions', Academic Press, London, 1970, p. 119
- (101) J. F. Bunnett and F. P. Olsen, Canad. J. Chem., 1966, 44, 1899, 1917
- (102) A. V. Willi, 'Homogeneous Catalysis of Organic Reactions' in 'Comprehensive Chemical Kinetics-Proton Transfer', eds. C. H. Bamford and C. F. H. Tipper, Elsevier, Oxford, 1977, vol. 8, ch. 1
- (103) R. Kintner and W. M. Schubert, 'Decarbonylation' in 'The Chemistry of the Carbonyl Group', ed. S. Patai, Interscience, London, 1966, ch. 14
- (104) K. Yates, Accounts Chem. Res., 1971, 4, 136
- (105) V. K. Kriehle and K. A. Holst, J. Am. Chem. Soc., 1938, 60, 2976
- (106) J. W. Barnett and C. J. O'Connor, J.C.S. Perkin II, 1972, 2378
- (107) D. W. Earls, J.C.S. Perkin II, 1976, 1641
- (108) A. R. Katritzky and R. A. Y. Jones, Chem. and Ind., 1961, 722

- (109) C. J. O'Connor, Quart. Rev., 1970, 24, 553
- (110) M. Liler, Adv. Phys. Org. Chem., 1975, 11, 267
- (111) R. Bonaccorsi, A. Pullman, E. Scrocco and J. Tomasi, Chem. Phys. Lett., 1972, 12, 622
- (112) A. C. Hopkinson and I. G. Csizmadia, Canad. J. Chem., 1973, 51, 1432
- (113) Y. A. Panteleev, Zh. Strukt. Khim., 1976, 17, 4
- (114) A. Pullman, Chem. Phys. Lett., 1973, 20, 29
- (115) H.S. Rzepa, Work to be published
- (116) M. J. S. Dewar and W. Thiel, J. Am. Chem. Soc., 1977, 99, 4899 ; Theor. Chem. Acta, 1977, 46, 89
- (117) M. J. S. Dewar and W. Thiel, J. Am. Chem. Soc., 1977, 99, 4907
- (118) M. J. S. Dewar and M. L. McKee, J. Am. Chem. Soc., 1977, 99, 523
- (119) M. J. S. Dewar and H. S. Rzepa, J. Am. Chem. Soc., 1978, 100, 58, 777
- (120) S. K. Pollack and W. J. Hehre, J. Am. Chem. Soc., 1977, 99, 4845
- (121) R. R. Li and S. I. Millar, J. Chem. Soc. (B), 1971, 2269
- (122) J. Toullec and J. E. Dubois, J. Am. Chem. Soc., 1974, 96, 3524
- (123) R. P. Bell, D. W. Earls and B. A. Timini, J.C.S. Perkin II, 1974, 811
- (124) E. F. Caldin and M. Kasparian, Discussions Faraday Soc., 1965, 39, 25
- (125) A. Streitwieser, Jr., M. R. Granger, F. Mares and R. A. Wolf, J. Am. Chem. Soc., 1973, 95, 4257
- (126) D. J. Cram, 'Fundamentals of Carbanion Chemistry', Academic Press, New York, 1965, p. 47

- (127) A. Streitwieser, Jr., 'Molecular Orbital Theory for Organic Chemists', Wiley, New York, 1961, p. 256
- (128) M. G. Evans, Trans. Faraday Soc., 1939, 35, 824
- (129) M. J. S. Dewar, Angew. Chem., 1971, 10, 761
- (130) N. Bodor, M. J. S. Dewar and A. J. Harget, J. Am. Chem. Soc., 1970, 92, 2929
- (131) V. Bocchi, L. Chierici and G. P. Gardini, Tetrahedron, 1970, 26, 4073
- (132) E. Wenkert, N. K. Bhattachargya, T. L. Reid and T. E. Stevens, J. Am. Chem. Soc., 1956, 78, 797
- (133) J. Burgers, W. van Hartingsveldt, J. van Keulen, P. E. Verkade, H. Visser and B. M. Wepster, Rec. Trav. Chim., 1956, 75, 1327
- (134) L. F. Fieser and M. Fieser, 'Reagents for Organic Synthesis', Wiley, New York, 1967, vol. 1, p. 1065
- (135) A. A. Pavlic and H. Adkins, J. Am. Chem. Soc., 1946, 68, 1471
- (136) G. Hahn and M. R. Tulus, Ber., 1941, 74, 500
- (137) 'Dictionary of Organic Compounds', ed. M. Heibron and H. M. Bunbury, Eyre and Spottiswoode, London, 1943
- (138) F. Mayer, L. van Zutphen and H. Philipps, Ber., 1927, 60, 858
- (139) P. G. Gassman, D. P. Gilbert and T. Y. Luh, J. Org. Chem., 1977, 42, 1340